

***At*NOGC1 protein bioelectrode for the determination of stress signalling molecules - Nitric Oxide (NO), Carbon Monoxide (CO) and Calcium ion (Ca<sup>2+</sup>).**

**Tsumbedzo Tertius Tshivhidzo**

**MSc Biotechnology**

**Faculty of Science**

**University of the Western Cape**



**Supervisor (s): Dr T Mulaudzi-Masuku**

**Prof E.I. Iwouha & Dr F. Ajayi**

**May 2018**

## **Declaration**

I Tsumbedzo Tertius Tshivhidzo declare that “*AtNOGCI protein bioelectrode for the determination of stress signalling molecules - Nitric Oxide (NO), Carbon Monoxide (CO) and Calcium ion (Ca<sup>2+</sup>)*” is my own work and that all the sources that I have used or quoted have been indicated and acknowledged by means of complete references and that this work has not been submitted by me before for any other degree at any institution.



Tsumbedzo Tertius Tshivhidzo

May 2018

Signature \_\_\_\_\_

Date \_\_\_\_\_

## **Dedication**

This is a special dedication to my late father **Tshililo John Tshivhidzo** (1960-2012), late mother **Mavhungu Esther Tshivhidzo** (1957-1997) and late brother **Tondani Stanley Tshivhidzo** (1986-2000). May their soul continue to rest in love and harmony.



## **Acknowledgements**

First and foremost I would like to thank **GOD** for the gift of life, wisdom and good health.

Thank you to my supervisor **Dr Takalani Mulaudzi-Masuku** for the opportunity to study my MSc degree under your supervision at the Molecular Sciences and Biochemistry Laboratory, this attainment wouldn't be possible if it was not for your academic and personal support to learn and acquire new scientific skills and continuous knowledge. I am grateful for the research's outcomes in a journey of seminars, symposiums, meetings and not forgetting the TV interview.

I would also thank my co-supervisor **Prof Emmanuel Iwuoha** for the financial support and to pursue this degree under your supervision at the SensorLab.

To my co-supervisor **Dr Fanelwa Ajayi**, members of the Molecular Sciences and Biochemistry Laboratory, SensorLab and Biotechnology department, I would like to appreciate all your support.

Lastly I would like to send warm gratitude to friends and family for all the support and for not giving up on me, lastly but not least I would appreciate my fiancée **Thembeke Mabiya** for the love and support.

I would like to thank **DST/NRF** for the financial support.



## **Abstract**

**Title:** *At*NOGC1 protein bioelectrode for the determination of stress signalling molecules - Nitric Oxide (NO), Carbon Monoxide (CO) and Calcium ion ( $\text{Ca}^{2+}$ ).

It has been estimated that the world population will reach about 10 billion by the year 2050 and in order to accommodate the increased demand of food, the world agricultural production needs to rise by 70 % in the year 2030. However, the realisation of the goal in food production is hindered by limited arable land caused by urbanisation, salinisation, desertification and environmental degradation. Furthermore, abiotic and biotic stresses affect plant growth and development, which lead to major crop losses. The long term goal of this study is to improve food security by producing genetically engineered agricultural crops that will be tolerant to diverse stresses. This research aims at developing stress tolerant crops through the determination of important signalling molecules and second messengers, such as nitric oxide (NO), carbon monoxide (CO) and calcium ion ( $\text{Ca}^{2+}$ ), which can bind to plant proteins such as *At*NOGC1 in order to induce stress tolerance in plants.

*At*NOGC1 is a novel plant protein that has been shown to have the guanylyl cyclase (GC) activity *in vitro* in the *Arabidopsis* sequence within the catalytic centre as well as the heme NO and or oxygen ( $\text{O}_2$ ) binding domain (H-NOX). Therefore, important signalling molecules and second messengers such as NO, CO and  $\text{Ca}^{2+}$ , that plays major roles in growth and development of plants and also in response to abiotic and biotic stresses, were investigated by developing electrochemical based biosensors to determine whether they will bind to *At*NOGC1 protein bioelectrode. The pET SUMO-*At*NOGC1 construct was expressed and purified by affinity chromatography under native conditions as a ~ 67.7 kDa protein. The purified protein was used to create an electrochemical enzyme based biosensor by immobilising the *At*NOGC1 protein onto the glassy carbon electrode

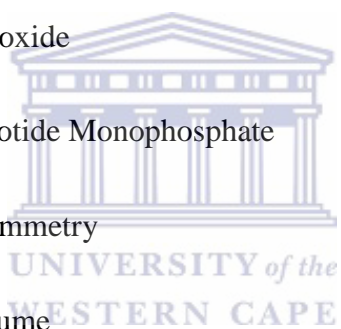
(GCE) surface. Electrochemistry technique such as cyclic voltammetry (CV) was used as a method of choice to determine the binding affinity of *At*NOGC1 protein to stress signalling molecules. Modification of the GCE surface with crosslinking agents and the *At*NOGC1 protein enhanced electron transfer in redox reactions. In the presence of O<sub>2</sub>, there was oxygenation of *At*NOGC1 coupling of the heme group from *At*NOGC1-Fe<sup>3+</sup> to *At*NOGC1-Fe<sup>2+</sup> state. However, imidazole restored the Fe<sup>3+</sup> state of the *At*NOGC1 protein through reduction reaction. The mono-oxygenation catalytic cycle of *At*NOGC1 binding towards NO took place in a reduction reaction at a catalytic potential peak of -500 mV (vs Ag/AgCl). Both the Fe<sup>3+</sup> and the Fe<sup>2+</sup> state of the heme binds to CO, since the cathodic peak potential of *At*NOGC1- Fe<sup>3+</sup>/Fe<sup>2+</sup> couple in redox reaction of CO response as a signalling molecule was in the peak potential range of -400 to -600 mV (vs Ag/AgCl). The dynamic linear range of the Ca<sup>2+</sup> concentration towards *At*NOGC1 binding was determined to be from 1 nM to 3 nM. The reaction of Ca<sup>2+</sup> on the *At*NOGC1/GCE biosensor is an adsorption controlled process as it showed excellent stability and reproducibility at the cathodic peak potential of -560 mV (vs Ag/AgCl). This study demonstrated that *At*NOGC1 protein plays an important role as an electron transporter in redox reactions and that *At*NOGC1 binds to NO, CO and Ca<sup>2+</sup>.

The advantage of biomolecules biosensors such as *At*NOGC1 protein bioelectrode, is that they are reproducible and can be used to determine the binding of many biological molecules in a short reliable period of time. This research aim to pave a way towards the development of stress tolerant crops to improve food security in order for the population to have an access to reliable, sufficient, affordable and nutritious food.

## **Abbreviations**

ABA	Abscisic Acid
AC	Adenylyl Cyclase
Ag/AgCl	Silver/Silver Chloride
AHLs	N-Acyl-homoserine-lactones
Al <sup>3+</sup>	Aluminum Ion
AR	Adventitious Root
AtBR1	<i>Arabidopsis thaliana</i> Brassinosteroid Receptor
AtDGK4	<i>Arabidopsis thaliana</i> diacylglycerol kinase 4
AtGC1	<i>Arabidopsis thaliana</i> guanylate cyclase 1
AtHO1	<i>Arabidopsis thaliana</i> heme oxygenase 1
AtPepR1	<i>Arabidopsis thaliana</i> Phytosulfokine Receptor 1
AtPNP-R1	<i>Arabidopsis thaliana</i> Plant Natriuretic Peptide Receptor 1
AtWAKL10	<i>Arabidopsis thaliana</i> Wall Associated Kinase-like 10
BH <sub>4</sub>	(6R-) 5,6,7,8-Tetrahydrobiopterin
BSA	Bovine Serum Albumin
cAMP	3', 5' cyclic Adenosine Monophosphate
Ca <sup>2+</sup>	Calcium Ion

[Ca <sup>2+</sup> ] <sub>cyt</sub>	Cytosolic calcium concentration
CAS	Calcium Ion-Sensing Receptors
Cat#	Catalogue Number
CaM	Calmodulin
CD	Calcium Dobesilate
cGMP	3', 5' cyclic Guanosine Monophosphate
CNGC	Cyclic Nucleotide Gated Channel
CO	Carbon Monoxide
cNMP	cyclic Nucleotide Monophosphate
CV	Cyclic Voltammetry
CV	Column Volume
DDAB	Didodecyldimethylammonium bromide
eNOS	Endothelial Nitric Oxide Synthase
ER	Endoplasmic Reticulum
$E_p^0$	Formal Peak Potential
$E_{pc}$	Cathodic Peak Potential
FAD	Flavin Adenine Dinucleotide
Fe <sup>2+</sup>	Iron (II)



Fe <sup>3+</sup>	Iron (III)
FMN	Flavin Mononucleotide
FMO	Flavin-dependent/containing Monooxygenase
GC	Guanylate Cyclase
GCE	Glassy Carbon Electrode
GCAPs	Guanylate Cyclase-Activating Proteins
GTP	Guanosine Triphosphate
H <sup>+</sup>	Hydrogen Ion
H <sub>2</sub> O <sub>2</sub>	Hydrogen Peroxide
HO	Heme Oxygenase
H-NOX	Heme Nitric oxide and/ or Oxygen
HR	Hypersensitive Response
HV	Hydrodynamic Voltammetry
IMAC	Immobilised metal-affinity chromatography
IP <sub>3</sub>	Inositol Triphosphate
<i>I</i> <sub>pc</sub>	Cathodic Peak Potential
K <sup>+</sup>	Potassium Ion
LSV	Linear Sweep Voltammetry



MAPK	Mitogen-Activated Protein Kinase
Mg <sup>2+</sup>	Magnesium Ion
mM	Millimolar
Na <sup>+</sup>	Sodium Ion
NaCl	Sodium Chloride
NADPH	Nicotinamide Adenine Dinucleotide Phosphate
NC	Nucleotide Cyclase
NO	Nitric Oxide
NO <sub>2</sub> <sup>-</sup>	Nitrite
NO <sub>3</sub> <sup>-</sup>	Nitrate
NOS	Nitric Oxide Synthase
NR	Nitrate Reductase
O <sub>2</sub>	Oxygen
OD	Optical Density
PBS	Phosphate Buffer Saline
PCD	Programmed Cell Death
PPs	Phosphatases
PSKR1	Phytosulfokine Receptor 1



PSV	Potential Step Voltammetry
PTMs	Protein Modifications
RNS	Reactive Nitrogen Species
ROS	Reactive Oxygen Species
SA	Salicylic Acid
SAR	Systemic Acquired Resistance
sGC	soluble Guanylate Cyclase
SLAC	Slow Anion Channel
SOS	Salt Overly Sensitive
SWV	Square-Wave Voltammetry
TFB1	Transfer Buffer 1
TFB2	Transfer Buffer 2



**Keywords**

*At*NOGC1

Biosensor

Calcium ion

Carbon monoxide

cGMP

Cyclic voltammetry

Electrochemistry

Guanylyl cyclase

H-NOX domain

Nitric oxide





## **List of tables and figures**

### **Tables**

#### **Chapter 2**

Table 2.1:	Preparation of 12 % SDS-PAGE for analysing recombinant proteins .....	36
Table 3.1:	The absorbance (595 nm) of the standard and unknown samples concentration (µg/mL).....	89

### **Figures**

#### **Chapter 1**

Figure 1.1:	Generic cyclic nucleotide transduction pathways in mammalian cells showing a role for cyclic nucleotide dependent kinases.....	5
Figure 1.2:	A schematic diagram of the NO-induced cGMP signalling pathway in plant development, abiotic and biotic stress responses.....	7
Figure 1.3:	Diagram showing the transduction sequences of auxins and cytokinins.....	9
Figure 1.4:	Summary of the main functions of NO in different plant physiological and pathological processes and its potential biotechnological applications.....	12
Figure 1.5:	Map showing crosstalk of NO with second messengers in plants defence responses against pathogen attack.....	14
Figure 1.6:	Schematic representation of CO production from different routes in the environment, animals and plants.....	15
Figure 1.7:	A ribbon representation of the typical EF-hand motif of Ca <sup>2+</sup> -binding proteins....	20

## Chapter 2

Figure 2.1:	Schematic representation of the apparatus used for the production of NO gas in the fume hood.....	41
-------------	---	----

## Chapter 3

Figure 3.1:	12 % SDS-PAGE analysis of the expression and affinity purification of the <i>At</i> NOGC1 protein.....	45
-------------	--	----

Figure 3.2:	12 % SDS-PAGE analysis of the concentrated <i>At</i> NOGC1 protein.....	46
-------------	---	----

Figure 3.3:	Standard curve of BSA to determine the <i>At</i> NOGC1 protein concentration by Bradford assay.....	90
-------------	---	----



## Chapter 4

Figure 4.1:	Cyclic voltammetry showing responses of bare GCE in the presence and absence of O <sub>2</sub> or imidazole as a chemical sensor.....	51
-------------	---	----

Figure 4.2:	Cyclic voltammetry showing responses of the <i>At</i> NOGC1/GCE biosensor in the presence and absence of O <sub>2</sub> .....	53
-------------	---	----

Figure 4.3:	Cyclic voltammetry showing responses of nitric oxide (NO) towards the <i>At</i> NOGC1/GCE biosensor in the presence and absence of O <sub>2</sub> . ....	55
-------------	--	----

Figure 4.4:	Cyclic voltammetry showing responses of the bare GCE, modified GCE with DDAB/BSA and <i>At</i> NOGC1/GCE biosensor in the presence of NO .....	58
-------------	--	----

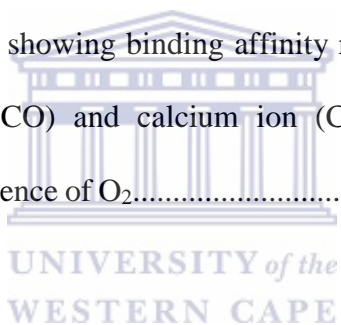
Figure 4.5: Cyclic voltammetry showing responses of the carbon monoxide (CO) towards the *At*NOGC1/GCE biosensor in the presence and absence of O<sub>2</sub>.....59

Figure 4.6: Cyclic voltammetry showing responses of the bare GCE, modified GCE with DDAB/BSA and *At*NOGC1/GCE biosensor in the presence of CO .....62

Figure 4.7: Cyclic voltammetry showing responses of the calcium ion (Ca<sup>2+</sup>) concentrations towards the *At*NOGC1/GCE biosensor in the presence and absence of O<sub>2</sub>.....63

Figure 4.8: Cyclic voltammetry showing responses of the bare GCE, modified GCE with DDAB/BSA and *At*NOGC1/GCE biosensor in the presence of Ca<sup>2+</sup>.....66

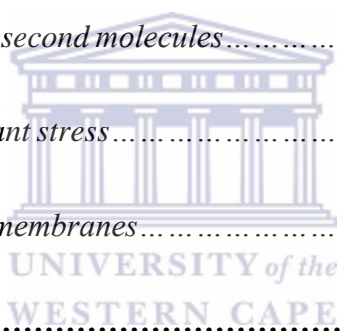
Figure 4.9: Cyclic voltammetry showing binding affinity responses of the nitric oxide (NO), carbon monoxide (CO) and calcium ion (Ca<sup>2+</sup>) towards the *At*NOGC1/GCE biosensor in the presence of O<sub>2</sub>.....67



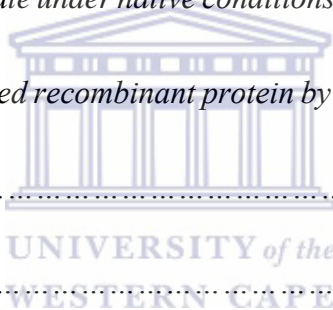
## Table of contents

<b>Declaration</b> .....	<b>i</b>
<b>Dedication</b> .....	<b>ii</b>
<b>Acknowledgements</b> .....	<b>iii</b>
<b>Abstract</b> .....	<b>iv</b>
<b>Abbreviations</b> .....	<b>vi</b>
<b>Keywords</b> .....	<b>xi</b>
<b>List of tables and figures</b> .....	<b>xii</b>
<b>CHAPTER 1: Literature Review</b> .....	<b>1</b>
<b>1.1 Introduction</b> .....	<b>1</b>
<b>1.2 Cyclic nucleotides monophosphate (cNMP)</b> .....	<b>5</b>
<i>1.2.1 Guanosine 3', 5' cyclic monophosphate (cGMP)</i> .....	<i>6</i>
<i>1.2.2 Adenosine 3', 5' cyclic monophosphate (cAMP)</i> .....	<i>8</i>
<b>1.3 Nitric Oxide (NO)</b> .....	<b>10</b>
<i>1.3.1 NO as a signalling molecule</i> .....	<i>10</i>
<i>1.3.2 NO generation</i> .....	<i>10</i>
<i>1.3.3 Functions of NO as a signalling molecule</i> .....	<i>11</i>
<i>1.3.4 NO regulation by second messengers</i> .....	<i>13</i>

1.3.5 Crosstalk of NO and second messengers.....	13
<b>1.4 Carbon Monoxide (CO).....</b>	<b>15</b>
1.4.1 CO production in the atmosphere.....	15
1.4.2 Role of CO in plants as a signalling molecule.....	16
<b>1.5 Calcium Ion (Ca<sup>2+</sup>).....</b>	<b>18</b>
1.5.1 Ca <sup>2+</sup> as a signalling molecule.....	18
1.5.2 Regulation of Ca <sup>2+</sup> .....	18
1.5.3 Interaction of Ca <sup>2+</sup> with other second molecules.....	19
1.5.4 Role of Ca <sup>2+</sup> in response to plant stress.....	21
1.5.5 Ca <sup>2+</sup> transporters in cellular membranes.....	22
<b>1.6 Electrochemistry.....</b>	<b>24</b>
1.6.1 Electrochemistry biosensors.....	25
1.6.2 Voltammetry techniques applied in electrochemistry.....	25
1.6.2.1 Cyclic voltammetry (CV).....	26
1.6.3 The electrochemistry of heme binding proteins.....	27
<b>1.7 Research hypothesis.....</b>	<b>27</b>
<b>1.8 Aim of the study.....</b>	<b>27</b>
<b>CHAPTER 2: Materials and Methods.....</b>	<b>29</b>



<b>2.1 Stock solutions, buffers and reagents.....</b>	<b>29</b>
<b>2.2 Molecular Biology: Preparation of the recombinant AtNOGC1 protein.....</b>	<b>33</b>
2.2.1 Preparation of competent <i>E.coli</i> cells for transformation.....	33
2.2.2 Transformation of the recombinant pET SUMO-AtNOGC1 plasmid into <i>E.coli</i> competent cells.....	33
2.2.3 Plasmid DNA isolation.....	34
2.2.4 Expression of the recombinant protein.....	34
2.2.5 Preparation of the cleared lysate under native conditions.....	35
2.2.6 Purification of the 6xHis-tagged recombinant protein by affinity chromatography.....	35
2.2.7 Setup of the gel plates.....	36
2.2.8 Running SDS-PAGE.....	37
2.2.9 Determination of the recombinant protein concentration by Bradford assay.....	37
2.2.10 Concentrating the recombinant protein.....	38
<b>2.3 Electrochemical preparation of AtNOGC1 protein bioelectrode as a biosensor for binding NO, CO and Ca<sup>2+</sup>.....</b>	<b>39</b>
<b>2.3.1 Cleaning the glassy carbon electrode (GCE).....</b>	<b>39</b>
<b>2.3.2. Immobilising the recombinant AtNOGC1 on the GCE surface.....</b>	<b>39</b>
<b>2.3.3. Electrochemical cell setup.....</b>	<b>39</b>
<b>2.3.4 Preparation of analytes.....</b>	<b>40</b>



2.3.4.1 Production of NO gas.....	40
2.3.4.2 Production of CO gas.....	41
2.3.4.3 Preparation of Ca <sup>2+</sup> solution.....	42
<b>2.3.5 Electrochemical procedure.....</b>	<b>42</b>
<b>CHAPTER 3: Recombinant expression and purification of the AtNOGC1 protein.....</b>	<b>44</b>
<b>3.1 Results.....</b>	<b>44</b>
3.1.1 Expression and purification of AtNOGC1.....	44
3.1.2 Determination of AtNOGC1's protein concentration.....	45
<b>3.2 Discussion.....</b>	<b>46</b>
<b>CHAPTER 4: Electrochemical characterisation of AtNOGC1 protein bioelectrode as a biosensor for binding NO, CO and Ca<sup>2+</sup>.....</b>	<b>50</b>
4.1 The electrochemical characterisation of the bare glassy carbon electrode (GCE) as a chemical sensor.....	50
4.2 The electrochemical behaviour of the immobilised AtNOGC1 on the GCE surface in the presence and absence of O <sub>2</sub> .....	52
4.3 Electrocalalytic activity of signalling molecules and second messengers.....	55
4.3.1 Electrocatalytic activity of nitric oxide (NO) on AtNOGC1/GCE biosensor.....	55
4.3.1.1 Electrochemical characterisation of the bare GCE, modified GCE with DDAB/BSA and AtNOGC1/GCE biosensor in the presence and absence of NO.....	57

4.3.2 Electrochemical activity of carbon monoxide (CO) on AtNOGC1/GCE biosensor.....	58
4.3.2.1 Electrochemical characterisation of the bare GCE, modified GCE with DDAB/BSA and AtNOGC1/GCE biosensor in the presence and absence of CO.....	61
4.3.3 Electrochemical activity of calcium ion (Ca <sup>2+</sup> ) on AtNOGC1/GCE biosensor.....	62
4.3.3.1 Electrochemical characterisation of the bare GCE, modified GCE with DDAB/BSA and AtNOGC1/GCE biosensor in the presence and absence of Ca <sup>2+</sup> .....	65
4.4 Electrochemical characterisation of the binding affinity of NO, CO and Ca <sup>2+</sup> to AtNOGC1/GCE biosensor.....	67
<b>4.7 Discussion.....</b>	<b>68</b>
<b>CHAPTER 5: Conclusion and future prospects.....</b>	<b>70</b>
<b>References.....</b>	<b>72</b>
<b>Appendix I: Determination of AtNOGC1 protein concentration.....</b>	<b>89</b>





# Chapter 1: Literature Review

## 1.1 Introduction

Abiotic and biotic factors are the major stresses that negatively affect agricultural plants globally (Dhlamini et al., 2005), consequences of such stresses result in depleted crop production, affected economy and hazardous health to the population (Boyer, 1982). Naturally, most plants have developed an ability to identify various stresses in such a way that they grow, develop and adapt to their environment. It is significant to understand mechanisms of plant's stress response, in order to produce plants that can withstand harsh environmental conditions. Abiotic factors such as high and low temperatures, salinity, soil erosion and continued droughts are caused by severe climatic change, which causes major crop losses and unstable food supply (Pachauri, 2007).

When plants respond to environmental stresses, their internal system is suppressed, which causes changes in their molecular, biochemical, physiological and morphological structure. Consequently, these changes should be balanced in order to obtain good plant growth, development and hence high crop yield. It has been reported that plants have multifaceted immune response system in which they respond to various biotic stresses such as insects and pathogen attack in a hypersensitive manner. Since plants use hypersensitive response (HR) to protect their system, any microbiological attack is terminated in a systematic acquired resistance (SAR) mechanism (Yu et al., 2014). Plants use signalling molecules and second messengers such as cyclic nucleotide monophosphate (cNMP), Calcium ions ( $\text{Ca}^{2+}$ ), Inositol polyphosphates, Nitric Oxide (NO), Carbon monoxide (CO) and other small molecules, to respond to signals perceived in their cells (Reddy et al., 2011).

For decades, it has been a challenge to identify and measure cyclic nucleotide monophosphate (cNMP) in plants. But with the aid of scientific techniques that are used in biochemical and molecular biology, recent studies discovered the presence of macromolecules such as enzymes, which are responsible for the synthesis of cNMP and these include adenylyl cyclase (AC) and guanylyl cyclase (GC) (Lemtiri-Chilieh et al., 2011). It was recently reported in the last two years that mass spectrometry based measurements, radiolabeled and antibody based immunoassays can be applied to measure and analyse cNMP levels in plants (Gross and Durner, 2016). Furthermore, fewer genes which are believed to code for nucleotide cyclases (NC's) have been discovered in lower plants, unlike in higher plants. These include; phytosulfokine (PSK) *Arabidopsis thaliana* leucine-rich repeat protein kinase receptor 1 (*AtPepR1*) (Qi et al., 2010), *Arabidopsis thaliana* guanylate cyclase 1 (*AtGC1*) (Ludidi and Gehring, 2003), *Arabidopsis thaliana* brassinosteroid receptor (*AtBRI1*) (Kwezi et al., 2007), *Arabidopsis thaliana* plant natriuretic peptide receptor 1 (*AtPNP-R1*) (Turek and Gehring, 2016) and *Arabidopsis thaliana* wall associated kinase-like 10 (*AtWAKL10*) (Meier et al., 2010). However, none of these GC's contained a heme binding motif that senses NO. Similarly to the existence of cAMP, which has been reported to be synthesised by purine nucleotide cyclases in plants remains unclear. Fewer AC's in higher plants have been reported which are responsible for growth and development of the pollen tube; the *Zea mays* pollen-signalling protein (*ZmPSiP*) (Moutinho et al., 2001); the *Arabidopsis thaliana* pentatricopeptide repeat protein responsible for apoptosis (*AtPPR*) (Ruzvidzo et al., 2013); also the reported *Nicotiana benthamiana* adenylyl cyclase protein (*NbAC*;) which causes cell death and many diseases such as wildfire disease (Ito et al., 2014); another AC protein known as the *Hippeastrum hybridum* (*HpAC1*), which is involved in signalling response of plants against abiotic

and biotic stresses (Swiezawska et al., 2014) and lastly the potassium uptake modulated in the *Arabidopsis* sequence (*AtKUP7*) (Al-Younis et al., 2015).

Mulaudzi et al (2011) identified a GC with a heme binding motif that is annotated as a flavin-containing monooxygenase (FMO; *At1g62580*) and shown to synthesise guanosine 3', 5' cyclic monophosphate (cGMP) from the guanosine triphosphate (GTP) in a 2-fold excess increase upon activation by NO (Mulaudzi et al., 2011). Based on its biochemical, electrochemical and structural characterisation, this GC was named as *Arabidopsis thaliana* NO/O<sub>2</sub> binding with a GC activity (*AtNOGC1*). Examination of *AtNOGC1* also supported the role of NO as an important signalling molecule in plants. Nitric oxide is involved in stomatal closure and plant senescence through cGMP pathway. It has been reported that NO/cGMP signalling is the main signalling pathway in animals that is well understood, but in plants it remains unclear. However, Judoi et al (2013) reported that nitrated cGMP derivative 8-nitro-cGMP functions in guard cell signalling and triggers stomatal opening and closure. These studies also demonstrated that in the presence of reactive oxygen species (ROS) in guard cells, abscisic acid (ABA) and NO induces the synthesis of 8-nitro-cGMP. In order to understand these signalling pathways, important second messengers that crosslink with NO such as cyclic nucleotide monophosphate (cNMP), carbon monoxide (CO) and calcium ions (Ca<sup>2+</sup>) should be further examined functionally using different scientific techniques.

The HNOX search motif was used again in *Arabidopsis* to search for another H-NOX candidate and discovered the *Arabidopsis thaliana* diacylglycerol kinase 4 (*AtDGK4*; *At5G57690*), which is responsible for Ca<sup>2+</sup> movement. The Ca<sup>2+</sup> movement is modulated by enhancing the phosphorylation of diacylglycerol to phosphatidic acid, therefore utilising and discharging Ca<sup>2+</sup> from intracellular stores. Since the growth of *Agapanthus umbellatus* is regulated by the cytosolic

Ca<sup>2+</sup> through phosphoinositides and phosphatidic acid, it is important to study the interaction of the *AtDGK4* and NO (Monteiro et al., 2005; Potocký et al., 2003). If binding could occur between the *AtDGK4* and NO it means that there might be a chance that NO may have an uninterrupted link towards Ca<sup>2+</sup> signalling (Wang et al., 2009). It has been reported that more than 24 000 genes have been verified for changes in gene expression when they responded to NO signalling in *Arabidopsis*. Therefore the study showed that several genes may be up-regulated which encodes for disease resistance proteins, transcription factors, zinc finger proteins, glutathione S-transferases and kinases. However in addition to NO-sensing molecules other biosynthetic genes such as phytohormones, lignin and alkaloids may have potential in gene expression when they respond to NO signalling (Parani et al., 2004).



## 1.2 Cyclic nucleotides monophosphate (cNMP)

In plants, cyclic nucleotide signalling is essential for the modulation of cation fluxes. Guanylate cyclase (GC) and adenylyate cyclase (AC) are responsible for the synthesis of cGMP and cAMP nucleotide cyclases, respectively (Martinez-Atienza et al., 2007). The effects of cyclic nucleotides has been explained clearly through their interaction with membrane transporters as shown in figure 1.1 (A) and (B).

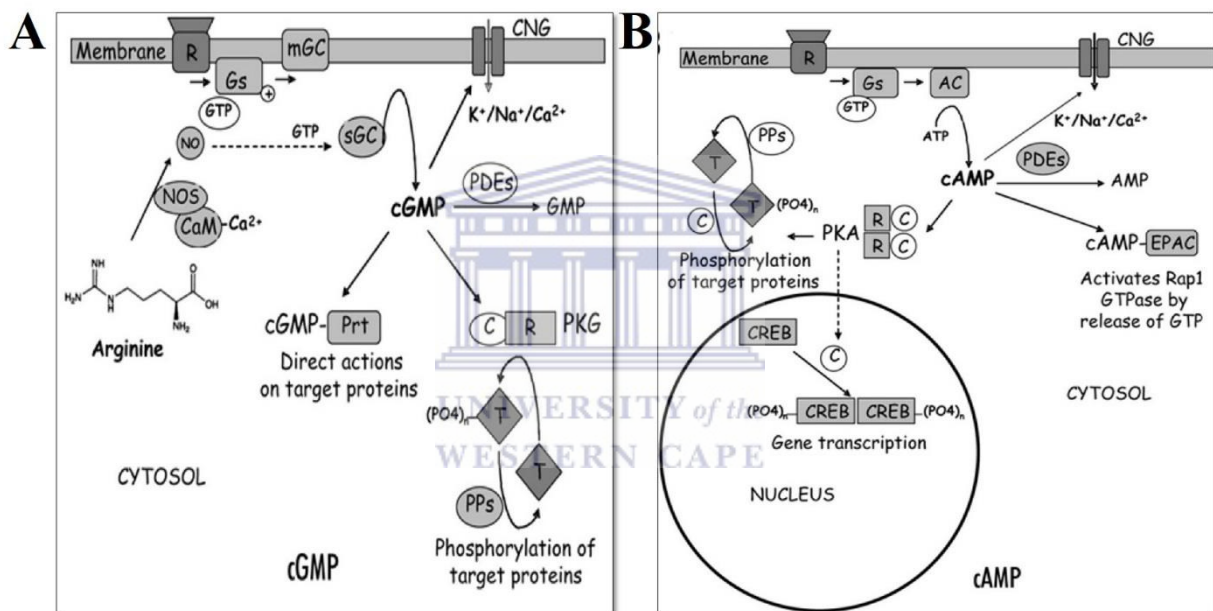


**Figure 1.1: Generic cyclic nucleotide transduction pathways in mammalian cells showing a role for cyclic nucleotide dependent kinases.** (A) NO synthesised from NO synthase (NOS) activates GC enzyme and synthesises cGMP from GTP which activates protein kinases, ion gated channels and phosphodiesterases. (B) Adenosine cyclase (AC) is activated by receptors (R) and G-proteins (Gs) which synthesises cAMP which is also involved in activating protein kinases and ion gated channels (Adapted from Martinez-Atienza et al., 2007).

The membrane bound guanylate cyclase (mGC) or the soluble guanylate cyclase (sGC) is activated in an NO or G-proteins (Gs) dependent manner by various stimuli perceived in a cell membrane. Therefore, the activated GC synthesise increased levels of cellular cGMP, which is either broken down by specific phosphodiesterases (PDEs) or can directly activates proteins such as cyclic nucleotide gated channels (CNGC). Therefore, the synthesised cGMP activates cGMP-dependent

protein kinase (PKG), which phosphorylate a large number of target proteins (T). Cyclic GMP plays its role as a second messenger in a similar manner as cAMP as shown in figure 1.1 (B) whereby the receptors (R) and G-proteins (Gs) are also involved in the synthesis of cAMP by activating the AC to synthesise the cellular cAMP in an increased level. Cyclic AMP is involved in activating cAMP-dependent protein kinases (PKA) which modifies gene transcription through binding proteins, CNGC and Rap-GTPases (Martinez-atienza et al., 2007).

### *1.2.1 Guanosine 3', 5' cyclic monophosphate (cGMP)*

Scientist discovered the guanosine 3', 5' cyclic monophosphate (cGMP) in the 1960's as a second messenger in prokaryotes and eukaryotes (Müller, 1997). The synthesis of cGMP is derived from guanosine triphosphate (GTP) by the action guanylyl cyclase (GC) enzyme. This second messenger is important because it is involved in many signalling cellular responses in plants including protein kinase activity, cyclic nucleotide gated ion channels and cGMP regulated cyclic nucleotide phosphodiesterases (Denninger and Marletta, 1999).

In mammals, the role of cGMP has been explored and shown to be important in the following; olfactory transduction, assisting with visual adaptation and widening of blood vessels (Pietrobon et al., 2011; Vielma et al., 2012; Thoonen et al., 2013). In plants on the other hand, this is still not well described (Gross and Durner, 2016). Recently several techniques have been developed in order to investigate the endogenous cytoplasmic cGMP levels *in vivo*, these techniques includes the non-invasive fluorescent cGMP biosensor called FlincG (Fluorescent indicator for cGMP) (Isner and Maathuis, 2011) and a cGMP responsive promoter which is fused to a luciferase reporter gene (Wheeler et al., 2013). Such investigations of cGMP in plants have shown a good relationship between the accumulation of cGMP, developmental process and response to abiotic and biotic stresses.

When a plant is under drought stress, abscisic acid (ABA) hormone is stimulated and activates the synthesis of NO (Dubovskaya et al., 2011). Therefore, NO stimulates the NO-dependent GC's to produce high concentrations of cGMP (Dubovskaya et al., 2011). Simultaneously, ABA also activates the production of hydrogen peroxide (H<sub>2</sub>O<sub>2</sub>), which reacts with NO to produce reactive nitrogen species (RNS) (Joudoi et al., 2013). Therefore, the reaction between the RNS and cGMP produces 8-Nitro-cGMP, which activates the slow anion channel 1 (SLAC1) and the accumulation of cytoplasmic calcium concentration ([Ca<sup>2+</sup>]<sub>cyt</sub>) which results in stomatal closure. Similarly, during a pathogen attack in plants stomatal closure occurs in a similar manner, except that the NO-cGMP pathway is activated by the hormone salicylic acid (SA) as shown in figure 1.2 (Hao et al., 2010).

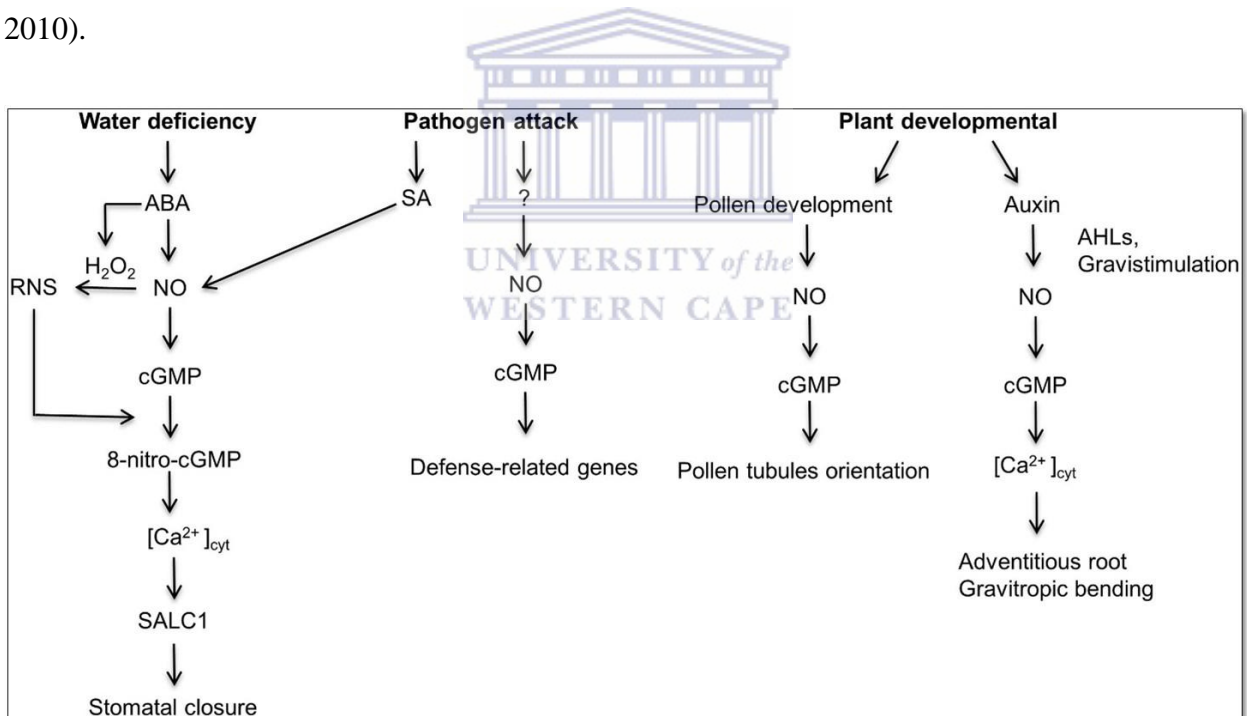


**Figure 1.2: A schematic diagram of the NO-induced cGMP signalling pathway in plant development, abiotic and biotic stress responses.** Under drought stress, abscisic acid (ABA) stimulates NO-cGMP mediated response which result in stomatal closure to avoid water loss and during pathogen attack in plants salicylic acid and unknown molecule also stimulates the NO-cGMP defence response. During plant development two signalling pathways are initiated whereby the other pathways involves growth hormone auxin and a second messenger, calcium ion (Ca<sup>2+</sup>) (Adapted from Gross and Durner, 2016).



The NO-cGMP signalling pathway is important as it is involved in growth and development of pollen tubule and adventitious roots formation. The formation of the adventitious roots is stimulated by exogenous and endogenous chemical, N-Acyl-homoserine-lactones (AHLs). AHLs are produced by the gram negative bacteria, the *rizobacteria* and they promote polar auxin transport, which activates the NO-cGMP dependent signalling cascade leading to the development of adventitious roots (Pagnussat et al., 2003; Hu et al., 2005).

### *1.2.2 Adenosine 3', 5' cyclic monophosphate (cAMP)*

In bacteria Adenosine 3', 5' cyclic monophosphate (cAMP) act primarily as a signalling molecule for relaying messages about the state of the metabolic cell by regulating the expression of many operons when it interacts with the catabolite gene activator protein (CAP) (Bolwell, 1995). In animals, cAMP act as a second messenger because it is involved in many signalling pathways such as the regulation of the glycogen and glucose synthesis by a process known as reverse protein phosphorylation (Bolwell, 1995). Recently, it has been reported that cAMP is an important second messenger and a growth factor in plants. Cyclic AMP is synthesised by the enzyme adenosine cyclase (AC) and it has been debated for more than 25 years that AC nor the cAMP does not exist in higher plants. It could not be concluded that cAMP exist in plants because it was believed that if it existed in plants it would behave in a similar manner as in animals and bacteria (Amrhein, 1977). Scientist were warned not to conclude because there were findings which opposed the existence of cAMP in plants since it was reported that cAMP levels in plants were lower when compared to that found in animals. Additionally, the assays that were conducted could not produce accurate conclusive evidence that there is a presence of cAMP in plants (Gehring, 2010).

Several promises have been made that justify the fact that cAMP exist in plants with the help of Trewavas (1997), as the author researched and found out that auxin signals were transduced



through cAMP and probably through cytosolic  $\text{Ca}^{2+}$ . The debate about whether plant cells contain cAMP was scientifically ended by identifying functional AC and showing that it can mediate the actions of the plant hormone auxin (Magyar et al., 1997). The growth-regulating effect of auxin is pre-eminent, and the main role of cytokinins is to attenuate this growth. Since, auxin can regulate growth in the absence of other growth regulators, cytokinins do so only in the presence of auxin as shown in figure 1.3 (Magyar et al., 1997;Trewavas, 1997).

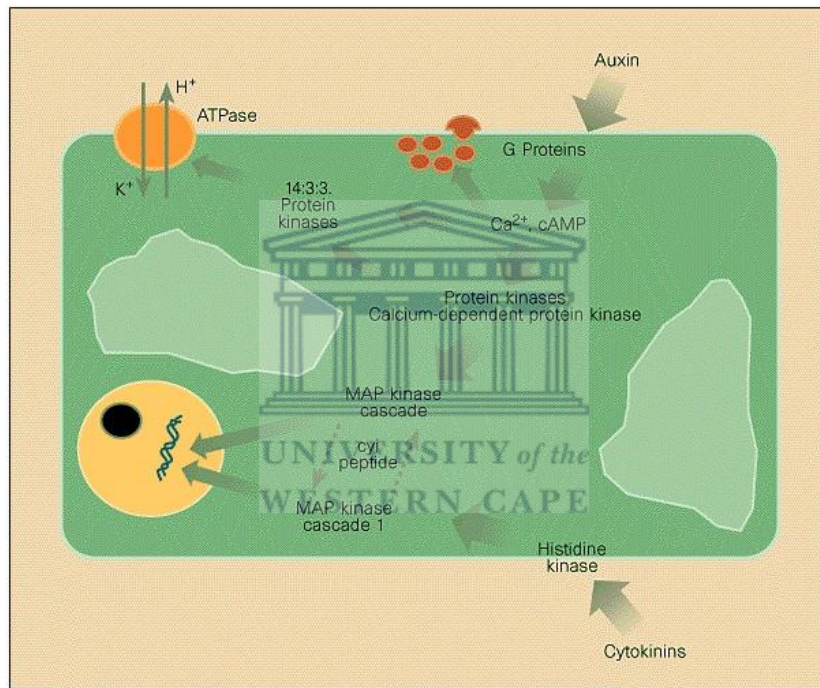
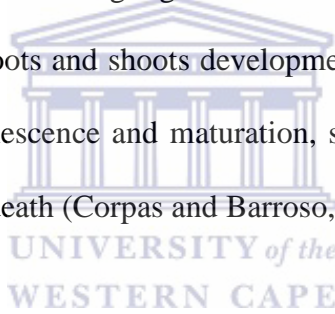


**Figure 1.3: Diagram showing the transduction sequences of auxins and cytokinins.** Auxin is required for growth and it stimulates second messengers  $\text{Ca}^{2+}$  and cAMP which activates protein kinases and calcium dependent protein kinases (CDPKs), which inhibits the cytokinins to decrease plant growth. The cyi peptide is suggested to join the two mitogen-activated protein (MAP) kinase signal-transduction cascades. The diagram includes only some of the known transduction information (Trewavas, 1997).

## 1.3 Nitric Oxide (NO)

### 1.3.1 NO as a signalling molecule

Nitric oxide (NO) is a universal diatomic gas that is very important as a regulator of a comprehensive array of physiological processes in animal model (Astier and Lindermayr, 2012; Martinez-Rutz et al., 2011). Several studies showed that NO production is not restricted to animal cells only but also in other kingdoms, such as plants (Astier and Lindermayr, 2012; Besson-Bard et al., 2008) and bacteria (Henares et al., 2012). Recent studies showed that NO has been well identified in plants in the last decade as well as its role as a signalling molecule is documented. NO in plants plays important roles including regulation of cell differentiation, lignification, seed germination, primary and lateral roots and shoots development, flowering, fruit ripening, pollen tube growth and reorientation, senescence and maturation, stomatal movement, plant-pathogen interactions and programmed cell death (Corpas and Barroso, 2015; Planchet and Kaiser, 2006).



### 1.3.2 NO generation

In mammals NO is synthesised by three different isoforms of nitric oxide synthase (NOS) (Forstermann and Sessa, 2011). All three NOS isoforms involves L-arginine as a substrate, molecular oxygen and nicotinamide-adenine-dinucleotide phosphate (NADPH) as co-substrates. Furthermore, flavin adenine dinucleotide (FAD), flavin mononucleotide (FMN), and (6R-) 5,6,7,8-tetrahydrobiopterin (BH<sub>4</sub>) are required as important cofactors by all isozymes. NOS is induced by NOS II to generate large quantity of NO (Forstermann and Sessa, 2011), and can be expressed in many cell types in response to lipopolysaccharide, cytokines, or other agents and this process also contributes to the pathophysiology of inflammatory diseases and septic shock. However, the large amounts of NO produced may have cytostatic effects on parasitic target cells (Forstermann and

Sessa, 2011). Haines et al (2012) reported that NO is also produced by endothelial NOS (eNOS), which converts L-arginine into L-citrulline and therefore into a final NO product.

The process of NO generation in plants is still challenging for researchers to understand (Astier and Lindermayr, 2012; Frohlich and Durner, 2011; Moreau et al., 2010), since it has been demonstrated that its synthesis occurs through non-enzymatic and enzymatic mechanism from nitrate ( $\text{NO}_3^-$ ), polyamines and L-arginine (Astier and Lindermayr, 2012; Gupta et al., 2011; Moreau et al., 2010). The enzymatic synthesis involves  $\text{NO}_3^-$  reduction to nitrite ( $\text{NO}_2^-$ ) which is catalysed by an NADPH-dependent nitrate reductase (NR), a cytosolic enzyme associated with nitrogen assimilation (Domingos et al., 2015; Yamasaki and Sakihama, 2000). Furthermore, in the presence of abscisic acid (ABA) and gibberellins (Berridge, 2004), NR reduces  $\text{NO}_2^-$  to NO under acidic conditions through mitochondrial electron transport-dependent reductase (Domingos et al., 2015; Planchet et al., 2005). NO generation process evidently shows that NO is a free radical molecule that is endogenously generated in green cells (Corpas, 2015). It has also been reported that in plants NO is produced by the photo-conversion of nitric dioxide ( $\text{NO}_2$ ) to NO, with the aid of carotenoids which reacts with nitrate reductases (NRs) (Garcia-Mata and Lamattina, 2003; Rockel et al., 2002) and glycine decarboxylase (Chandok et al., 2003).

### *1.3.3 Functions of NO as a signalling molecule*

Nitric Oxide plays an important role as a signalling molecule and as a regulator in plants since it influences growth and development, responses to abiotic and biotic stresses. It binds to the heme group of the mammalian soluble guanylyl cyclase (sGC), and activates the enzyme to convert GTP to a large concentration of cGMP. The heme binding NO and/or  $\text{O}_2$  (H-NOX) domains contains a protein fold which is significantly unique and different from other known heme-binding proteins in terms of structure across various species groups ranging from bacteria to animals (Boon and

Marletta, 2005). In plants, NO signal transduction pathways which contains GC and other enzymatic reactions occurs through cGMP dependent (Berridge, 2004) or none dependent mediated processes (Davis et al., 2001; Durzan and Pedroso, 2002) which allows gene expression. In addition, when NO interacts with the heme moiety of the sGC, its activity increases and that result in an increased cGMP production whereby the NO signal is transferred by sGC to downstream components of signalling cascades (Durzan and Pedroso, 2002; Murad, 1999; Pfeiffer et al., 1994). NO promotes a better adaptation to stress and increase defence against invading pathogens as shown in figure 1.4.

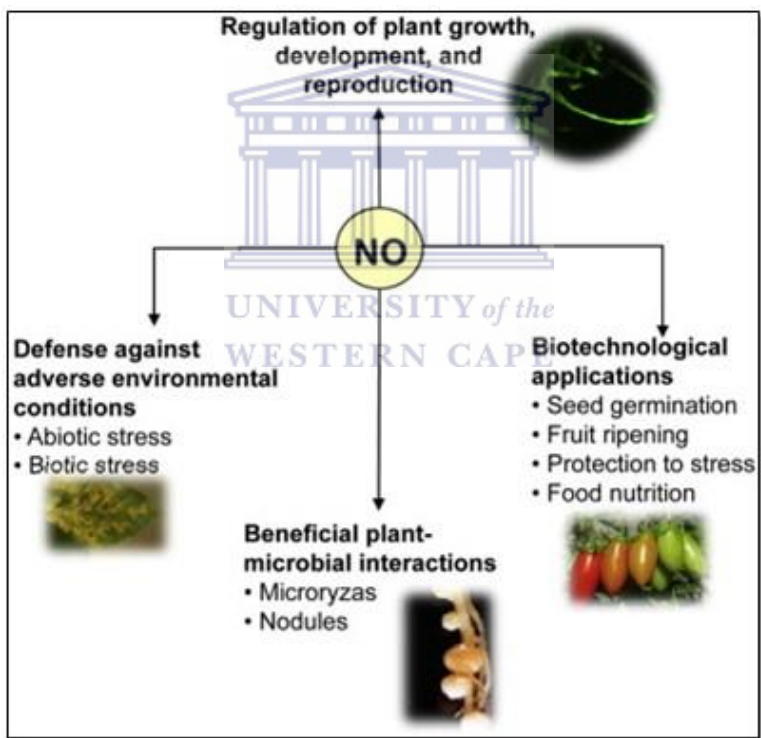


**Figure 1.4: Summary of the main functions of NO in different plant physiological and pathological processes and its potential biotechnological applications.** NO plays an important role in plants as a signalling molecule through different mediated pathways in response to abiotic and biotic stresses. Besides being a signalling molecule it interacts with some microorganisms enhances their functions. NO also plays a beneficial role in industrial application of food as it increases food nutrition (Adapted from Corpas, 2015).

#### 1.3.4 NO regulation by second messengers

When NO is present in large quantities, it is regulated by various second messengers such as calcium ion ( $\text{Ca}^{2+}$ ) and mitogen-activated protein kinase (MAPK) (Frohlich and Durner, 2011). Furthermore, if NO levels increase in the system, they can affect signalling either directly via protein modifications (PTMs) or indirectly via activation of other second messengers like metal nitrosylation, S-nitrosylation and 3-nitrotyrosine (Leitner et al., 2009). However, investigations made by Gaupels et al., (2011) showed that S-nitrosylation and 3-nitrotyrosine are two NO-dependent direct PTMs which are involved in plant defence signalling.

#### 1.3.5 Crosstalk of NO and second messengers

Nitric oxide diffuses regularly due to its gaseous nature, therefore it does not require a carrier to cross membranes and reach intracellular targets. NO falls between reactive oxygen species (ROS) and reactive nitrogen species (RNS) (Berridge, 2004). In plants, ROS play various important roles including the regulation and division of growth cells in the tips. In addition ROS also play an important signalling role in response to abiotic and biotic environmental stimuli and programmed cell death (Bailey-Serres and Mittler, 2006). However, high amount of ROS are found in apical levels of the *Arabidopsis* root hairs, which activates  $\text{Ca}^{2+}$  channel (Berridge, 2004). During plant stress responses, signalling cascades are transmitted mostly by calcium (Ca) molecule which brings the insights of  $\text{Ca}^{2+}$  cation as an important node at which crosstalk between signalling molecules and second messengers pathways occurs (Arimura and Maffei, 2010).

NO and  $\text{Ca}^{2+}$  work simultaneously in plants whereby NO is involved in regulating stomatal opening whereas extracellular  $\text{Ca}^{2+}$  promotes stomatal closure through  $\text{Ca}^{2+}$  oscillations. The extracellular and intracellular  $\text{Ca}^{2+}$  signal is regulated by  $\text{Ca}^{2+}$ -sensing receptors (CAS) through an

action of NO during salt stress or multiple stress response. NO elongates intracellular  $\text{Ca}^{2+}$  oscillations and increases the generation of ROS and salicylic acid (SA). NO generation is also increased which promotes programmed cell death (PCD) that prevent pathogen attacks to plants as shown similarly in figure 1.5 (Gaupels et al., 2011).

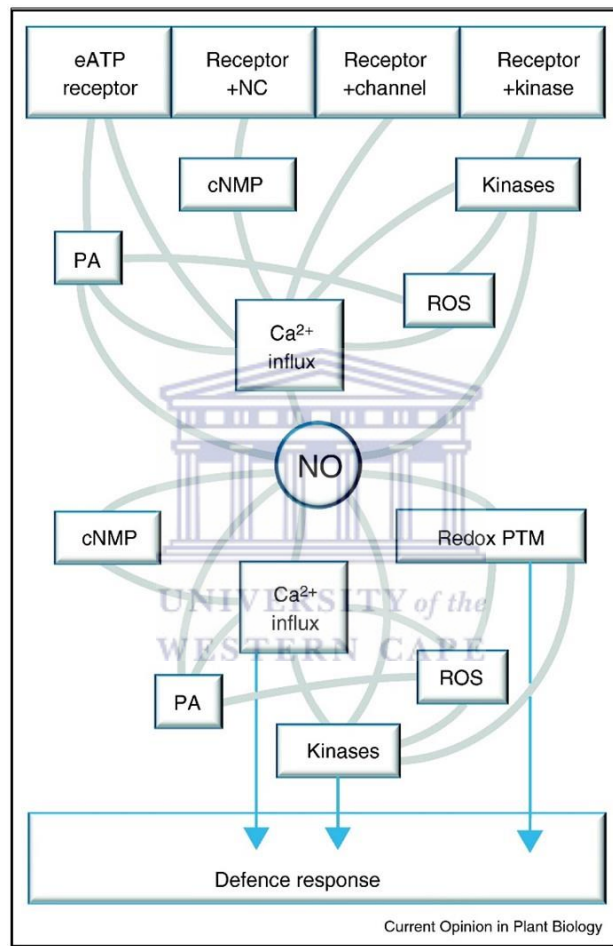


**Figure 1.5: Map showing crosstalk of NO with second messengers in plants defence responses against pathogen attack.** NO in plants is stimulated during any stress conditions, when plants are attacked by pathogens NO-dependent cAMP is induced through calcium influx in which an awareness of a pathogen present triggers the cNMP production by the nucleotide cyclase domain of the receptor. Therefore, cNMPs stimulate a CNGC2-mediated calcium which is in transit of the response pathway by producing a calcium-dependent NO and ROS and induce defence of the gene expression against pathogen attack (Adapted from Gaupels et al., 2011).



## 1.4 Carbon Monoxide (CO)

### 1.4.1 CO production

Carbon monoxide (CO) is defined as a very low molecular weight diatomic trace gas which is significant in the troposphere as a vital regulator for both animal and plant cells. CO has been long considered as a poisonous gas, since it is mainly generated by an incomplete combustion of organic materials in the atmosphere, as a significant element of tobacco smoke and vehicle exhaust fumes as shown in figure 1.6.

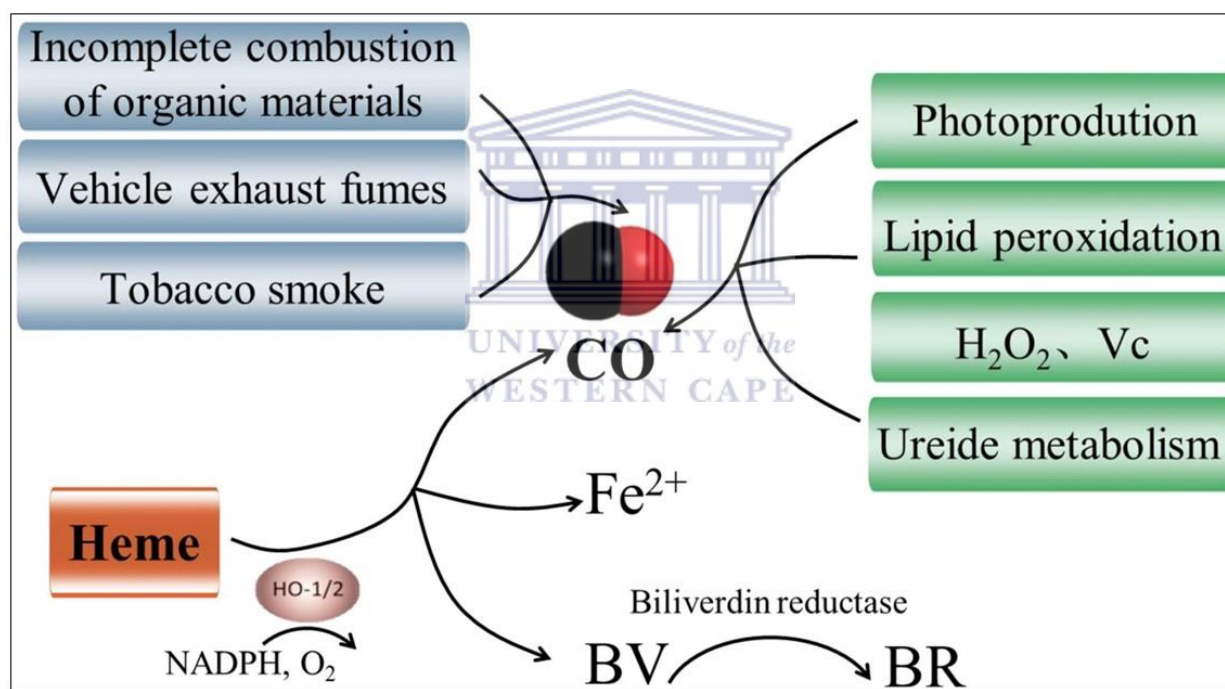


**Figure 1.6: Schematic representation of CO production from different routes in the environment, animals and plants.** CO gas (black and red) is produced from the heme in animals and plants which is considered the main source of production (Bilban et al., 2008). Therefore, in the atmosphere if there is an incomplete combustion of an organic material, pollution of air by smoke from tobacco and motor vehicle exhaust forms CO. Other non-heme sources which include photo-production taking place in the leaves (Schade et al., 1999), lipid peroxidation occurring in the roots, hydrogen peroxide (H<sub>2</sub>O<sub>2</sub>), ascorbic acid (AA) (Dulak and Józkwicz, 2003) and ureide metabolism have also been recently suggested to generate CO in plants (Zilli et al., 2014; Adapted from Wang and Liao, 2016).

Carbon monoxide is also considered toxic when is exposed to humans and animals at high concentrations, although at low concentrations it relaxes smooth muscles and lowers the blood pressure (Heinemann et al., 2014). Recent investigations indicated that CO is also produced through the activity of heme oxygenase (HO) in animals. Following that, the biosynthesis and photo-production of CO in living plants was demonstrated by identifying a plastid *Arabidopsis thaliana* heme oxygenase 1 (*AtHO1*) recombinant protein, which was able to catalyse the formation of CO from heme molecules *in vitro*. It has been reported that HOs are the main enzymatic source of CO in plants (Xuan et al., 2008), but investigations by Zilli et al (2014) are contrary to the above statement.

#### *1.4.2 Role of CO in plants as a signalling molecule*

High levels of exogenous CO are toxic in animals and plants, because uncontrolled CO is detrimental to normal cell function. Therefore, it is important to control CO levels to an adequate level since it plays an important role as an active signalling mediator in many physiological processes. In animals, CO plays a vital role in controlling important physiological processes that take part in neurotransmission (Boehning et al., 2003), vasodilation (Motterlini, 2007), and platelet aggregation (Brüne and Ullrich, 1987). CO gives plants a good advantage as it stimulates growth and development under normal or stress conditions by promoting seed germination, root development and regulating stomatal closure (Wang and Liao, 2016).

CO uses catalytically dose-dependent CO donors known as heme aqueous and CO aqueous which also promotes physiological processes such as seed germination and regulation of plant root development (Liu et al., 2007). Based on these findings CO perform its roles in a similar manner as the growth hormone auxin and signalling molecule NO, and this was evidently demonstrated by the ability of exogenous CO to promote root elongation in wheat seedlings (Xuan et al., 2007).



Additionally exogenous CO also up-regulated NO production by stimulating adventitious root formation in seedlings without auxin (Xuan et al., 2012).

CO plays several roles as a signalling molecule required for inflammatory responses of plants against abiotic stresses such as salinity, drought, heavy metals and ultraviolet radiation. One of the important roles of signalling molecules is to stimulate plant responses to drought stress through controlling the opening and closing the stomata (Cao et al., 2007). Under drought stress it was clearly demonstrated that abscisic acid (ABA), a hormone that is responsible for regulating stomatal movement increased the levels of CO in *Triticum aestivum* (Grondin et al., 2015). These findings have demonstrated that CO influences stomatal closure in a comparable manner to NO (Cao et al., 2007) and H<sub>2</sub>O<sub>2</sub> (She and Song, 2008; Song et al., 2008), whereby *vicia faba* leaves were treated with ABA which increased the HO activity. Carbon monoxide has a similar interaction with NO as a signalling molecule in response to external environmental stresses in plants, however the biological roles of CO signal transduction in plants remain unknown (Wang and Liao, 2016).

## 1.5 Calcium Ion ( $\text{Ca}^{2+}$ )

### 1.5.1 $\text{Ca}^{2+}$ as a signalling molecule

Calcium (Ca) is a chemical element with an atomic number 20 which is the third most abundant metal in nature and has a positive charge of 2, making it an ion. Calcium is an essential element needed by living organisms in large quantities and it can also be used in steel making since it has strong chemical affinity for oxygen ( $\text{O}_2$ ) and sulphur (S). Calcium ion ( $\text{Ca}^{2+}$ ) is an important signalling molecule, which is involved in many different signalling transduction pathways (Tuteja and Mahajan, 2007), because all living organisms need it for growth, development and responses to abiotic and biotic stresses (Dodd et al., 2010). In the kingdom plantae,  $\text{Ca}^{2+}$  often form links between cells and is it also a requirement for maintaining the stringency of the whole plant (Ranty et al., 2006). The vacuoles, endoplasmic reticulum (ER), mitochondria and cell wall are responsible for regulating the concentration of  $\text{Ca}^{2+}$ . Calcium ion concentration in the cell wall and vacuoles is measured in millimolar (mM) units and it can be released at any time when is required by the cell (Tuteja and Mahajan, 2007).

### 1.5.2 Regulation of $\text{Ca}^{2+}$

Calcium ion is an intracellular second messenger in plants and an increase in the cytosolic concentration of  $\text{Ca}^{2+}$  ( $[\text{Ca}^{2+}]_{\text{cyt}}$ ) pair a diverse array of signals and responses. In the resting state, the  $\text{Ca}^{2+}$  signalling system comprises of a receptor and a component that is responsible for  $[\text{Ca}^{2+}]_{\text{cyt}}$  regulation. Hetherington and Brownlee (2004) suggested that the  $\text{Ca}^{2+}$  signalling system is very complicated, because it was previously reported that plant  $\text{Ca}^{2+}$  elevations mainly act as switches during the signalling process rather than just converting specific information. Since the cell has several mechanisms for generating an increase in  $[\text{Ca}^{2+}]_{\text{cyt}}$ , therefore it requires highly complex

patterns of regulating it. There are many proteins which respond to any changes in the  $[Ca^{2+}]_{\text{cyt}}$  and these include calmodulin (CaM),  $Ca^{2+}$ -dependent protein kinases and CaM-binding proteins. Therefore, the involvement of many other intracellular messengers and signalling proteins in the regulation of  $Ca^{2+}$  signalling lead to complicated pathway (Hetherington and Brownlee, 2004), which might be beneficial for plant survival under stress conditions.

Calcium ion has been studied well as a second messenger, and any increase in its cellular levels, triggers  $Ca^{2+}$  sensors or  $Ca^{2+}$ -binding proteins, resulting in the activation of protein kinases (Mahajan and Tuteja, 2005). The activated protein kinases are responsible for phosphorylating various proteins, which regulate  $Ca^{2+}$  level. Transcription factors regulate expression level of these regulatory proteins by changing their metabolism and phenotypic response thus stimulating a better stress tolerance. The phenotypic response of the elevated  $Ca^{2+}$  level depends on the kind of stimuli which has been perceived in order to know the kind of genes that should be up or down-regulated and which ones can lead to the inhibition of growth or cell death. However, if  $Ca^{2+}$  levels are high above the physiological levels, they result in the accumulation of toxic cations such as aluminum ion ( $Al^{3+}$ ) and sodium ion ( $Na^{+}$ ) from the soil. So it is important for  $Ca^{2+}$  levels to be regulated, which is taken care of by the presence of none toxic cations such as potassium ion ( $K^{+}$ ) and magnesium ion ( $Mg^{2+}$ ). Additionally, calcium regulation is also important since its deficiency can cause inhibition of plant root development and undesired leaf forms (Tuteja and Mahajan, 2007).

### *1.5.3 Interaction of $Ca^{2+}$ with other second molecules*

The most commonly known  $Ca^{2+}$  sensor is calmodulin (CaM), which is highly conserved and widely distributed in all members of the fungi, protozoa, animal and plant kingdom. CaM contains two unique structures in the globular domains, each globular structure contains a pair of EF-hand

motifs which is joined together by a central helix and a type of a target protein site as shown in figure 1.7. Upon  $\text{Ca}^{2+}$  binding to the CaM domains there are certain openings which are observed between the  $\alpha$ -helices which displays a complementary binding site for CaM to interact with other various target proteins. Therefore, the target enzymes are recognised easily when the terminal helix has been untwisted by the effector protein, which interacts with both the C and N terminal domains (Haeseleer et al., 2002).

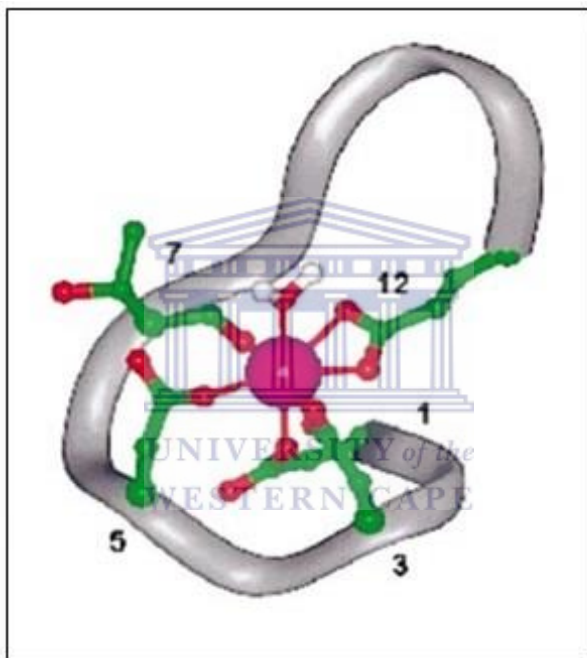


**Figure 1.7:** A ribbon representation of the typical EF-hand motif of  $\text{Ca}^{2+}$ -binding proteins.  $\text{Ca}^{2+}$  (Pink) is bound to six oxygen atoms (red) of the EF-hand which is involved in the direction of the  $\text{Ca}^{2+}$ . The carbonyl oxygen atoms (1, 3 and 5) arrange straight direction and carbonyl oxygen atoms (7 and 12) arrange indirect direction through  $\text{Ca}^{2+}$  backbone (Adapted from Haeseleer et al., 2002).

The interaction of the  $\text{Ca}^{2+}$  with other second messengers is through the coordination of two oxygen atoms of amino acids side chains such as glutamic acid and aspartic acid. The natural chemical structure of the  $\text{Ca}^{2+}$  is regarded as the largest of the  $2+$  ions group and it allows maximum interaction with other second messengers and other divalent metal ions. Since  $\text{Ca}^{2+}$  is regarded as the largest  $2+$  ions group, it incorporates a large number of unique sequences in the

EF-hand motif. The structure of the loop is strengthened by two specifically oriented helices on the ends of the EF-hand motif that differs from the  $\beta$ -strand domain which is known as the C2 domains. However at the C2 domains, the loops are fixed together by the  $\beta$ -strand structure and  $\text{Ca}^{2+}$  is further stabilised by phospholipids. Furthermore, it is believed that  $\text{Ca}^{2+}$ -binding proteins are closely related to the CaM superfamily which is known as the guanylate cyclase-activating proteins (GCAPs). These GCAPs are mostly involved in the regulation of photoreceptor guanylate cyclase (GC) and CaM is responsible for activating the cell through cellular responses as an effect of high  $[\text{Ca}^{2+}]$  elevation (Haeseleer et al., 2002).

#### *1.5.4 Role of $\text{Ca}^{2+}$ in response to plant stress*

It has been long studied that  $\text{Ca}^{2+}$  plays an important role as a nutrient component in animals and plants and as a main ion in maintaining the structural rigidity of the cell wall and membrane (Ranty et al., 2006). The role of  $\text{Ca}^{2+}$  as a significant messenger in stimulating plant responses to various abiotic and biotic stress signals is well documented (Hepler, 2005). Previous evidence from Clapharm (1995) shows that  $\text{Ca}^{2+}$  is used by animals and plants as a second messenger more than any other studied and discovered second messengers, since nearly all stimulated signals including developmental, hormonal and stress have an effect on the cellular  $\text{Ca}^{2+}$  (Berridge, 2004). In plants, calcium is needed for growth and development of the meristematic root and shoot tip which divides by mitosis. Thus, in the anaphase stage  $\text{Ca}^{2+}$  participate in the formation of microtubules which are important for the movement of chromosomes.  $\text{Ca}^{2+}$  is also required for pollen tube growth and elongation where it strengthen the cell wall and membrane by accumulating large amounts of calcium pectate which binds the cells together. Since  $\text{Ca}^{2+}$  act as a divalent cation in the cell wall and membrane, it is required as a counter ion for inorganic and organic anions in other cellular organelles such as vacuoles and cytosol.  $\text{Ca}^{2+}$  also minimises the damage which is caused by high

salt content and therefore reduces salinity stress (Tuteja and Mahajan, 2007). It does this by activating the salt overlay sensitive signalling pathway, which result in well maintained ion homeostasis. Calcium ion maintains ion homeostasis in the cytoplasm salt overly sensitive (*SOS*) stress signalling pathway by activating a salt stress signalling *SOS2*, as an amino acid coupled kinase of serine/threonine (Liu and Zhu, 1998). The *SOS* signalling pathway consist of three *SOS* important proteins; the *SOS3*, a calcium binding protein which is responsible for sensing any increase in  $[Ca^{2+}]_{cyt}$  (Zhu et al., 1998). Calcium ion binding to *SOS3* is important because, it prepares a good environment for *SOS3* to bind and activate *SOS2*, a serine/threonine protein kinase. Lastly, *SOS1* is a  $Na^+/H^+$  antiporter, which is activated by the *SOS3-SOS2* complex, this results in the extrusion of excess  $Na^+$  from the cytoplasm (Shi et al., 2000).

#### 1.5.5 $Ca^{2+}$ transporters in cellular membranes

There are two different  $Ca^{2+}$  transporters which are required for maintaining a balanced cytosolic  $Ca^{2+}$  concentration ( $[Ca^{2+}]_{cyt}$ ) after a signalling event has occurred: These include the high affinity  $Ca^{2+}$ -ATPases with low transport capacity and the low affinity  $H^+/Ca^{2+}$ -antiporters with high transport capacity for  $Ca^{2+}$  transport (Hirschi et al., 1996). When there is a response against any stress in plants, the  $[Ca^{2+}]_{cyt}$  eventually increases and result in an elevated  $[Ca^{2+}]_{cyt}$  which is caused by the  $Ca^{2+}$  influx into the cytosol. The source of the  $Ca^{2+}$  is not well defined, as to whether is directly from the apoplast or it enters the cytoplasm through the plasma membrane of other cell organelles. When  $Ca^{2+}$  concentration is high in the cytosol, it is rapidly dispersed through a mechanism which opens  $Ca^{2+}$ , before they can be closed. An increase in  $[Ca^{2+}]_{cyt}$  may lead to the production of inositol triphosphate ( $IP_3$ ), which is well known second messenger responsible for transferring chemical signals received by the cell.  $IP_3$  also play a role in rapidly activating a relay of  $Ca^{2+}$  channels (Trewavas, 1999; Drøbak and Watkins, 2000). Since plant tissues are not only

affected by an increased  $[Ca^{2+}]_{cyt}$ , due to repeated increase in  $[Ca^{2+}]_{cyt}$ , cells forms a cellular memory, which helps cells to respond better to any stress without disturbing the normal  $Ca^{2+}$  levels and maintaining cellular  $[Ca^{2+}]_{cyt}$  homeostasis (Tuteja and Mahajan, 2007).



## 1.6 Electrochemistry

Electrochemistry involves any study of chemical processes that could be responsible for the movement of electrons and this movement of electrons is called electricity, which can be generated by movements of electrons from one element to another in an oxidation-reduction (redox) reaction (Marcus, 1964). An electrochemical system is not homogeneous but it is heterogeneous and is constituted by a very large field, which includes electro-analysis, sensors, energy storage devices, energy conversion devices, corrosion, electro-synthesis, and metal electroplating (Dayton et al., 1980). The use of electrochemistry in the study of redox-active biomolecules has become increasingly widespread among chemical and biological scientists within the last three decades. Direct electrochemistry of redox proteins immobilised on different electrodes has recently attracted great attention. These methods have been reported to provide a suitable required model for understanding the electron transfer mechanisms in biological systems and to establish a foundation for the production of electrochemical biosensors and devices (Feng et al., 2005). Recently there have been successful approaches that have included cast films of redox proteins or enzymes with different materials and membranes. Therefore, by achieving a great sensitive and accurate direct electron transfer between redox proteins or enzymes and electrodes simplifies the studies and application of these devices, which has a great significance in preparing the third generation of biosensors (Hong et al., 2013).

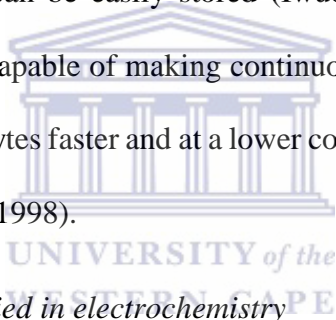
Recent studies of redox active biomolecules such as proteins or enzymes from native chemical sensors have been improved. Since the behaviour of chemical sensors are used in the investigations of biomolecules, therefore biomolecules are immobilised on the electrode surfaces as biosensors. Nowadays these biosensors are implemented in different important sectors such as in health care practices, biotechnology research, industries, environmental monitoring, defence and security.



Scientists take advantage of using enzymes in electrochemistry to create a biosensor, because enzymes display a specific binding due to their catalytic activity in nature for a better bio-recognition and quantification (Ashe et al., 2007).

### *1.6.1 Electrochemical biosensors*

A biosensor is a device, which consists of a biological molecule that is directly interfaced to a sensitive transducer, such as an electrode. This combination measures the response of an analyte or a group of analytes depending on their concentration. It has been stated that the use of suitable biosensors would be a very good advantage since biosensors are generally made in a very small portable size and therefore, they can be easily stored (Iwuoha et al., 1998). Furthermore, the authors added that biosensors are capable of making continuous measurements as they are easily reusable and they can measure analytes faster and at a lower cost than complicated time-consuming traditional methods (Iwuoha et al., 1998).



### *1.6.2 Voltammetry techniques applied in electrochemistry*

Voltammetry is a technique used to investigate the electrolysis mechanisms of different molecules by using analytical methods to measure and quantify electron movements in a redox reaction. Voltammetry techniques measure current taking into consideration applied time, under conditions that favour polarization in an electrochemical cell. There is a wide variety of voltammetric techniques, namely; potential step voltammetry (PSV), linear sweep voltammetry (LSV), hydrodynamic voltammetry (HV), cyclic voltammetry (CV), and square-wave voltammetry (SWV). Voltammetric techniques differ in their application because they use different unique waveforms. These waveforms are acquired in an electrochemical cell in a process whereby a

voltage or series of voltages are applied to the electrode and the corresponding current that flows is monitored as a redox reaction (Andrienko, 2008).

#### *1.6.2.1 Cyclic voltammetry (CV)*

Cyclic voltammetry (CV) is one of the technique that utilises potentiodynamic electrochemical measurements and that makes it the most widely used technique, because it acquires qualitative information about complex elements, compounds and molecules through electrochemical reactions. CV was used to study the biosynthetic reaction pathways in which they showed to generate free radicals electrochemically (Mabbott, 1983). Since then there have been several studies that have been reported about an increasing number of inorganic chemist whereby they applied CV to investigate the properties of ligands on the redox potential upon binding. In addition, they further assessed the complexity of the metal ion and other multinuclear clusters of ligands. Therefore, the overall studies opened doors for different approaches such as in solar energy conversion and in model studies of enzymatic catalysis (Mabbott, 1983).

The operating process of CV is a potential-controlled reversible experiment in a circular direction, whereby the initial electric potential is scanned before turning to the reverse direction after reaching the final potential and then it scans back to the initial potential. CV technique is considered as a very important analytical characterisation in the field of electrochemistry, because various processes that include electron transfer can be studied from the investigation of catalytic reactions, analysing of complex compounds by stoichiometry and determination of the photovoltaic materials band gap. The other advantage of CV is that it offers a rapid location of redox potentials of the electroactive species that is being investigated.

### 1.6.3 The electrochemistry of heme binding proteins

Proteins can naturally bind to target molecules with a high binding affinity in a selective sensitive manner, they can be used as sensing biomolecules in electrochemistry due to their natural binding and sensing property (Das et al., 2006). Therefore, there is no need to add any reagents to facilitate the naturally occurring binding property of proteins in which mostly they bind through ligand-substrate mechanism. Molecular and electrochemical studies reported that heme proteins can perform a variety of electrochemical functions because the heme co-factor is often used as an electron transport that facilitate redox chemistry, for example it can function in the detoxification processes (Fufezan et al., 2008).

### 1.7 Research hypothesis

In order to determine the binding affinity of the *At*NOGC1 protein bioelectrode to stress signalling molecules; NO, CO and Ca<sup>2+</sup>, the following hypothesis was proposed: Different signalling molecules for responsive against abiotic and biotic stresses in plant will bind to the *Arabidopsis* plant protein, *At*NOGC1 for conferring stress tolerant in plants.

### 1.8 Aim of the study

The *At*NOGC1 was successfully characterised as a novel *Arabidopsis thaliana* signalling protein, which is made up of the H-NOX and the GC motif, that are responsible for sensing NO/O<sub>2</sub> and the synthesis of cGMP. NO is an important signalling molecule in plants since it is involved in many signalling responses when plants are under abiotic and biotic stresses. However, other signalling molecules and second messengers such as CO and Ca<sup>2+</sup> have also been reported to be involved in similar signalling responses as NO. In order to generate stress tolerant crops, signalling pathways that involves novel proteins need to be understood. In this study, molecular biology techniques

were used to express and purify *At*NOGC1, followed by characterising its ability to bind different signalling molecules including NO, CO and Ca<sup>2+</sup> by using electrochemical techniques. The aim of this study was to determine the binding affinities of *At*NOGC1 to these signalling molecules NO, CO and Ca<sup>2+</sup>, and this was achieved by the following objectives:

- i. To recombinantly express and purify *At*NOGC1 protein by affinity chromatography.
- ii. To prepare a biosensor, using the recombinant *At*NOGC1.
- iii. To determine the bioelectrode binding of *At*NOGC1 protein based biosensor to NO, CO and Ca<sup>2+</sup> using cyclic voltammetry.



## Chapter 2: Materials and Methods

### 2.1 Stock solutions, buffers and reagents

All buffers and solutions were prepared at the University of the Western Cape at the life sciences building (Molecular Sciences and Biochemistry Laboratory) and chemical sciences building (SensorLab). All the chemicals, reagents and instruments used in this study were purchased from Merck-Sigma Aldrich, ThermoScientific, Fermentas, BioRAD, Inqaba Biotech, BMG Labtech unless otherwise stated in the main text.

**2x SDS sample buffer:** 4 % SDS, 0.125 M Tris pH 6.8, 15 % glycerol and 1 mg/mL Bromophenol Blue. Stored at  $-20^{\circ}\text{C}$ . 0.2 M DTT was added to the buffer immediately prior to use.

**APS (Ammonium persulphate):** 10 % APS stock solution was prepared by dissolving 100 mg in 1 mL distilled water ( $\text{dH}_2\text{O}$ ) and stored at  $-20^{\circ}\text{C}$ .

**BSA (Bovine serum albumin):** 2 mg/mL BSA stock solution was prepared by dissolving 2 mg BSA into 2 mL  $\text{dH}_2\text{O}$ . The solution was stored at  $4^{\circ}\text{C}$  wrapped in aluminum foil.

**$\text{Ca}^{2+}$  (Calcium ion):** 1 mM  $\text{Ca}^{2+}$  stock solution was prepared by dissolving 1.11 mg calcium chloride ( $\text{CaCl}_2$ ) into 10 mL  $\text{dH}_2\text{O}$  and stored at room temperature.

**Coomassie staining solution:** 250 mg Coomassie Brilliant Blue R-250 dye, 45 % methanol and 10 % acetic acid.

**DDAB (Didodecyldimethylammonium bromide):** 10 mM DDAB stock solution was prepared by dissolving 4.63 mg DDAB into 1 mL  $\text{dH}_2\text{O}$ . The solution was sonicated for 8 hours and stored at  $4^{\circ}\text{C}$ .

**Destaining solution:** 40 % methanol and 10 % glacial acetic acid, was added to dH<sub>2</sub>O to a final volume of 1000 mL.

**DTT (DL-dithiothreitol):** 1 M DTT stock solution was prepared by dissolving 1.5 g DTT into 10 mL dH<sub>2</sub>O. The solution was stored at -20 °C as 1 mL aliquots (wrapped in aluminum foil).

**Glucose:** 20 % glucose stock solution was prepared by dissolving 2 g glucose (D + glucose, #200114) into 10 mL dH<sub>2</sub>O, the solution was filter sterilised and stored at -20 °C.

**Glutaraldehyde:** 2.5 % glutaraldehyde working solution was prepared by diluting 50 % glutaraldehyde in 1 mL dH<sub>2</sub>O and the solution was stored at 4 °C.

**HNO<sub>3</sub> (Nitric acid):** 5 M HNO<sub>3</sub> working solution was prepared by diluting 70 % HNO<sub>3</sub> into 10 mL dH<sub>2</sub>O.

**Imidazole:** 1 M imidazole stock solution was prepared by dissolving 17.02 g imidazole into 250 mL dH<sub>2</sub>O and stored at room temperature covered with aluminum foil.

**IPTG (Isopropyl-1-thio-D-galactoside):** 0.1 M IPTG stock solution was prepared by dissolving 1.19 g IPTG into 10 mL dH<sub>2</sub>O. The solution was filter sterilised and stored at -20 °C as 1 mL aliquots.

**Kanamycin:** 50 mg/mL kanamycin stock solution was prepared by dissolving 0.5 g kanamycin into 10 mL dH<sub>2</sub>O, filter sterilised and stored at -20 °C as 1 mL aliquots.

**Luria Agar:** 10 g peptone, 5 g yeast extract, 5 g NaCl, and 12 g agar, was made up to 1000 mL with dH<sub>2</sub>O and autoclaved.

**Luria Broth:** 10 g peptone, 5 g yeast extract and 5 g NaCl, was made up to 1000 mL with dH<sub>2</sub>O and autoclaved.

**Lysis Buffer:** 0.001 M PMSF, 100 µg/mL lysozyme, 1x DNase I reaction buffer, 0.5 U/µL DNase I, RNase free, 0.1 % Triton X-100, 0.001 M DTT and 1x protease inhibitor cocktail and was made up to 10 mL with 0.1 M Sodium Phosphate Buffer Solution (0.05 M Na Phosphate buffer, 0.3 M NaCl and 0.04 M imidazole; pH 8.0).

**Lysozyme:** 100 mg/mL lysozyme stock solution was prepared by dissolving 10 g lysozyme into 10 mL dH<sub>2</sub>O and stored at -20 °C as 1 mL aliquots.

**NaCl (Sodium Chloride):** 2 M NaCl stock solution was prepared by dissolving 29.2 g NaCl into 250 mL dH<sub>2</sub>O and stored at room temperature.

**NaH<sub>2</sub>PO<sub>4</sub> (mono-basic):** 0.2 M NaH<sub>2</sub>PO<sub>4</sub> stock solution was prepared by dissolving 0.24 g NaH<sub>2</sub>PO<sub>4</sub> into 10 mL dH<sub>2</sub>O and stored at room temperature.

**Na<sub>2</sub>HPO<sub>4</sub> (di-basic):** 0.2 M Na<sub>2</sub>HPO<sub>4</sub> stock solution was prepared by dissolving 2.84 g Na<sub>2</sub>HPO<sub>4</sub> into 100 mL dH<sub>2</sub>O and stored at room temperature.

**Na (sodium) Phosphate buffer:** 0.1 M Na Phosphate buffer stock solution was prepared from mixing 0.2 M NaH<sub>2</sub>PO<sub>4</sub> and 0.2 M Na<sub>2</sub>HPO<sub>4</sub> with dH<sub>2</sub>O to a final volume of 200 mL.

**NaOH (Sodium hydroxide):** 5 M NaOH working solution was prepared by dissolving 100 mg NaOH into 10 mL dH<sub>2</sub>O.

**PMSF (Phenylmethylsulfonyl fluoride):** 0.1 M PMSF stock solution was prepared by dissolving 0.17 g PMSF into pure 10 mL isopropanol and stored at -20 °C as 1 mL aliquots.

**SDS (Sodium dodecyl sulfate):** 10 % SDS stock solution was prepared by dissolving 10 g SDS into 100 mL dH<sub>2</sub>O and stored at room temperature.

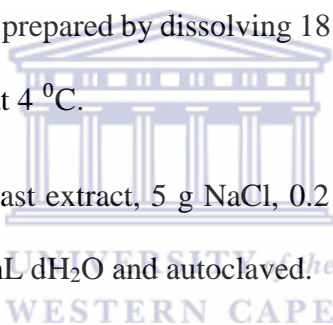
**TFB1 (Transfer Buffer 1):** 0.03 M potassium acetate, 0.05 M manganese chloride, 0.1 M potassium chloride, 0.01 M calcium chloride and 15 % glycerol was made up with 250 mL dH<sub>2</sub>O and stored at 4 °C.

**TFB2 (Transfer Buffer 2):** 0.009 M sodium 3-(*N*-morpholino) propanesulfonic acid (MOPS), 0.1 M potassium chloride, 0.05 M calcium chloride and 15 % glycerol was made up with 250 mL dH<sub>2</sub>O and stored at 4 °C.

**Tris:** 1.5 M Tris stock solution was prepared by dissolving 181.65 g Tris into 1000 mL dH<sub>2</sub>O. The pH was adjusted to 8.8 and stored at room temperature.

**Tris:** 0.5 M Tris stock solution was prepared by dissolving 181.65 g Tris into 1000 mL dH<sub>2</sub>O. The pH was adjusted to 6.8 and stored at 4 °C.

**TYM Broth:** 10 g peptone, 5 g yeast extract, 5 g NaCl, 0.2 % glucose and 0.01 M magnesium chloride, was made up with 1000 mL dH<sub>2</sub>O and autoclaved.





## 2.2 Molecular Biology: Preparation of the recombinant *At*NOGC1 protein

### 2.2.1 Preparation of competent *E.coli* cells for transformation

All glassware's were washed with 10 % bleach and rinsed with distilled water (dH<sub>2</sub>O), followed by washing with 10 % sodium hydroxide (NaOH) aqueous solution and autoclaved at 125 °C for 20 minutes. About 50 µL glycerol stock of the competent cells were inoculated into 10 mL TYM broth and incubated at 37 °C with shaking at 150 rpm overnight. The following day, 3 mL of cells were scaled up to 100 mL with TYM broth and allowed to grow at 37 °C with shaking at 150 rpm until the optical density (OD)<sub>550 nm</sub> reached 0.2. The cell culture was scaled up to 400 mL with TYM broth under the same conditions until OD<sub>550 nm</sub> reached 0.5. Therefore, cells were chilled on ice and centrifuged at 4 300 rcf for 10 minutes. The supernatant was discarded and cells were re-suspended in 50 mL transfer buffer 1 (TFB1) and allowed to incubate on ice for 30 minutes. Cells were recovered by centrifugation at 4 300 rcf for 10 minutes and the supernatant was discarded followed by re-suspending the pellet with 30 mL transfer buffer 2 (TFB2). Cells were frozen with liquid nitrogen as aliquots of 100 µL and stored at -80 °C.

### 2.2.2 Transformation of the recombinant *pET SUMO-At*NOGC1 plasmid into *E.coli* competent cells

The *pET SUMO-At*NOGC1 plasmid was received from Dr T. Mulaudzi-Masuku (Molecular Sciences and Biochemistry Laboratory; Department of Biotechnology, University of the Western Cape). The *E.coli* competent cells and autoclaved 1.5 mL eppendorf tubes were chilled on ice. About 100 ng/µL of the *pET SUMO-At*NOGC1 plasmid was added into 50 µL of competent cells and mixed by gentle tapping. Cells were incubated on ice for 30 minutes, followed by heat shocking at 42 °C for 45 seconds and then incubated on ice for 2 minutes. Pre-warmed 450 µL LB

was added to the cells and incubated at 37 °C with shaking at 150 rpm for 1 hour. About 100 µL of the cell culture was plated on LB agar plates containing 50 µg/mL kanamycin and incubated at 37 °C overnight (~16 hours). The XL-GOLD strain was used for propagation and the BL-21 CodonPlus strain was used for expression.

### *2.2.3 Plasmid DNA isolation*

Small scale plasmid DNA isolation was performed using the alkaline method (Birnboim and Doly, 1979). A single colony from the XL-GOLD plate was inoculated into 10 mL LB which contained 50 µg/mL kanamycin and incubated at 37 °C with shaking at 150 rpm overnight. From the overnight culture 900 µL was mixed with 100 µL of 100 % glycerol and stored at -80 °C. The remaining 5 mL culture was centrifuged at 4 300 ref for 10 minutes and the supernatant was discarded. The plasmid DNA isolation was performed according to the manufacturer's instructions using the GeneJET plasmid Miniprep kit (Fermentas, Cat# K0503, EU). The concentration of the pET SUMO-AtNOGC1 plasmid was determined using the nanodrop 2000 spectrophotometer (Thermo Scientific, USA).

### *2.2.4 Expression of the recombinant protein*

A single colony from the BL-21 CodonPlus plate was inoculated into 5 mL LB containing 50 µg/mL kanamycin and 0.2 % glucose, the culture was incubated at 37 °C with shaking at 150 rpm. After 7 hours the culture was scaled up to 150 mL with LB containing the same concentration of kanamycin and glucose, followed by incubation at 37 °C with shaking at 150 rpm overnight. The following morning, the overnight culture was scaled up to 1 500 mL with LB containing the same concentration of kanamycin and glucose, the large scale culture was incubated at 37 °C with shaking until the OD<sub>600 nm</sub> reached 0.5. From the same culture, about 10 mL was removed as an

un-induced culture and the remaining culture was induced by the addition of Isopropyl-1-thio-D-galactoside (IPTG) to a final concentration of 2 mM. The expression was induced at 30 °C with shaking for 2.5 hours. Both the induced and un-induced cultures were centrifuged at 4 300 rcf for 10 minutes at 4 °C, and the pellet was stored at -20 °C until further use.

#### *2.2.5 Preparation of the cleared lysate under native conditions*

The pellet was thawed on ice and re-suspended with 5 mL of the lysis buffer followed by incubation on ice with shaking at 100 rpm for 1 hour. The lysed solution was sonicated for 4 minutes (30 seconds on and 30 seconds off rotational) followed by centrifugation at 4 300 rcf for 30 minutes. The lysate was collected and stored at 4 °C.

#### *2.2.6 Purification of the 6xHis-tagged recombinant protein by affinity chromatography*

Purification of the 6xHis SUMO-A $\alpha$ NOGCl protein was performed under native conditions by the use of affinity chromatography. The column matrix comprised of Ni-NTA system with 50 % of His-Nickel select beads which is an immobilised metal-affinity chromatography (IMAC). A volume of 5 mL of the column resin was prepared and washed with 5 column volume (CV) of dH<sub>2</sub>O. The column was equilibrated by adding 5 CV of the binding buffer (0.05 M Na Phosphate buffer, 0.3 M NaCl and 0.04 M imidazole; pH 8.0), followed by the addition of 6 mL lysate and the column was allowed to incubate for few minutes before collecting the flow through. The column was washed with 2 CV of wash buffer 1-4 (wash 1: 0.05 M Na Phosphate buffer and 0.3 M NaCl; wash 2: 0.05 M Na Phosphate buffer, 0.3 M NaCl, 0.005 M imidazole; wash 3: 0.05 M Na Phosphate buffer, 0.3 M NaCl, 0.02 M imidazole; wash 4: 0.05 M Na Phosphate buffer, 0.3 M NaCl, 0.04 M imidazole; pH 8.0) and the flow through was collected. The protein was eluted by 2 CV of elution buffer (0.05 M Na Phosphate buffer, 0.3 M NaCl, 0.25 M imidazole; pH 8.0) and

the eluate was collected. The column matrix was washed with 2 CV of 2 M NaCl and was stored in 10 mL of 20 % Ethanol at 4 °C. Samples collected for each step were stored at 4 °C.

**Table 2.1: Preparation of 12 % SDS-PAGE for analysing recombinant proteins**

Components	12 % Separating gel	5 % Stacking gel
30 % acrylamide	2.4 mL	0.7 mL
1.5 M Tris (pH 8.8)	2 mL	0 mL
0.5 M Tris (pH 6.8)	0 mL	1.5 mL
10 % SDS	0.08 mL	0.05 mL
10 % APS	0.08 mL	0.05 mL
dH <sub>2</sub> O	3.4 mL	2.9 mL
Tetramethylethylenediamine (TEMED)	0.008 mL	0.005 mL

### 2.2.7 Set up of the gel plates

The surface of the gel plates were cleaned with 70 % ethanol and wiped with paper towel. The glass plates were then assembled and locked into green clips (BioRad Laboratories Inc, USA). Both the 5 % stacking and 12 % separating gels were prepared according to the set up shown in Table 2.1. The separating gel was added by gently pipetting from side to side to fill the plates. Pure isopropanol was added to level the separating gel layer and the gel was allowed to solidify (~30 minutes) at room temperature. When the separating gel had solidified, isopropanol was discarded and the gel plate rinsed with dH<sub>2</sub>O followed by adding the stacking gel. The comb was inserted

gently to avoid bubbles and the gel was allowed to solidify for ~30 minutes at room temperature. The gels were immersed in 1x SDS running buffer.

#### *2.2.8 Running SDS-PAGE*

To run the SDS-PAGE 2x SDS sample buffer and 250 kDa unstained protein marker (Thermo Scientific, Cat# 26614) were thawed on ice. About 15  $\mu$ L of the samples to be analysed on the SDS-PAGE were mixed with 10  $\mu$ L of 2x SDS sample buffer and boiled at 95  $^{\circ}$ C for 5 minutes. About 20  $\mu$ L of the mixture was loaded on adjacent lanes. The dye mixture was electrophoresed at 80 V from the stacking gel and then the voltage was increased to a constant 100 V until the dye reached the bottom of the gel. The gel was stained with the coomassie staining solution overnight and de-stained the following day using destaining solution until the bands were visible.

#### *2.2.9 Determination of the recombinant protein concentration by Bradford assay*

Bovine Serum Albumin (BSA) concentrations ranging from 2.5-25  $\mu$ g/mL were prepared from 2 mg/mL stock solution to act as standards. The 1x dye reagent (Sigma, Cat# SLBP3810V) was removed from 4  $^{\circ}$ C storage and allowed to warm to ambient temperature. The 1x dye reagent was inverted a few times before use. The dilutions for measuring the standards were performed in triplicates, using 0.1 M PBS (0.05 M Na Phosphate buffer, 0.3 M NaCl, 0.25 M imidazole; pH 8.0) as a diluent. Protein solutions were also assayed in triplicate and 2 dilutions of 1:50 and 1:1000 were prepared. A blank sample was prepared with dH<sub>2</sub>O and dye reagent. About 5  $\mu$ L of the samples were pipetted into a separate clean 96 well microplate. A total volume of 250  $\mu$ L 1x dye reagent was added to each microplate well and mixed. The absorbance of the standards and unknown samples were measured at 595 nm using multi-detection spectrophotometer (FLUOstar OPTIMA; BMG LABTECH, Germany, 2010). The calculations of the average triplicate were

performed and the standard curve was plotted from the average absorbance values against the concentrations using Microsoft Excel 2013 software (Microsoft office 2013, Windows 8).

#### *2.2.10 Concentrating the recombinant protein*

For downstream analyses of the recombinantly expressed and purified protein, about 5 mL of the cleared lysate was centrifuged at 4 300 rcf for 6 hours in a 3K molecular weight cutoff (MWCO) ultrafiltration centrifugal tube (Amicor<sup>®</sup> ultra centrifugal filters, Cat# UFC200324). The concentrated protein sample was collected and stored at 4 °C.



## **2.3 Electrochemical preparation of *At*NOGC1 protein bioelectrode as a biosensor for binding NO, CO and Ca<sup>2+</sup>**

### **2.3.1 Cleaning the glassy carbon electrode (GCE)**

The glassy carbon electrode (GCE) (Bioanalytical System Inc., USA) with an area of 0.071 cm<sup>2</sup> was polished using different concentrations of micro-polish alumina (Buehler, USA) powder slurry from 1.0 μM for 5 minutes, 0.5 μM for 15 minutes and 0.03 μM for 20 minutes then rinsed with dH<sub>2</sub>O. The previously polished GCE was sonicated in 95 % absolute ethanol and dH<sub>2</sub>O for 10 minutes followed by drying out with argon gas.

### **2.3.2 Immobilising the recombinant *At*NOGC1 on the GCE surface**

The previously purified and concentrated *At*NOGC1 protein was immobilised on the GCE surface using the method described by Iwuoha et al., (1998). About 4.63 mg of Didodecyldimethylammonium bromide (DDAB) was dissolved into 1 mL of dH<sub>2</sub>O and the solution was sonicated for 8 hours. Then 10 μL of the sonicated DDAB solution was mixed with 2 mg BSA to make solution A. An *At*NOGC1 (3.1 mg/mL) dilution of 1:100 was made and 10 μL of *At*NOGC1 (0.01 mg/mL) was mixed with 10 μL of solution A to make solution B. Solution C was prepared by mixing 5 μL of 2.5 % glutaraldehyde with 10 μL of solution B. Then 5 μL of solution C was drop coated on the GCE surface and the immobilised DDAB/BSA-*At*NOGC1/GCE was stored at 4 °C overnight before it was used.

### **2.3.3 Electrochemical cell set up**

Three electrochemical cell system was used; the working electrode (GCE), counter electrode (platinum wire) and the reference electrode (Ag/AgCl). The BASi Epsilon system (Bioanalytical

System Inc., USA) was used to conduct the electrochemical experiments at room temperature. Ag/AgCl was stored in 3 M NaCl and the bare GCE with immobilised DDAB/BSA-AtNOGC1/GCE was rinsed with dH<sub>2</sub>O before use. The platinum wire was first rinsed with acetone and then rinsed with dH<sub>2</sub>O before use. Different conducting wires from the BASi epsilon system were connected to different electrodes (red wire was connected to the counter electrode, black wire connected to the working electrode and the white wire was connected to the reference electrode). The electrochemical cell was filled with 10 mL of Phosphate buffer saline (PBS) of pH 8.0. The argon gas was used to remove excess O<sub>2</sub> from the solution by purging for more than 30 minutes and the argon blanket was kept on a surface to stabilise an anaerobic conditions.

## 2.3.4 Preparation of analytes

### 2.3.4.1 Production of NO gas



The NO gas was produced in the laboratory according to the method of Mori and Bertotti (2000). The reaction was achieved by adding droplets of 5 M nitric acid (HNO<sub>3</sub>) into 10 g copper (Cu) chips while stirring in the presence of a continuous argon gas. The presence of the argon gas was to avoid the formation of toxic nitric dioxide (NO<sub>2</sub>) gas which produces a brownish smoke and a blue solution. The NO gas was produced by the indication of the green colour solution as shown in figure 2.1 (B) and it was trapped in a 5 M sodium hydroxide (NaOH) solution. The final produced NO gas was collected in a 10 mL PBS (pH 8.0). The reaction was conducted in the fume hood as shown in figure 2.1 (A).



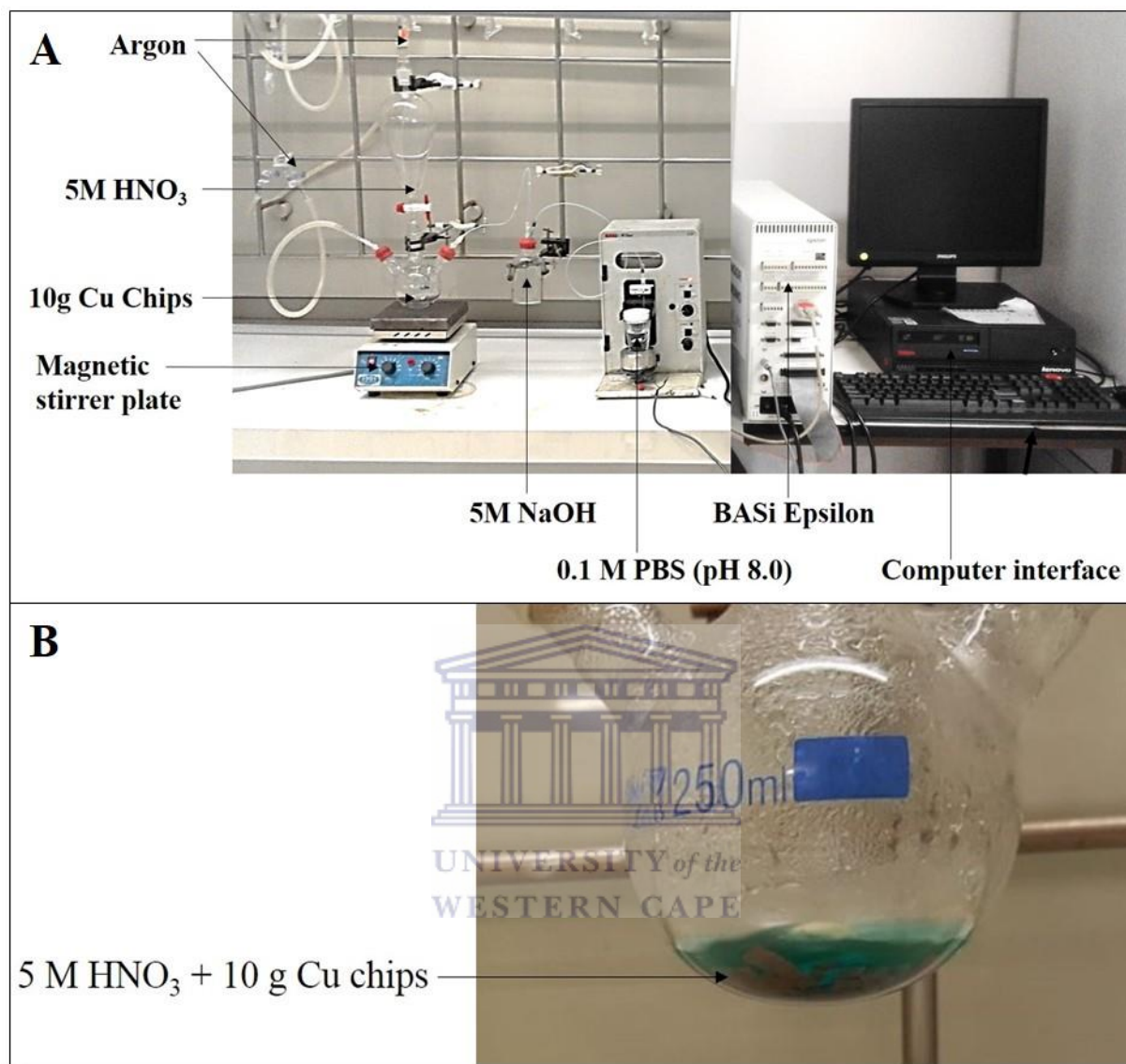
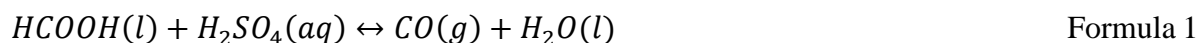


**Figure 2.1: Schematic representation of the apparatus used for the production of NO gas in the fume hood.** (A) NO gas was produced in the fume hood by reacting droplets of 5 M HNO<sub>3</sub> with 10 g Cu chips under a continuous flow of argon gas into the reaction solution. When the solution turned into a green colour, the colourless NO gas was produced and trapped into 5 M NaOH. The NO gas was collected in 10 mL PBS (pH 8.0) of the electrochemical cell connected to the BASi epsilon system which is operated on the computer interface. (B) Reaction of HNO<sub>3</sub> and Cu chips as the green colour solution indicated that NO was produced.

#### 2.3.4.2 Production of CO gas

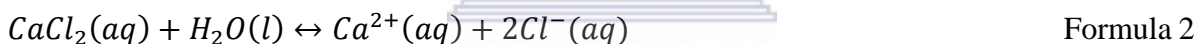
Carbon monoxide (CO) gas was produced in the laboratory, whereby 98 % sulphuric acid (H<sub>2</sub>SO<sub>4</sub>) reacted with 90 % formic acid (HCOOH) and the concentrated H<sub>2</sub>SO<sub>4</sub> dehydrated the HCOOH

producing a colourless CO gas as shown in formula 1. The CO produced was collected in a 10 mL PBS (pH 8.0), the reaction was conducted in the fume hood.



#### 2.3.4.3 Preparation of $\text{Ca}^{2+}$ solution

Stock solution of 1 mM  $\text{Ca}^{2+}$  was prepared by dissolving 1.11 mg calcium chloride ( $\text{CaCl}_2$ ) (molecular weight = 110.98  $\text{g}\cdot\text{mol}^{-1}$ ) into 10 mL  $\text{dH}_2\text{O}$ .  $\text{CaCl}_2$  dissociated into aqueous  $\text{Ca}^{2+}$  and  $\text{Cl}^-$  as shown in formula 2. A further dilution of  $\text{Ca}^{2+}$  concentration from 1 mM to 1  $\mu\text{M}$  stock solution was prepared and several concentrations from 1 nM to 16 nM were used in the electrochemical experiments.



#### 2.3.5 Electrochemical procedure

The BASi Epsilon software was used to run cyclic voltammetry (CV). Parameters used for activating the cell were from +2000 mV to -2000 mV potential window and 2 cycles with a sensitivity of 1 mA at a scan rate of 100 mV/s. For cell stabilisation, the potential window between +150 mV and -800 mV in 10 cycles with a sensitivity of 100  $\mu\text{A}$  at a scan rate of 100 mV/s was used. The potential window for running all the CV experiments was between +150 mV and -800 mV in 2 cycles with a sensitivity of 10 nA at a scan rate of 2 mV/s. For anaerobic conditions the solution was degassed with argon gas and the argon blanked was kept on the surface of the solution for an  $\text{O}_2$  free environment. Different concentrations of analytes were added in 10 mL PBS (pH

8.0) electrochemical cell. All the results were saved and converted into textfiles (DAT) format and analysed using Origin 7 (Origin Lab, USA).

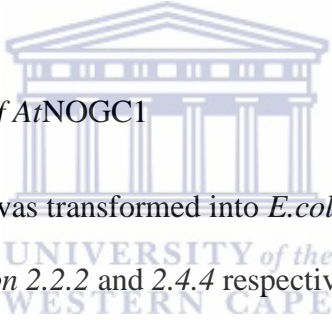


## Chapter 3: Recombinant expression and purification of the *At*NOGC1 protein

The *Arabidopsis thaliana* proteome has been searched for the presence of the heme-Nitric Oxide (NO) and oxygen (O<sub>2</sub>) binding (H-NOX) motif. The guanylyl cyclase (GC) and the extended H-NOX motifs were used as search engines for heme-binding and identified an *Arabidopsis* flavin-containing monooxygenase (At1g62580) as a candidate. The *At*NOGC1 has been successfully expressed as a His SUMO protein which is fused to the N-terminus of the protein and it was purified under native conditions by affinity chromatography using a metal-chelating resin of nickel-nitrilotriacetic acid (Ni-NTA).

### 3.1 Results

#### 3.1.1 Expression and purification of *At*NOGC1



The pET SUMO-*At*NOGC1 clone was transformed into *E.coli* BL-21 CodonPlus competent cells and expressed as described in section 2.2.2 and 2.4.4 respectively. When the OD<sub>600nm</sub> reached 0.5, induction was achieved by adding IPTG to a final concentration of 2 mM at 30 °C and the expected band at ~ 67.7 kDa was well prominent in the induced soluble fraction as shown in figure 3.1 (lane 2) as compared to the uninduced fraction (lane 1). The recombinant protein was successfully expressed and the pET SUMO-*At*NOGC1 was purified under native conditions by affinity chromatography as confirmed by a clear band of ~ 67.7 kDa on the eluted fraction (lane 8).

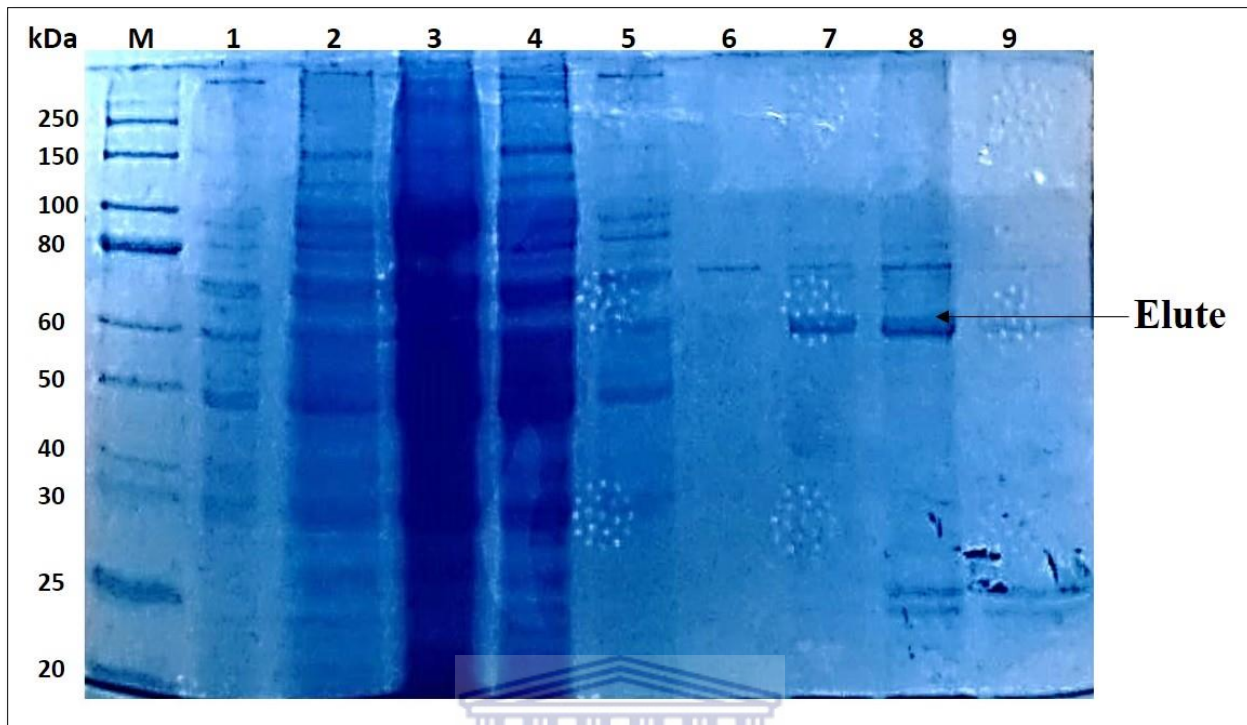


**Figure 3.1: 12 % SDS-PAGE analysis of the expression and affinity purification of the *AtNOGC1* protein.** M: 250 kDa Molecular weight unstained protein marker (New England Biolabs, Cat# P7703); Lane 1: Lysate Un-induced; Lane 2: Lysate Induced; Lane 3: Lysate Induced flow through; Lane 4-7: Wash 1-4; Lane 8: Elute; Lane 9: 2 M NaCl.

UNIVERSITY of the  
WESTERN CAPE

### 3.1.2 Determination of *AtNOGC1*'s protein concentration

Sample fractions corresponding to the fusion *AtNOGC1* protein in lanes 7-8 of figure 3.1 were pulled together and concentrated as described in *section 2.2.10*. The final concentration of the fusion *AtNOGC1* protein was determined by Bradford assay as described in *section 2.2.9*. Different absorbance values of the BSA standard and the unknown protein sample were recorded at the same wavelength of 595 nm as shown in table 3.1 Appendix I. The standard curve was constructed according to the absorbance values of the standard samples (Appendix I, Figure 3.3). The protein concentration was calculated to a final of 3.1 mg/mL (Appendix I, Equation 1) and the final concentrated fusion protein was analysed on the SDS PAGE as shown in figure 3.2. The

expected band size of the concentrated *At*NOGC1 protein was observed at ~ 67.7 kDa on lane 1 at a final concentration of 50 µg.

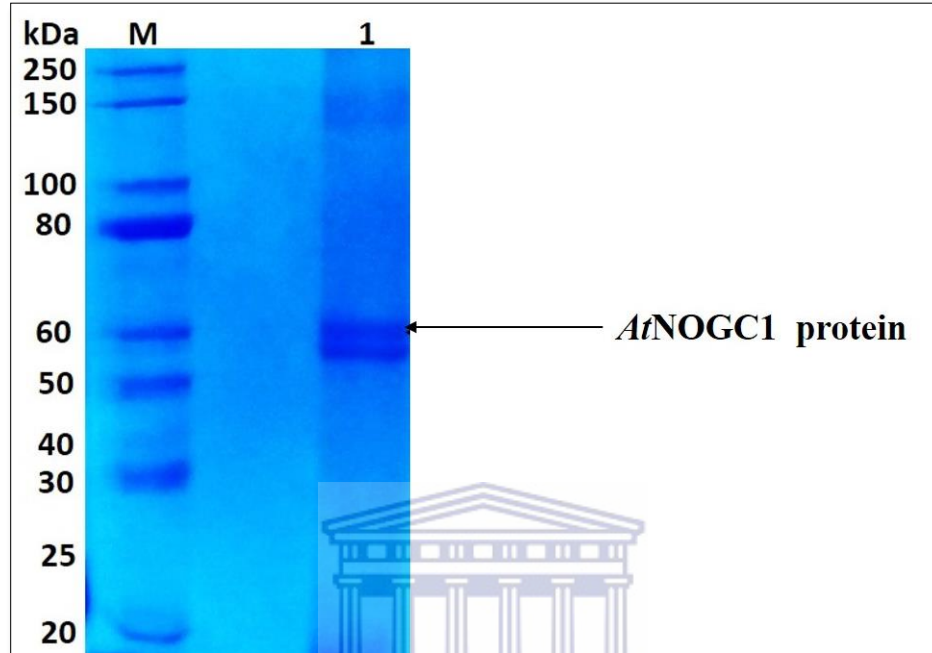


**Figure 3.2: 12 % SDS-PAGE analysis of the concentrated *At*NOGC1 protein.** M: 250 kDa Molecular weight unstained protein marker (New England Biolabs, Cat#P7703); Lane 1: *At*NOGC1 (50µg). The band on lane 1 is visible at ~ 67.7 kDa as an expected size of the recombinant *At*NOGC1 protein after ultra-centrifugation using 3k filter for 6 hours.

### 3.2 Discussion

The main objective for this chapter was to express and purify the novel signalling molecule *At*NOGC1, which has been previously identified and characterised by Mulaudzi et al (2011). The author searched for the H-NOX domain and GC activity within the *Arabidopsis* sequence and discovered that *At*NOGC1 contains the H-NOX motif at the N terminus followed by a GC motif towards the C-terminus. *E.coli* competent cells such as XL-GOLD and BL-21 CodonPlus were previously prepared for the propagation and expression of the pET SUMO-*At*NOGC1 construct.



The expected size of the pET SUMO-*AtNOGC1* was ~ 67.7 kDa protein which represent ~1 kDa 6xHis tag, 11 kDa SUMO fusion tag and 56.7 kDa for *AtNOGC1*. The *AtNOGC1* protein was expressed as a fusion protein to SUMO, a *Saccharomyces cerevisiae* (Smt3) protein which is a homolog of the mammalian SUMO-1 protein (Saitoh et al., 1997). Smt3 is a member of ubiquitin-like protein family involved in some of the major cellular mechanisms such as apoptosis, nuclear transport and cell cycle progression (Muller et al., 2001). SUMO's mechanism of action include covalently binding to lysine side chains on target proteins to modulate the protein function. This work demonstrate that binding of SUMO to the N-terminus of under-expressed proteins extensively enhances their expression in *E.coli* (Malakhov et al., 2004).

The protocol optimised for the expression of the novel *AtNOGC1* protein was followed (Mulaudzi et al., 2011). Large scale expression was conducted in a final volume of 1 500 mL culture which was induced by 2 mM of IPTG. The ubiquitin and SUMO families of proteins are highly stable and resistant to heat and proteolysis. Since *in silico* analysis indicated that *AtNOGC1* is a non-stable insoluble protein (unpublished data), its attachment to the SUMO increased its solubility and stabilised its expression (Mulaudzi, 2011). These results correlate with the work done by Malakhov et al (2004), who indicated that attachment of a highly stable structure (SUMO) at the N-terminus of a partner protein helps to stabilise and increase the yield of the recombinant protein (Malakhov et al., 2004).

The recombinant pET SUMO protein was purified under native conditions by affinity chromatography with Ni-NTA, which contains a nickel-charged agarose resins. The advantage of the Ni-NTA resin is that it can be regenerated and re-used many times due to its stable binding metallic property (Bornhorst and Falke, 2000). Since there was a presence of the N-terminal polyhistidine (6xHis) tag in pET SUMO which is ~ 1 kDa, therefore affinity chromatography was

used because it allows purification of the recombinant fusion protein with a metal-chelating resin of Ni-NTA. Elution of AtNOGC1 was efficiently achieved with the elution buffer (0.05 M Na Phosphate buffer; 0.3 M NaCl; 0.25 M imidazole; pH 8.0), since it has been reported that eluting proteins with mild buffer conditions and imidazole result in biologically active proteins either under native or denatured conditions by IMAC (Bornhorst and Falke, 2000). The expressed and purified recombinant protein was analysed on 12 % SDS PAGE as confirmed by a protein band at ~ 67.7 kDa on the induced soluble fraction, compared to the negative control on the un-induced soluble fraction and a well pronounced band on the eluted lane at the same band size as shown in figure 3.1. These results indicate that the protein was successfully expressed and purified under these conditions.

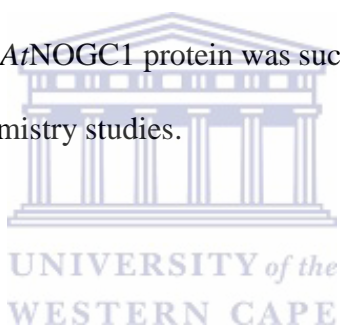
The concentration of the expressed and purified AtNOGC1 protein was determined using the Bradford assay method. Bradford assay is a protein determination method that involves the binding of Coomassie Brilliant Blue G-250 dye to proteins (Bradford, 1976). However, when the dye binds to the protein, it is converted to a stable unprotonated blue form ( $A_{\max} = 595 \text{ nm}$ ) (Sedmack and Grossberg, 1977). The blue protein-dye form is detected at a wavelength of 595 nm in the assay using a spectrophotometer or microplate reader. The two most common protein standards used for protein assays are bovine serum albumin (BSA) and gamma-globulin, however BSA was preferred (BioRad Laboratories Inc, USA). Standard proteins of the BSA were used to prepare known protein concentrations from 0 to 25  $\mu\text{g/mL}$  (Appendix I, Table 3.1). The recombinant AtNOGC1 protein dilutions of 1:50 and 1:1000 showed average absorbance values of 0.254 and 0.253 which were within the range of the standard samples absorbance values (Appendix I, Table 3.1).

The standard curve was plotted from the standard absorbance values against the concentration. A standard curve, also known as a calibration curve was used as a quantitative research technique in



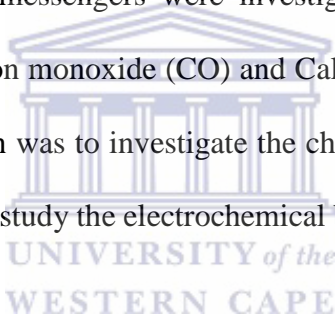
which standard samples with known concentrations were measured and graphed. Therefore the concentration of the unknown *At*NOGC1 protein was determined by interpolation on the graph with a good linear relationship of  $R^2 = 0.9336$  (Appendix I, Figure 3.3).

The last steps of preparing a protein sample for analyses, such as activity assays or structural studies, involve ensuring that the protein is in its native, soluble form and without any impurities. The *At*NOGC1 protein was concentrated to a final concentration of 3.1 mg/mL by using a 3K molecular weight cutoff (MWCO) of an ultrafiltration centrifugal tube which contains a polyethersulfone (PES) membrane for a rapid and high recovery concentration process. The concentrated *At*NOGC1 protein was observed on the expected ~ 67.7 kDa size when analysed on 12 % SDS-PAGE (figure 3.2). The *At*NOGC1 protein was successfully expressed and purified for preparing a biosensor in electrochemistry studies.



## **CHAPTER 4: Electrochemical characterisation of *At*NOGC1 protein bioelectrode as a biosensor for binding NO, CO and Ca<sup>2+</sup>**

Chemical materials are mainly converted into a useful analytical signal by a device called a chemical sensor. The data from a chemical sensor is converted in a form of composition, existence of a certain element or ion, its concentration, chemical activity and its partial pressure (Kreno et al., 2011). The chemical data may be a reaction involving analytes or from a physical property of an electrode (Šljukić et al., 2006). Electrochemistry techniques were used to investigate redox reactions, since the activity of a reaction is directly related to the current measured. In this study, signalling molecules and second messengers were investigated as biological analytes which includes; Nitric Oxide (NO), Carbon monoxide (CO) and Calcium ion (Ca<sup>2+</sup>). The application of the chemical sensor in this research was to investigate the chemical responses of the bare glassy carbon electrode (GCE) in order to study the electrochemical behaviour of the *At*NOGC1/GCE as a biosensor.



### *4.1 The electrochemical characterisation of the bare glassy carbon electrode (GCE) as a chemical sensor*

Cyclic voltammetry (CV) of the bare GCE in PBS (0.05 M Na Phosphate buffer and 0.3 M NaCl; pH 8.0) was conducted in aerobic and anaerobic conditions. For anaerobic conditions, the solution was purged with argon gas for 30 minutes and the argon blanket was kept on the surface level as previously described in *section 2.3.3*. Distilled water (dH<sub>2</sub>O) and imidazole were added as analytes as shown in figure 4.1 (A) and (B). The CV experiments were carried out at a scan rate of 2 mV.s<sup>-1</sup> at a potential window between +150 mV and -800 mV.

For anaerobic conditions, there was no catalytic peak current formed in figure 4.1 (A) (green and blue) and 4.1 (B) (green and black). For aerobic conditions in figure 4.1 (A), in the absence of dH<sub>2</sub>O (black), there was a cathodic peak current ( $I_{pc}$ ) of 1.4  $\mu$ A observed around cathodic peak potentials ( $E_{pc}$ ) of -400 mV (vs Ag/AgCl). When 0.25 mL dH<sub>2</sub>O was added as a control analyte (red) an  $I_{pc}$  of 2  $\mu$ A was observed around the same  $E_{pc}$  of -400 mV (vs Ag/AgCl). Therefore, there was an  $I_{pc}$  of 0.6  $\mu$ A difference between aerobic solutions in the presence (red) and absence (black) of dH<sub>2</sub>O.

In figure 4.1 (B), for aerobic conditions without imidazole (red), there was an  $I_{pc}$  of 1.3  $\mu$ A observed around  $E_{pc}$  of -400 mV (vs Ag/AgCl). When 0.25 M imidazole (blue) was added a new catalytic peak was generated with an  $I_{pc}$  of 1.65  $\mu$ A and there was a catalytic peak potential shift with a value of -300 mV (vs Ag/AgCl). Therefore, there was an  $I_{pc}$  of 0.35  $\mu$ A difference between aerobic solutions in the presence (blue) and absence (red) of imidazole.

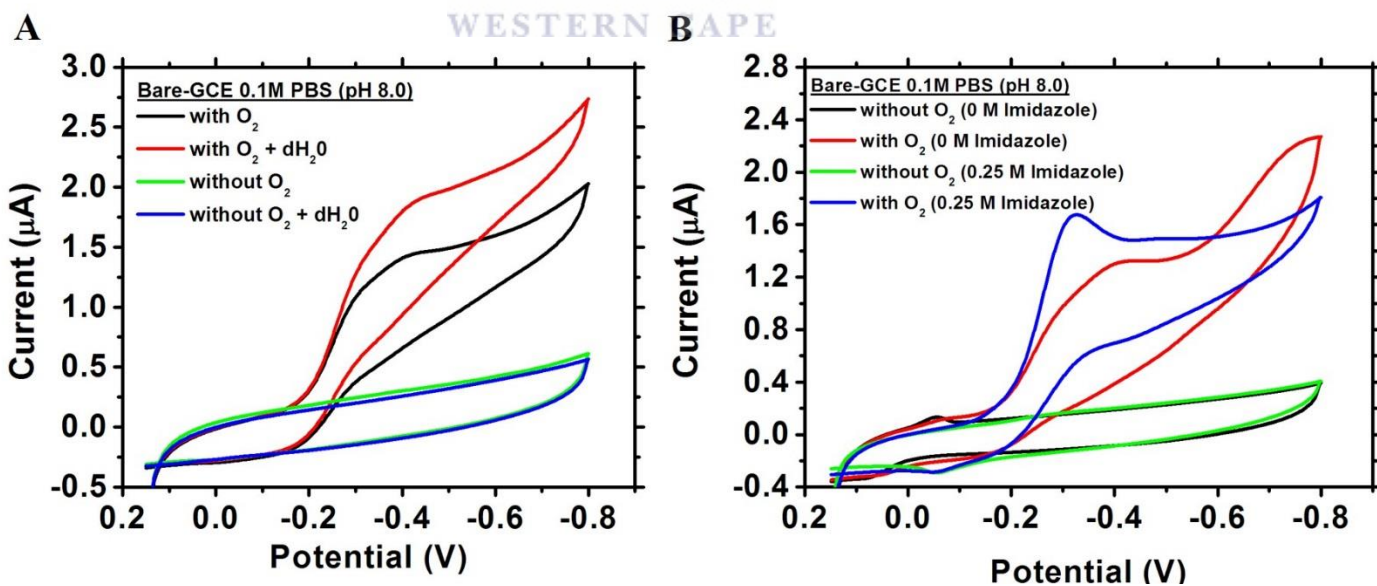


**Figure 4.1: Cyclic voltammetry showing responses of bare GCE in the presence and absence of O<sub>2</sub> or imidazole as a chemical sensor.** All CV experiments were conducted in PBS (0.05 M Na Phosphate buffer and 0.3 M NaCl; pH 8.0) at a scan rate of 2 mV.s<sup>-1</sup> and a potential window between +150 mV and -800 mV. (A) For anaerobic conditions; Green: 0.1 M PBS without O<sub>2</sub> and blue: 0.25 mL dH<sub>2</sub>O without O<sub>2</sub>. For aerobic conditions; Black: O<sub>2</sub> only and red: 0.25 mL dH<sub>2</sub>O with O<sub>2</sub>. (B) For anaerobic conditions; Black: without O<sub>2</sub> and green: 0.25 M imidazole without O<sub>2</sub>. For aerobic conditions; Red: O<sub>2</sub> only and blue: 0.25 M imidazole with O<sub>2</sub>.

Imidazole is incorporated into many important biological molecules and the most obvious is the amino acid histidine, which has an imidazole side chain. Imidazole can act as a cation and as an anion when it combines with salts. The electroactive ions diffuse to the electrode surface and adsorb to it in the presence of  $O_2$ . Therefore, the bare GCE showed response as a chemical sensor to both the control ( $dH_2O$ ) and experimental (Imidazole) analytes in anaerobic and aerobic conditions. The chemical sensor was characterised electrochemically in response to an electron transfer mechanism in redox reactions.

In order to study the biochemical sensor, the chemical sensor was first characterised electrochemically in response to an electron transfer mechanism in a redox reaction as shown in figure 4.1 (A and B). Whereby the results demonstrated the diffusion of electroactive ions on the surface of the bare GCE in anaerobic solution, since flat voltammograms were observed. However, when the solution was saturated with excess  $O_2$  and different analytes;  $dH_2O$  (figure 4.1 A) and imidazole (figure 4.1 B), adsorption took place hence there was an increase in the catalytic peak currents and potential shift in a reduction reaction. Therefore, these results depict that the bare GCE is involved in electron transfer as a chemical sensor with no interference and it can further be used to create an electrochemical enzyme based biosensor such as *AtNOGC1*/GCE biosensor (Zhu et al., 2014).

#### *4.2 The electrochemical behaviour of the immobilised AtNOGC1 on the GCE surface in the presence and absence of $O_2$ .*

The immobilisation of *AtNOGC1* protein onto the GCE surface was performed by the method described in section 2.3.2, whereby crosslinking agents such as didodecyldimethylammonium bromide (DDAB), Bovine Serum Albumin (BSA) and glutaraldehyde were used. The cyclic voltammetry (CV) responses of *AtNOGC1*/GCE biosensor in the presence and absence of  $O_2$  was

conducted in PBS (0.05 M Na<sub>2</sub>HPO<sub>4</sub> and 0.3 M NaCl; pH 8.0) at 2 mV.s<sup>-1</sup> scan rate and a potential window between +150 mV and -800 mV as shown in figure 4.2.

In anaerobic (black) solution with 0.25 M imidazole, there was no catalytic peak current responses observed. However, in aerobic (green) solution without imidazole the onset potential was observed at -200 mV (vs Ag/AgCl) and a reduction wave with  $E_{pc}$  of -550 mV (vs Ag/AgCl). The aerobic (red) solution with 0.25 M imidazole showed increased response with  $I_{pc}$  of 0.8  $\mu$ A at the same peak potential value of -550 mV (vs Ag/AgCl). Therefore, an  $I_{pc}$  difference of 0.3  $\mu$ A between the aerobic solutions with 0.25 M imidazole (red) and without imidazole (green) was observed at the same peak potential of -550 mV (vs Ag/AgCl).

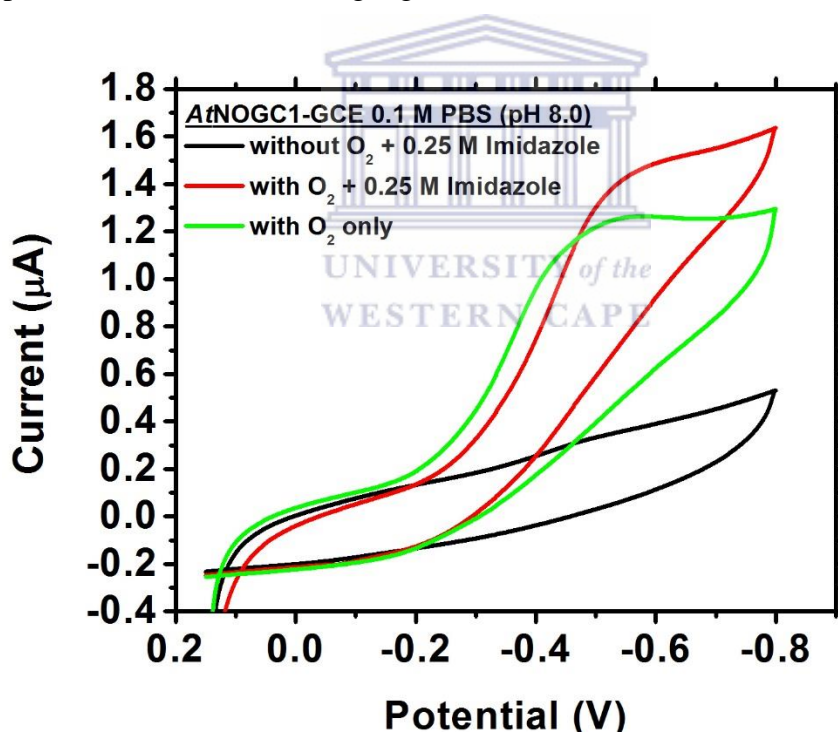


**Figure 4.2:** Cyclic voltammetry showing responses of the AtNOGC1/GCE biosensor in the presence and absence of O<sub>2</sub>. All CV experiments were conducted in PBS (0.05 M Na<sub>2</sub>HPO<sub>4</sub> and 0.3 M NaCl; pH 8.0) at a scan rate of 2 mV.s<sup>-1</sup> and a potential window between +150 mV and -800 mV. Argon gas was used to purge the solution for anaerobic (black) condition with no catalytic peak current generated and was saturated by bubbling to acquire excess O<sub>2</sub> for aerobic (red and green) conditions. The solution with 0.25 M imidazole (red) displayed a high cathodic peak current of 1.5  $\mu$ A as compared to a slow reaction rate (green) without imidazole with an  $I_{pc}$  of 1.2  $\mu$ A in the presence of the O<sub>2</sub>.

The overall comparison of the O<sub>2</sub> free solution (black) to the O<sub>2</sub> rich solution (red and green) in the reaction rate was about 1.15 μA excess increase. The electrochemical properties of the immobilised heme protein such as *At*NOGC1 aid in the determination of whether electrons are able to move from the electrode surface to the active site of the immobilised *At*NOGC1/GCE.

The binding affinity of *At*NOGC1/GCE biosensor to signalling molecules and second messengers was studied under anaerobic and aerobic conditions. The electrochemical reduction of *At*NOGC1 protein was determined to be greatly influenced by the presence of O<sub>2</sub> on the *At*NOGC1/GCE biosensor surface. For redox reaction to take place, O<sub>2</sub> is essential in the electron transfer between prosthetic heme groups of the protein and electrode surface (Gorton et al., 1999). Since, adsorption took place at the surface of the *At*NOGC1/GCE biosensor in the presence of O<sub>2</sub> and imidazole as shown in figure 4.2.

Imidazole is believed to restore the Fe<sup>3+</sup> state of the heme through reduction, as demonstrated with the FixL heme-based sensor which is more reactive towards the large polar imidazole (Mansy et al., 1998) and our results also showed that imidazole assisted O<sub>2</sub> to bind to *At*NOGC1 with more affinity as shown in figure 4.2 (green voltammogram). The *At*NOGC1 protein is also annotated as a flavin containing mono-oxygenase (FMO), which specialises in oxidation reactions. Since, FMO's requires O<sub>2</sub> in their reactions as a co-factor such as nicotinamide adenine dinucleotide phosphate (NADPH) and flavin adenine dinucleotide (FAD) (Förstermann and Sessa, 2011). Therefore, in the presence of O<sub>2</sub>, there was oxygenation of *At*NOGC1 coupling of the heme group from *At*NOGC1-Fe<sup>3+</sup> to *At*NOGC1-Fe<sup>2+</sup> state, but when 0.25 M imidazole was added, the reduction peak potential shifted to a more reduction potential as illustrated in figure 4.2 (from green to red voltammogram), therefore it shows that imidazole restored the *At*NOGC1-Fe<sup>2+</sup> back to the *At*NOGC1-Fe<sup>3+</sup> state (Kokhan et al., 2010).



### 4.3 Electrocalalytic activity of signalling molecules and second messengers

#### 4.3.1 Electrocatalytic activity of nitric oxide (NO) on AtNOGC1/GCE biosensor

The AtNOGC1 protein comprises of a heme-nitric oxide and/or oxygen (H-NOX) binding domain for binding NO and O<sub>2</sub>. NO was produced in the laboratory by a method previously described in section 2.3.4.1. The CV responses of the AtNOGC1/GCE based biosensor were evaluated at milliliter (mL) concentration arrays of the NO analyte from 0.5 mL to 2.5 mL in PBS (0.05 M Na<sub>2</sub>HPO<sub>4</sub>, 0.3 M NaCl and 0.25 M imidazole; pH 8.0) at 2 mV.s<sup>-1</sup> scan rate and a potential window between +150 mV and -800 mV. Figure 4.3 shows the CV of the biosensor under anaerobic or aerobic conditions, in the presence and absence of NO.

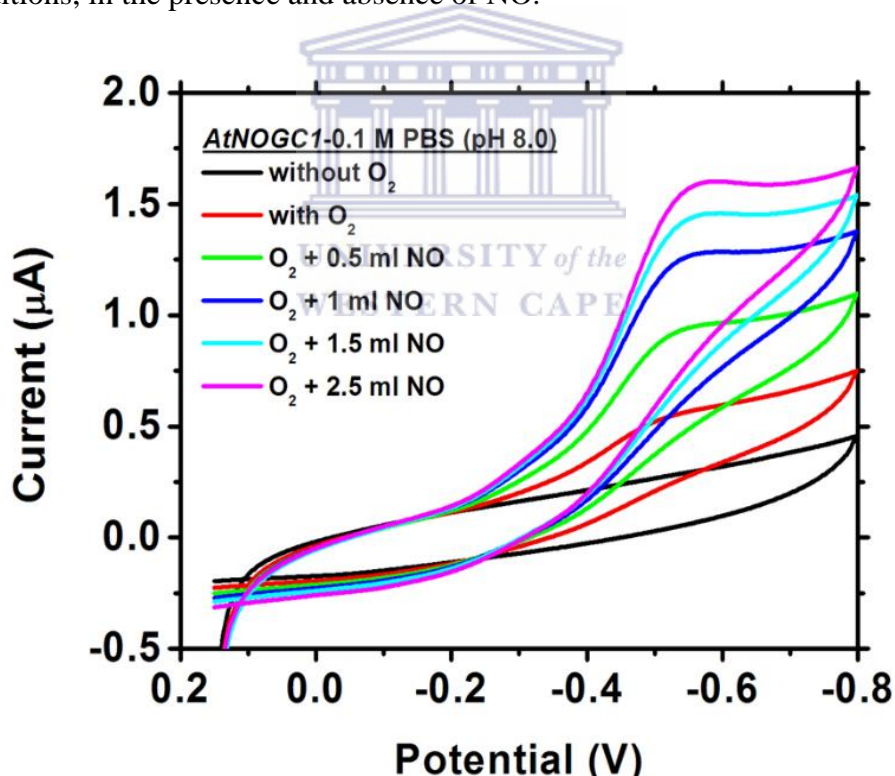


**Figure 4.3. Cyclic voltammetry showing responses of the nitric oxide (NO) towards the AtNOGC1/GCE biosensor in the presence and absence of O<sub>2</sub>.** All CV experiments were conducted in PBS (0.05 M Na<sub>2</sub>HPO<sub>4</sub>, 0.3 M NaCl and 0.25 M imidazole; pH 8.0) at a scan rate of 2 mV.s<sup>-1</sup> and a potential window between +150 mV and -800 mV. Argon gas was used to purge the solution for anaerobic (black) conditions and was saturated by bubbling to acquire excess O<sub>2</sub> for aerobic (red) conditions which displayed a higher I<sub>pc</sub> of 0.5 µA. Therefore, when different volumes of NO were added into the aerobic solution from 0.5 mL (green), 1 mL (blue), 1.5 mL (cyan) to 2.5 mL (magenta) a constant increase of I<sub>pc</sub> from 0.9 to 1.7 µA was observed around E<sub>pc</sub> of -500 mV (vs Ag/AgCl).

In the absence of O<sub>2</sub> and NO (black) solution, there was no catalytic response observed since the voltammogram consist of a flat wave. When the solution was saturated with excess O<sub>2</sub> (red), the reduction current suddenly increased with  $I_{pc}$  of 0.48  $\mu$ A around  $E_{pc}$  of -500 mV (vs Ag/AgCl). Therefore when 0.5 mL PBS saturated with NO gas was added in the solution (green), an  $I_{pc}$  of 1.8  $\mu$ A was observed around the same peak potential value of -500 mV. Thereafter, a constant catalytic increase in  $I_{pc}$  of 0.25  $\mu$ A when 1 mL (blue), 1.5 mL (cyan) and 2.5 mL (magenta) were added around the same peak parameters of -500 and -540 mV (vs Ag/AgCl).

Cyclic voltammetric responses of the *At*NOGC1/GCE biosensor corresponding to different concentrations of NO showed a cathodic shift potential as the concentration of NO was increased. The reverse voltammetric waves did not have any anodic current as they showed plain voltammograms. The reduction cyclic voltammetric current of *At*NOGC1-NO responses showed only one redox species due to the observation of only one cathodic peak in the CV.

The binding of NO to *At*NOGC1 was investigated in an *At*NOGC1-Fe<sup>3+</sup> to *At*NOGC1-Fe<sup>2+</sup> conversion. Since it has been reported by Mulaudzi et al (2011) that under anaerobic conditions, NO binds to *At*NOGC1 protein in its resting state (*At*NOGC1-Fe<sup>3+</sup>) and the bound *At*NOGC1-NO remains bound in its reduced state (*At*NOGC1-Fe<sup>2+</sup>). The increase in the reduction current peak with a cathodic shift peak potential was observed in the presence of O<sub>2</sub> as shown in figure 4.3, whereby the catalytic peak also increased with an increase in NO. Therefore, these observations suggested that the *At*NOGC1-Fe<sup>3+</sup> reduction was accompanied by the oxygenation step i.e. the binding of two O<sub>2</sub> molecules. The first O<sub>2</sub> molecule bind to the *At*NOGC1-Fe<sup>3+</sup> and results in *At*NOGC1-Fe<sup>2+</sup>-O<sub>2</sub> form and the second O<sub>2</sub> molecule was involved in the cleavage of the O<sub>2</sub> to O<sub>2</sub> bond (O-O) (Ignaszak et al., 2009). The CV responses of the constant increase in the catalytic current peak from 0.5 mL to 2.5 mL NO at the same potential peak of -500 mV (vs Ag/AgCl) was



observed in figure 4.3, these results can be explained by the mono-oxygenation catalytic cycle of heme enzymes such as *At*NOGC1 as it took place in a reduction reaction (Lewis and Pratt, 1998).

#### *4.3.1.1 Electrochemical characterisation of the bare GCE, modified GCE with DDAB/BSA and AtNOGC1/GCE biosensor in the presence and absence of NO*

In order to study the electrochemical behaviour of the modified DDAB/BSA-*At*NOGC1/GCE biosensor, several control parameters were performed to monitor the catalytic responses of the crosslinking agents. The CV experiments were performed in aqueous solution of PBS (0.05 M Na<sub>2</sub>HPO<sub>4</sub>, 0.3 M NaCl and 0.25 M imidazole; pH 8.0) in aerobic conditions at 2 mV.s<sup>-1</sup> scan rate with a potential window between +150 mV and -800 mV. Figure 4.4 shows the CV responses of the (A) bare GCE, (B) DDAB/BSA/GCE and (C) *At*NOGC1/GCE biosensor in the presence and absence of 0.5 mL NO in aerobic solution.

In figure 4.4 (A), a chemical sensor which is the bare GCE showed a high catalytic reduction peak with a potential value of -500 mV and an  $I_{pc}$  increase from 1.5 to 1.6  $\mu$ A when 0.5 mL PBS with NO was added to the aerobic solution. Addition of 0.5 mL PBS with NO in the electrochemical solution of *At*NOGC1/GCE biosensor resulted in a drastic decrease in the electrochemical current response as shown in figure 4.4 (D), indicating the possibility of adsorption of NO molecules on the *At*NOGC1/GCE biosensor surface at the same  $E_{pc}$  of -500 mV. However, when GCE was coated with the recombinant *At*NOGC1 protein, the reduction peak potential was decreased when compared to the bare GCE and DDAB/BSA/GCE. Redox potential of all different coated and non-coated GCE shown to vary in the range from -400 to -500 mV (vs Ag/AgCl) when 0.5 mL NO was added into the electrochemical solution.

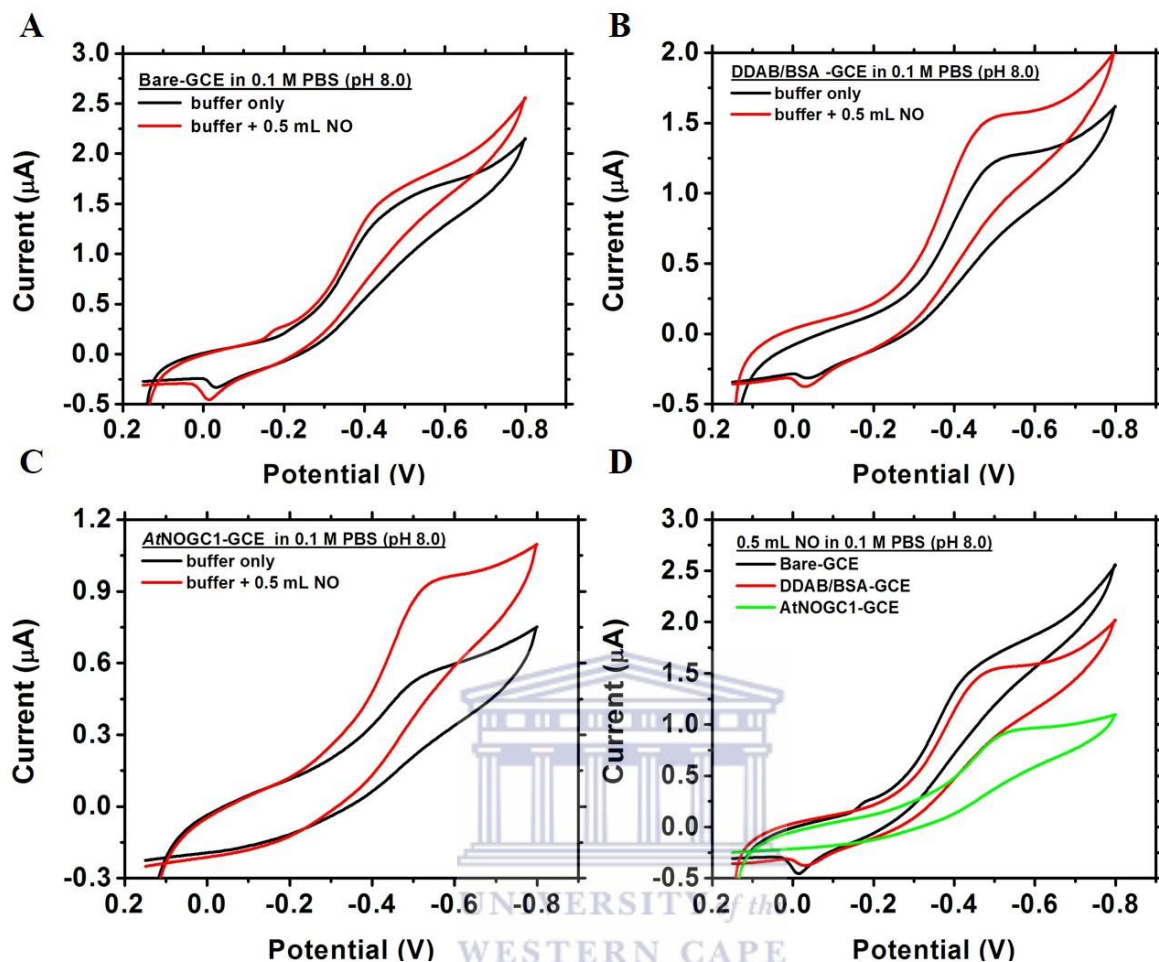


**Figure 4.4:** Cyclic voltammetry showing responses of the bare GCE, modified GCE with DDAB/BSA and *AtNOGC1*/GCE biosensor in the presence of NO. All CV experiments were conducted in PBS (0.05 M Na<sub>2</sub>HPO<sub>4</sub>, 0.3 M NaCl and 0.25 M imidazole; pH 8.0) at a scan rate of 2 mV.s<sup>-1</sup> and a potential window between +150 mV and -800 mV. (A) Bare GCE generated a reduction peak in aerobic (black) solution with  $I_{pc}$  of 1.45  $\mu$ A around  $E_{pc}$  of -500 mV (vs Ag/AgCl) and a solution (red) which contained 0.5 mL NO showed an increase in the catalytic current and a shift towards more reduction. (B) When bare GCE was immobilised with 10 mM DDAB and 2 mg/ml BSA, the reduction reaction rate of aerobic (black) solution with buffer only was observed with  $I_{pc}$  of 1.25  $\mu$ A and when 0.5 mL NO was added to the solution (red), there was an increase in the catalytic current responses around same  $E_{pc}$  of -500 mV. (C) Cyclic voltammetry response of *AtNOGC1*/GCE biosensor in aerobic (black) solution without NO, showed a drastic decrease in the catalytic current peak at a potential value of -500 mV. However when 0.5 ml NO was added, the  $I_{pc}$  increased from 0.4 to 9.5  $\mu$ A at the same potential value of -500 mV. (D) CV response of aerobic solution in the presence of 0.5 mL NO, the bare GCE (black) displaced a high catalytic peak than both DDAB/BSA/GCE (red) and *AtNOGC1*/GCE (green) with  $I_{pc}$  of 1.75  $\mu$ A. Therefore, redox potential coated and non-coated GCE showed to vary in the range from -400 to -500 mV in the presence of NO.

#### 4.3.2 Electrocatalytic activity of carbon monoxide (CO) on *AtNOGC1*/GCE biosensor

Carbon monoxide (CO) uses catalytically dose-dependent CO donors known as heme aqueous and CO aqueous which also promotes physiological processes such as seed germination in plants. Due

to its catalytic activity and selectivity in aqueous solutions, it is important to determine its binding affinity as a signalling molecule to *At*NOGC1/GCE biosensor as shown in figure 4.5.

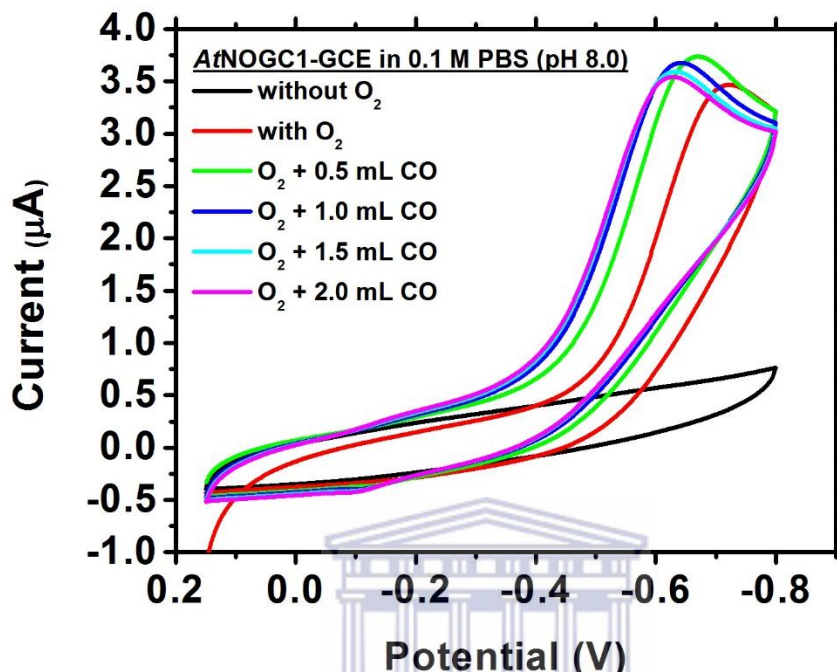
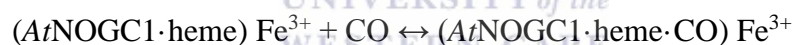


**Figure 4.5. Cyclic voltammetry showing responses of the carbon monoxide (CO) towards the *At*NOGC1/GCE biosensor in the presence and absence of O<sub>2</sub>.** All CV experiments were conducted in PBS (0.05 M Na<sub>2</sub>HPO<sub>4</sub>, 0.3 M NaCl and 0.25 M imidazole; pH 8.0) at a scan rate of 10 mV.s<sup>-1</sup> with a potential window between +150 mV and -800 mV. Argon gas was used to purge the solution for anaerobic (black) solution and was saturated by bubbling to acquire excess O<sub>2</sub> for aerobic (red) solution which display a high *I*<sub>pc</sub> of 3.4 µA. Different volumes of CO were added into the aerobic solution from 0.5 mL (green), 1.0 mL (blue), 1.5 mL (cyan) to 2.0 mL (magenta) of CO. A constant decrease in *I*<sub>pc</sub> from 3.6 to 3.4 µA was observed from -680 mV to -610 mV with cathodic peak shift potential towards an oxidizing agent region.

In the absence of O<sub>2</sub> and CO (black) free analyte solution, there was no catalytic response observed in PBS (0.05 M Na<sub>2</sub>HPO<sub>4</sub>, 0.3 M NaCl and 0.25 M imidazole; pH 8.0) at 10 mV.s<sup>-1</sup> scan rate with a potential window between +150 mV and -800 mV. Therefore, when the solution was saturated with excess O<sub>2</sub> (red), there was an increase in the catalytic response with *I*<sub>pc</sub> of 3.5 µA around *E*<sub>pc</sub> of -700 mV (vs Ag/AgCl) and when 0.5 mL of PBS with CO gas was added in the solution (green), an *I*<sub>pc</sub> increased to a maximum reduction peak of 3.75 µA around *E*<sub>pc</sub> of -680 mV (vs Ag/AgCl). The electrode showed a shift to less negative potential as a strong oxidizing agent. Thereafter, a constant catalytic decrease in *I*<sub>pc</sub> and a shift in potential to a more positive potential was observed

when CO concentration was increased from 1 mL (blue), 1.5 mL (cyan) and to 2 mL (magenta). CO reduction may be caused by the adsorption of the heme group as the concentration of CO with O<sub>2</sub> is added to the electrolyte solution. The reaction rate is influenced by the current which is dependent on the potential.

The effect of CO saturation on the *At*NOGC1/GCE based biosensor in figure 4.5 can be explained by CO binding to the heme group, which affects the reduction potentials of the Fe<sup>3+</sup>/Fe<sup>2+</sup> couple. However, it has been reported that CO can inhibit the mono-oxygenation reaction of the heme oxygenase (HO) catalytic cycle by binding to the ferrous heme complex such as *At*NOGC1-Fe<sup>3+</sup>/Fe<sup>2+</sup> (Migita et al., 1998). Carbon monoxide rapidly and strongly binds to the reduced *At*NOGC1-Fe<sup>3+</sup> heme, which produces a shift in the reduction formal redox potential to a less (negative) reduction potential as shown in figure 4.5. This can be well illustrated by the following reaction:



The shift in potential to a less (negative) reduction by ~ 50 mV for *At*NOGC1 when different CO concentrations were added into the solution was observed as shown in figure 4.5. Fleming et al (2007) also reported the same magnitude of the shift in potential that is consistent with the results obtained in this study for other heme enzymes such as P450 (Fleming et al., 2007). Both the Fe<sup>3+</sup> and the Fe<sup>2+</sup> state of the heme can bind to CO, since the cathodic peak potential of the *At*NOGC1-Fe<sup>3+</sup>/Fe<sup>2+</sup> couple in the presence of O<sub>2</sub> agreed well with the value reported by Mulaudzi et al (2011), that redox responses of gas signalling molecules vary in the peak potential range of -400 to -600 mV (vs Ag/AgCl) (Mulaudzi et al., 2011).

#### 4.3.2.1 Electrochemical characterisation of the bare GCE, modified GCE with DDAB/BSA and *AtNOGC1*/GCE biosensor in the presence and absence of CO

Electrochemical response of the *AtNOGC1*/GCE biosensor in the presence of CO was studied to confirm that the reduction was not influenced from the direct electron transfer of the bare GCE nor the solid support DDAB/BSA vesicle. The CV experiment was conducted in aerobic solution of PBS (0.05 M Na<sub>2</sub>HPO<sub>4</sub>, 0.3 M NaCl and 0.25 M imidazole; pH 8.0) at 2 mV.s<sup>-1</sup> scan rate with a potential window between +150 mV and -800 mV as shown in figure 4.6 (A) Bare GCE, (B) DDAB/BSA/GCE and (C) *AtNOGC1*/GCE biosensor in the presence and absence of 0.5 mL PBS saturated with CO.

In figure 4.6 (A) represent voltammograms of the bare GCE in the absence (black) and presence (red) of 0.5 mL CO, an addition of CO to the electrochemical solution led to an increase in the reduction peak. Similarly, to the GCE modified with DDAB/BSA in figure 4.6 (B). However, a well-defined cathodic peak was observed when the GCE was modified with *AtNOGC1* protein with  $I_{pc}$  of 1.4  $\mu$ A (black) and 1.5  $\mu$ A (red) at a potential peak value of -500 mV (vs Ag/AgCl). This crosslinkers provides an excellent environment for rapid electron exchange between heme proteins and electrode surface, whereby they carried a solid support as a carrier between *AtNOGC1* protein and GCE surface.



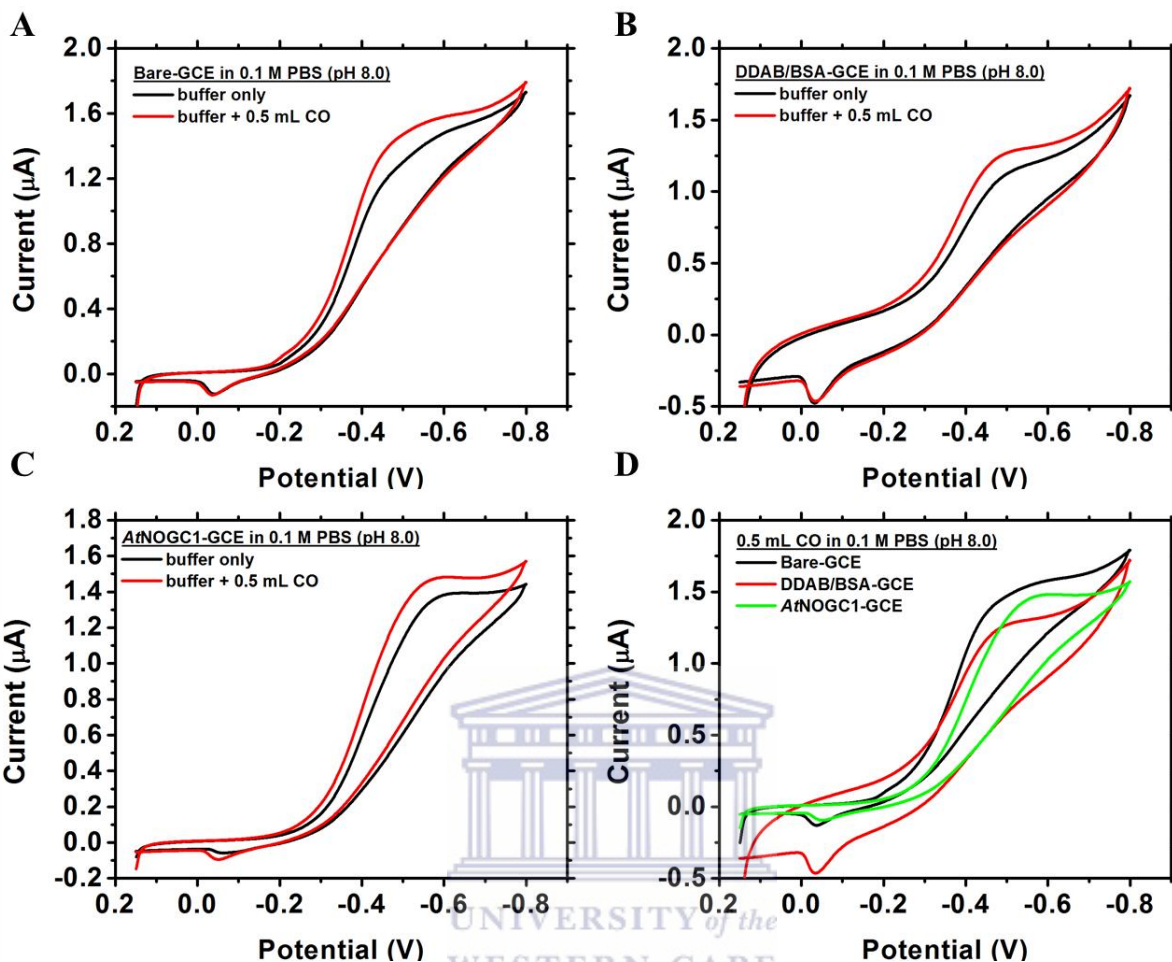


**Figure 4.6: Cyclic voltammety showing responses of the bare GCE, modified GCE with DDAB/BSA and *AtNOGC1*/GCE biosensor in the presence of CO.** All CV experiments were conducted in PBS (0.05 M Na<sub>2</sub>HPO<sub>4</sub>, 0.3 M NaCl and 0.25 M imidazole; pH 8.0) at a scan rate of 2 mV.s<sup>-1</sup> and a potential window between +150 mV and -800 mV. (A) The bare GCE generated a reduction peak in aerobic (black) solution with  $I_{pc}$  of 1.4  $\mu$ A and a solution (red) which contained 0.5 mL CO showed an increase in the catalytic current with  $I_{pc}$  of 1.55  $\mu$ A around  $E_{pc}$  of -500 mV (vs Ag/AgCl). (B) The modified GCE with 10 mM DDAB and 2 mg/ml BSA showed a decrease in the reduction peak of aerobic (black) solution with buffer only, as it was observed with  $I_{pc}$  of 1.15  $\mu$ A and when 0.5 mL CO was added to the solution (red), there was an increase in  $I_{pc}$  of 1.25  $\mu$ A around same  $E_{pc}$  of -500 mV (vs Ag/AgCl). (C) Cyclic voltammety response of the *AtNOGC1*/GCE biosensor in aerobic (black) solution without CO displayed a well-defined catalytic current peak at a potential value of -500 mV. However when 0.5 ml CO was added, the  $I_{pc}$  increased from 1.4 to 1.45  $\mu$ A at the same potential value of -500 mV. (D) CV response of aerobic solution in the presence of 0.5 mL CO, the bare GCE (black) showed a maximum catalytic peak than both DDAB/BSA/GCE (red) and *AtNOGC1*/GCE biosensor (green) at  $I_{pc}$  of 1.55  $\mu$ A. Redox potential of immobilised and none-immobilised GCE showed to vary in the range from -450 to -500 mV in the presence of CO.

#### 4.3.3 Electrocatalytic activity of calcium ion ( $Ca^{2+}$ ) on *AtNOGC1*/GCE biosensor

Electrochemical responses of the *AtNOGC1*/GCE biosensor were evaluated at nano-molar (nM) concentration arrays of the calcium ion ( $Ca^{2+}$ ) analyte from 1 nM to 7 nM in PBS (0.05 M

Na<sub>2</sub>HPO<sub>4</sub>, 0.3 M NaCl and 0.25 M imidazole; pH 8.0). The *At*NOGC1/GCE biosensor activity was analysed in the presence and absence of O<sub>2</sub> and Ca<sup>2+</sup> as shown in figure 4.7 (A). Therefore, in an O<sub>2</sub> and Ca<sup>2+</sup> free solution (black), there was no catalytic peak response observed. In the presence of O<sub>2</sub> (red) only, there was a generated reduction catalytic peak with an *I*<sub>pc</sub> of 1 μA around *E*<sub>pc</sub> of -560 mV (vs Ag/AgCl). Therefore, when 1 nM Ca<sup>2+</sup> (green) was added to the solution, there was an increase in the catalytic reduction peak to an *I*<sub>pc</sub> of 1.25 μA around the same *E*<sub>pc</sub>. A constant increase of an *I*<sub>pc</sub> from 1.35 to 1.6 μA (blue, cyan, magenta, yellow and dark yellow) was observed at the same *E*<sub>pc</sub> when different Ca<sup>2+</sup> concentrations were added to the solution. An increase in the electrochemical response current correspond to an increase in the Ca<sup>2+</sup> concentrations from 1 nM to 7 nM.

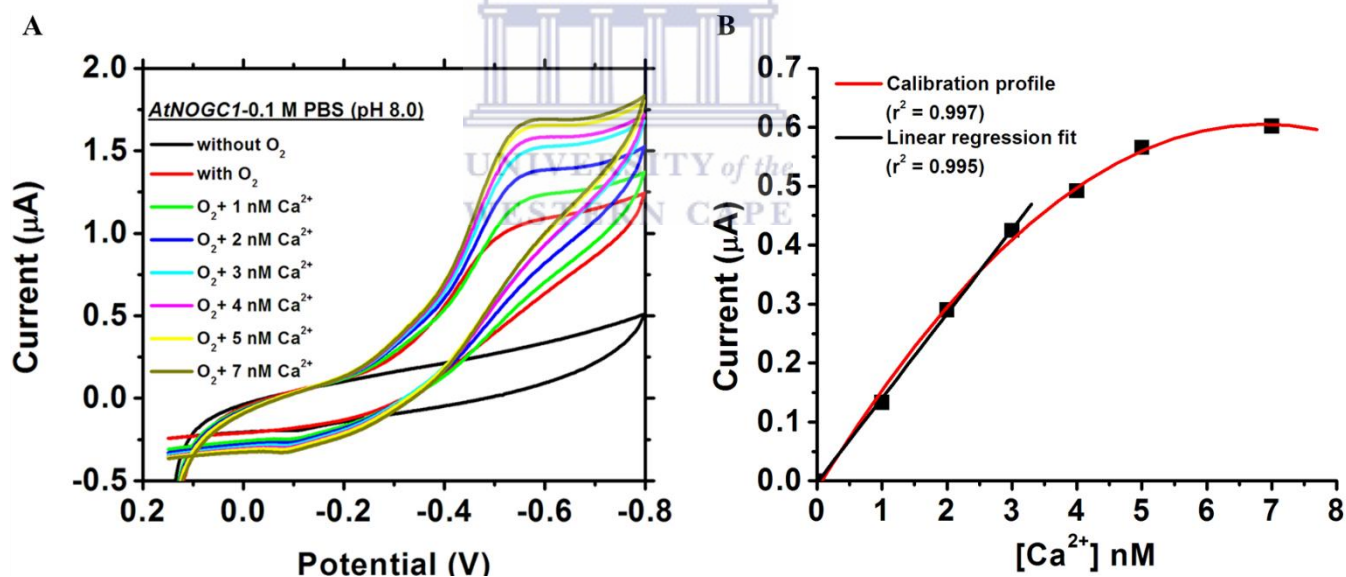


**Figure 4.7: Cyclic voltammetry showing responses of calcium ion (Ca<sup>2+</sup>) concentrations towards the *At*NOGC1/GCE biosensor in the presence and absence of O<sub>2</sub>.** (A) All CV experiments were conducted in PBS (0.05 M Na<sub>2</sub>HPO<sub>4</sub>, 0.3 M NaCl and 0.25 M imidazole; pH 8.0) at 2 mV.s<sup>-1</sup> scan rate with a potential window between +150 and -800 mV. The argon gas was used to purge the solution for anaerobic (black) conditions and was saturated by bubbling to acquire excess O<sub>2</sub> for aerobic (red) conditions which displayed a high *I*<sub>pc</sub> of 1 μA around *E*<sub>pc</sub> of -560 mV (vs Ag/AgCl). Different concentrations of Ca<sup>2+</sup> were added into the aerobic solution from 1 nM (green), 2 nM (blue), 3 nM (cyan), 4 nM (magenta), 5 nM (yellow) to 7 nM (dark yellow). Therefore, a constant increase of *I*<sub>pc</sub> from 1 μA to 1.7 μA was observed around *E*<sub>pc</sub> of -550 mV (vs Ag/AgCl). (B) Calibration profile curve (red) and linear relationship (black) of *At*NOGC1/GCE biosensor of current (μA) vs Ca<sup>2+</sup> concentration (nM).

The electrochemical kinetic response of the *At*NOGC1/GCE biosensor on the  $\text{Ca}^{2+}$  concentrations were further analysed by plotting a calibration curve of current ( $\mu\text{A}$ ) vs  $\text{Ca}^{2+}$  concentrations (nM) as shown in figure 4.7 (B). A standard linear regression (black) was fitted from 1 nM to 3 nM  $\text{Ca}^{2+}$  concentrations with a maximum adsorption current of  $4.25 \mu\text{A}$  at 3 nM  $\text{Ca}^{2+}$  concentration. The calibration curve (red) was plotted from 4 nM to 7 nM  $\text{Ca}^{2+}$  concentrations as the solution indicated that a saturation point was reached at  $6 \mu\text{A}$  corresponding to 7 nM  $\text{Ca}^{2+}$ .

The electrochemical concentration-dependent responses of the *At*NOGC1/GCE biosensor statically standard curve was fitted by using origin 7 software (Origin Lab, USA). The maximum effective concentration of the  $\text{Ca}^{2+}$  towards the *At*NOGC1/GCE based biosensor was observed at a cathodic current value of  $0.3 \mu\text{A}$ , which corresponded to the 2 nM  $\text{Ca}^{2+}$  concentration as shown in figure 4.7 (B). The maximum inhibition current response was observed at a cathodic current value of  $0.57 \mu\text{A}$  which corresponded to the 7 nM  $\text{Ca}^{2+}$  concentration of the biosensor's electroactive surface in figure 4.7 (B).

The dynamic linear range of the  $\text{Ca}^{2+}$  concentration towards the *At*NOGC1/GCE based biosensor was evaluated from 1 nM to 3 nM. The electrode reaction of  $\text{Ca}^{2+}$  on the *At*NOGC1/GCE biosensor is an adsorption controlled process due to the linear regression fit ( $r^2 = 0.995$ ) of the cathodic peak current from 1 nM to 3 nM. These results showed excellent stability and reproducibility at the same  $E_{pc}$  of  $-560 \text{ mV}$  (vs Ag/AgCl). Similar electrochemical studies of calcium dobesilate (CD) have been reported by Xu et al (2009), whereby electrochemical behaviour of CD showed excellent activity on gold nanoparticle modified glass carbon electrode with a couple of diffusion controlled stable redox peaks (Xu et al., 2009).



#### 4.3.3.1 Electrochemical characterisation of the bare GCE, modified GCE with DDAB/BSA and *AtNOGC1*/GCE biosensor in the presence and absence of $\text{Ca}^{2+}$

Immobilisation of proteins of interest by using crosslinkers enables for an indirect determination of whether the immobilisation process affects the properties of the protein, as it can be deduced from the crosslinkers behaviour as shown in figure 4.8 (A) Bare GCE, (B) DDAB/BSA/GCE and (C) *AtNOGC1*/GCE biosensor, when 7 nM  $\text{Ca}^{2+}$  was added to aerobic solution. The CV experiments were performed in aqueous solution of PBS (0.05 M  $\text{Na}_2\text{HPO}_4$ , 0.3 M NaCl and 0.25 M imidazole; pH 8.0) at  $2 \text{ mV}\cdot\text{s}^{-1}$  scan rate with a potential window between +150 mV and -800 mV.

Figure 4.8 (A) shows the CV response of the bare GCE with a catalytic reduction current peak of 1  $\mu\text{A}$  (black) without  $\text{Ca}^{2+}$  and catalytic reduction current peak of 1.25  $\mu\text{A}$  (red) with 7 nM  $\text{Ca}^{2+}$  at a potential value of -450 mV (vs Ag/AgCl). However, when the GCE was coated with *AtNOGC1*, there was a shift in the reduction peak potential to a value of -550 mV (vs Ag/AgCl). In addition to the observation of the GCE modified with *AtNOGC1* there was an increase in the catalytic current peak of 1.7  $\mu\text{A}$  as shown in figure 4.8 (D) when compared to the bare GCE and DDAB/BSA/GCE.

Modification of the electrode surface showed an increase in the electron transfer. Since, cationic lipid DDAB form a stable lipid bilayer at room temperature and the positive charge on the ammonium ion allows it to interact electrostatically with negatively charged graphite electrodes such as GCE. In addition, the structure of glutaraldehyde is not limited to monomeric form in aqueous solution and it has weak absorbance (at 235 nm). The advantage with glutaraldehyde as a crosslinker is that it can react with several functional groups of proteins.

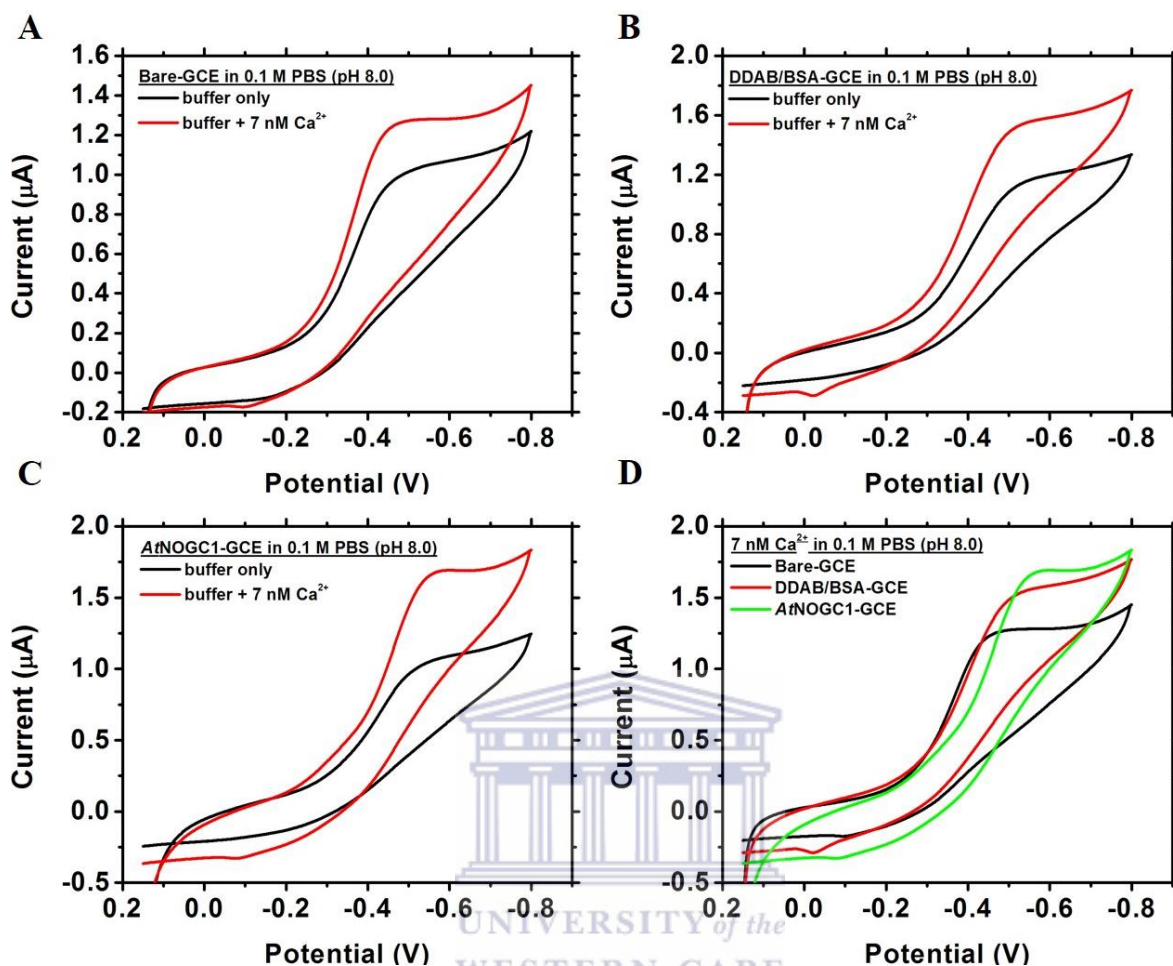


**Figure 4.8: Cyclic voltammety showing responses of the bare GCE, modified GCE with DDAB/BSA and *At*NOGC1/GCE biosensor in the presence of  $\text{Ca}^{2+}$ .** All CV experiments were conducted in PBS (0.05 M Na Phosphate buffer, 0.3 M NaCl and 0.25 M imidazole; pH 8.0) at a scan rate of  $2 \text{ mV}\cdot\text{s}^{-1}$  and a potential window between +150 mV and -800 mV. (A) The bare GCE generated a reduction peak in aerobic (black) solution with  $I_{pc}$  of  $1 \mu\text{A}$  and a solution (red) which contained  $7 \text{ nM } \text{Ca}^{2+}$  showed an increase in the catalytic current with  $I_{pc}$  of  $1.25 \mu\text{A}$  around  $E_{pc}$  of  $-450 \text{ mV}$  (vs Ag/AgCl). (B) The modified GCE with 10 mM DDAB and 2 mg/ml BSA showed an increase in the reduction peak when  $7 \text{ nM } \text{Ca}^{2+}$  was added into the aerobic (red) solution with  $I_{pc}$  of  $1.5 \mu\text{A}$  around  $E_{pc}$  of  $-500 \text{ mV}$  (vs Ag/AgCl). (C) Cyclic voltammety response of the *At*NOGC1/GCE biosensor in aerobic (black) solution without  $\text{Ca}^{2+}$  displayed a well-defined catalytic current peak at a potential value of  $-550 \text{ mV}$ . However, when  $7 \text{ nM } \text{Ca}^{2+}$  was added, the  $I_{pc}$  increased from  $1.1$  to  $1.7 \mu\text{A}$  at the same potential value of  $-550 \text{ mV}$ . (D) CV response in aerobic solution in the presence of  $7 \text{ nM } \text{Ca}^{2+}$  when bare GCE (black) showed a less catalytic peak than both DDAB/BSA/GCE (red) and *At*NOGC1/GCE (green). Redox potential of all different coated and non-coated GCE showed to vary in the range from  $-450$  to  $-550 \text{ mV}$  (Ag/AgCl) in the presence of  $7 \text{ nM } \text{Ca}^{2+}$ .

#### 4.4 Electrochemical characterisation of the binding affinity of NO, CO and Ca<sup>2+</sup> to AtNOGC1/GCE biosensor

In order to study the binding affinity of AtNOGC1 protein to signalling molecules such as NO and CO, and second messenger; Ca<sup>2+</sup> in combination, CV experiments with different analytes were performed in PBS (0.05 M Na<sub>2</sub>HPO<sub>4</sub>, 0.3 M NaCl and 0.25 M imidazole; pH 8.0) at room temperature with a potential window between +150 mV and -800 mV at a scan rate of 2 mV.s<sup>-1</sup> as shown in figure 4.9.

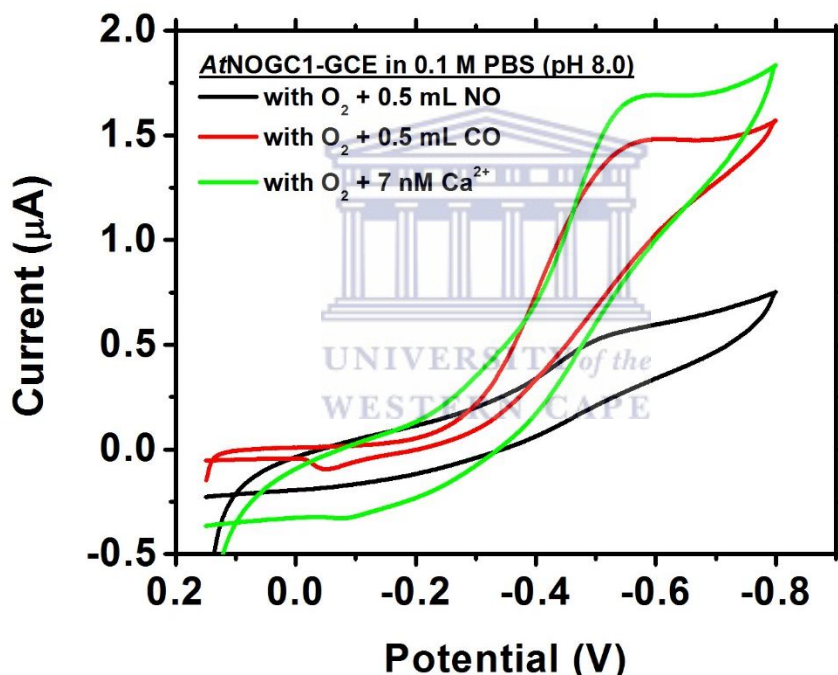


**Figure 4.9.** Cyclic voltammetry showing binding affinity responses of the nitric oxide (NO), carbon monoxide (CO) and calcium ion (Ca<sup>2+</sup>) towards the AtNOGC1/GCE biosensor in the presence of O<sub>2</sub>. Cyclic voltammetric experiments were conducted in PBS (0.05 M Na<sub>2</sub>HPO<sub>4</sub>, 0.3 M NaCl and 0.25 M imidazole; pH 8.0) at a scan rate of 2 mV.s<sup>-1</sup> with a potential window between +150 mV and -800 mV. When 0.5 mL NO (black) was added to the aerobic solution an  $I_{pc}$  of 0.5 µA was observed at  $E_{pc}$  -500 mV (vs Ag/AgCl). Therefore, when 0.5 mL CO (red) was added to the solution an  $I_{pc}$  of 1.5 µA was observed at  $E_{pc}$  -550 mV (vs Ag/AgCl) and when 7 nM Ca<sup>2+</sup> (green) was added to the solution, maximum catalytic peak was generated with  $I_{pc}$  of 1.7 µA around at  $E_{pc}$  -550 mV (vs Ag/AgCl).

CV responses of the aerobic (green) solution with 7 nM Ca<sup>2+</sup> which displaced the highest reduction catalytic peak with  $I_{pc}$  of 1.7 µA around  $E_{pc}$  of -550 mV (vs Ag/AgCl), when compared to the catalytic responses of solutions which contains 0.5 mL NO (black) and 0.5 mL CO (red). There is

a potential peak value of NO solution observed at -500 mV in comparison to the  $\text{Ca}^{2+}$  and CO peak potential value of -550 mV. The difference in the rate of electron transfer can determine the binding affinity of different analytes to the *At*NOGC1/GCE based biosensor. Therefore, addition of analytes in the electrochemical solution may increase the rate of oxygenation of the *At*NOGC1.

#### 4.7 Discussion

The aim of this chapter was to determine the binding affinity of signalling molecules; NO and CO and second messenger;  $\text{Ca}^{2+}$  to an *Arabidopsis* protein, *At*NOGC1. Since *At*NOGC1 has been annotated as a flavin containing mono-oxygenase, therefore it was important to monitor its responses in the presence and absence of  $\text{O}_2$  in all electrochemical experiments. *At*NOGC1 is a heme containing protein which is characterised by an H-NOX domain and a GC domain (Mulaudzi et al., 2011). The *At*NOGC1 is a heme protein which is a co-factor consisting of  $\text{Fe}^{3+}$  in the centre of the large heterocyclic porphyrin ring made up of pyrrolic groups (Gorton et al., 1999).

The biological sensor was composed by immobilising *At*NOGC1 protein on the bare GCE surface with crosslinking agents which include; didodecyldimethylammonium bromide (DDAB), bovine serum albumin (BSA) and glutaraldehyde to develop an electrochemical enzyme based biosensor. These crosslinking agents are stable at room temperature and they do not interfere with electron transfer on graphite electrodes such as GCE (Migneault et al., 2004). The results obtained in figure 4.4, 4.6 and 4.8 support that electrochemical response of the *At*NOGC1/GCE biosensor was not influenced from the direct electron transfer of the solid support crosslinking vesicle. Therefore, modification of the GCE surface with crosslinking agents and the *At*NOGC1 protein enhanced electron transfer (Iwuoha et al., 1998), since there was a more reduction shift in the peak potentials of the immobilised GCE.

It has been identified that graphite electrodes such as GCE showed their excellent promotion of direct electron transfer of heme proteins such as *At*NOGC1 than noble metal electrodes such as gold and platinum. The GCE showed a good selectivity to determine the binding affinity of *At*NOGC1 protein bioelectrode to stress signalling molecules; NO, CO and  $\text{Ca}^{2+}$  in the presence of imidazole. This study demonstrated that *At*NOGC1 protein plays an important role as an electron transporter in redox reactions. Similarly, Fufezan et al (2008) reported that heme co-factors are essential part of life because of their role in electron transportation. Furthermore, heme co-factors showed the ability to transport, store and detect many important molecules. In addition to its involvement in modulating gene expression, heme co-factors has been mostly used in redox chemistry (Fufezan et al., 2008).

The electrochemical reduction of the *At*NOGC1 protein was determined to be greatly influenced by the presence of the reactive  $\text{O}_2$  molecule on the *At*NOGC1/GCE surface. Biosensors are analytical tools which offer quantitative or semi quantitative analytical information by means of a biological recognition element in contact with a suitable transducer. The binding of the *At*NOGC1 protein to stress signalling molecules; NO, CO and  $\text{Ca}^{2+}$  was successful with no interference. The advantage of biomolecules biosensors such as *At*NOGC1 bioelectrode is that they are reproducible and can be used to determine the binding of many biological molecules in a research level. This study has shown for the first time that *At*NOGC1 is able to bind and sense CO in addition to NO and this is a characteristics of the human soluble guanylyl cyclase (Schmidt, 1992). Furthermore its ability to bind  $\text{Ca}^{2+}$ , also mean that *At*NOGC1 might have dual functions and maybe a novel  $\text{Ca}^{2+}$  binding protein in higher plants.

## Chapter 5: Conclusion and future prospects

Identification and characterisation of proteins that are involved in signalling pathways through binding different stress signals is important to understand mechanisms of stress tolerance towards the development of stress tolerant crops. Identification of guanylyl cyclases in higher plants is one of the major breakthroughs which indicated the importance of NO in cGMP synthesis (Mulaudzi et al., 2011) and the in planta existence of the NO/cGMP signalling cascade (Jodoui et al., 2013). However the amount of cGMP generated in an NO activation manner is not comparable to that which is produced by human sGC, this raised a lot of questions as to whether *At*NOGC1 is the only NO activated GC (Gross and Durner, 2016).

To further elucidate the role of *At*NOGC1 in binding stress signalling molecules, the recombinant protein was prepared as previously described in chapter 2 according to the method of Mulaudzi et al (2011). An enzyme (*At*NOGC1)-based biosensor was prepared and utilised in this study (Chapter 4) using electrochemical techniques. Previous investigations indicate that in addition to sensing NO, the human sGC also sense CO which activates its GC domain to synthesise cGMP (Stones and Marletta, 1994), this is interesting since CO has been shown to perform similar functions as NO. This information stimulated the need to further investigate the ability of *At*NOGC1 to bind CO. The *At*NOGC1 protein bioelectrode was able to bind CO as demonstrated in chapter 4 through an increase in the reduction peaks with  $I_{pc} = 3.75 \mu\text{A}$  at  $E_{pc} = -680 \text{ mV}$  (vs Ag/AgCl). Although its activation by CO to synthesise cGMP is still outstanding, this work has demonstrated the involvement of *At*NOGC1 in signalling CO, and thus a possible role in plant stress response. In addition, CO has been confirmed to be produced by many pathways in plants and so far hemoglobin is one of the well-known scavenger of CO (Liu et al., 2010). This study has also added new information that since *At*NOGC1 is able to bind CO, it might also play a role as a



CO scavenger through regulating it in plants to avoid its negative toxic effects, however further research is required to support this statement. In addition, plant breeders or engineers who wish to increase the production of CO in plants for better stress tolerance have a better chance, since in addition to hemoglobin as a scavenger, *AtNOGC1* might also serve the same purpose. This study has supported future work to investigate the ability of CO to indirectly synthesise cGMP through the activation of *AtNOGC1*. This is important since cGMP is a second messenger that is involved in many important physiological and biochemical processes in plants especially increasing plant tolerance to abiotic and biotic stresses (Donaldson et al., 2004; Durner et al., 1998).

Additionally and uniquely our protein based bioelectrode demonstrated the ability of *AtNOGC1* to bind  $\text{Ca}^{2+}$ , another important and well-studied stress signalling molecule both in animals and in plants (Fujita et al., 2006). Britt et al (2015) indicated that molecules that activate and stimulate human sGC might have a role in  $\text{Ca}^{2+}$  regulation (Britt et al., 2015). But till today there are no clear reports indicating the direct involvement of GC's with  $\text{Ca}^{2+}$ , except for the ability of cGMP to modulate various  $\text{Ca}^{2+}$  processes (Bazan-Perkins, 2012; Perez-Zoghbu et al., 2010; Koch and Stryer, 1988). Previous study indicated that  $\text{Ca}^{2+}$  was able to increase cGMP synthesis however at lower concentrations (Mulaudzi T, PhD thesis unpublished data, 2011). The response observed in this study upon addition of different  $[\text{Ca}^{2+}]$  on the *AtNOGC1* protein bioelectrode suggests a direct interaction and probably regulation of  $\text{Ca}^{2+}$  by *AtNOGC1*.

*AtNOGC1* is a plant sGC which signals NO (Mulaudzi et al., 2011), thus this study supported this statement by demonstrating that *AtNOGC1* also signals CO and  $\text{Ca}^{2+}$ . These results suggest that *AtNOGC1* is involved in many plant physiological processes including growth, development and response to abiotic and biotic stresses.

## References

- Al-Younis, I., Wong, A., & Gehring, C. (2015). The *Arabidopsis thaliana* K<sup>+</sup>-uptake permease 7 (AtKUP7) contains a functional cytosolic adenylate cyclase catalytic centre. *FEBS letters*, **589**(24), 3848-3852.
- Amrhein, N. (1977). The current status of cyclic AMP in higher plants. *Annual Review of Plant Physiology*, **28**(1), 123-132.
- Andrienko, D. (2008). Cyclic voltammetry. *John Wiley & Sons Publish., New York*, 3-12.
- Arimura, G. I., & Maffei, M. E. (2010). Calcium and secondary CPK signalling in plants in response to herbivore attack. *Biochemical and Biophysical Research Communications*, **400**(4), 455-460.
- Ashe, D., Alleyne, T., & Iwuoha, E. (2007). Serum cytochrome c detection using a cytochrome c oxidase biosensor. *Biotechnology and Applied Biochemistry*, **46**(4), 185-189.
- Astier, J., & Lindermayr, C. (2012). Nitric oxide-dependent posttranslational modification in plants: an update. *International Journal of Molecular Sciences*, **13**(11), 15193-15208.
- Bailey-Serres, J., & Mittler, R. (2006). The roles of reactive oxygen species in plant cells. *Plant Physiology*, **141**(2), 311-311.
- Bazán-Perkins, B. (2012). cGMP reduces the sarcoplasmic reticulum Ca<sup>2+</sup> loading in airway smooth muscle cells: a putative mechanism in the regulation of Ca<sup>2+</sup> by cGMP. *Journal of Muscle Research and Cell Motility*, **32**(6), 375-382.
- Berridge, M. J. (2004). Calcium signal transduction and cellular control mechanisms. *Biochimica et Biophysica Acta (BBA)-Molecular Cell Research*, **1742**(1-3), 3-7.



Besson-Bard, A., Pugin, A., & Wendehenne, D. (2008). New insights into nitric oxide signalling in plants. *Annual Review of Plant Biology*, **59**, 21-39.

Bilban, M., Haschemi, A., Wegiel, B., Chin, B. Y., Wagner, O., & Otterbein, L. E. (2008). Heme oxygenase and carbon monoxide initiate homeostatic signaling. *Journal of Molecular Medicine*, **86**(3), 267-279.

Boehning, D., Moon, C., Sharma, S., Hurt, K. J., Hester, L. D., Ronnett, G. V., & Snyder, S. H. (2003). Carbon monoxide neurotransmission activated by CK2 phosphorylation of heme oxygenase-2. *Neuron*, **40**(1), 129-137.

Bolwell, G. P. (1995). Cyclic AMP, the reluctant messenger in plants. *Trends in Biochemical Sciences*, **20**(12), 492-495.

Boon, E. M., & Marletta, M. A. (2005). Ligand specificity of H-NOX domains: from sGC to bacterial NO sensors. *Journal of Inorganic Biochemistry*, **99**(4), 892-902.

Bornhorst, J. A., & Falke, J. J. (2000). Purification of proteins using polyhistidine affinity tags. In *Methods in enzymology*. Academic Press, **326**, 245-254.

Boyer, J. S. (1982). Plant productivity and environment. *Science*, **218**(4571), 443-448.

Bradford, M. M. (1976). A rapid and sensitive method for the quantitation of microgram quantities of protein utilizing the principle of protein-dye binding. *Analytical Biochemistry*, **72**(1-2), 248-254.

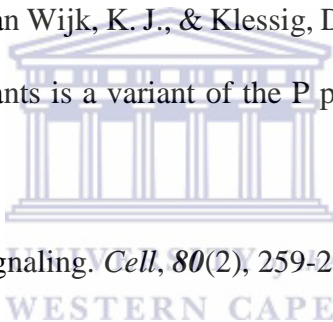
Britt Jr, R. D., Thompson, M. A., Kuipers, I., Stewart, A., Vogel, E. R., Thu, J., & Prakash, Y. S. (2015). Soluble guanylate cyclase modulators blunt hyperoxia effects on calcium responses of

developing human airway smooth muscle. *American Journal of Physiology-Lung Cellular and Molecular Physiology*, **309**(6), 537-542.

Brüne, B., & Ullrich, V. O. L. K. E. R. (1987). Inhibition of platelet aggregation by carbon monoxide is mediated by activation of guanylate cyclase. *Molecular Pharmacology*, **32**(4), 497-504.

Cao, Z., Huang, B., Wang, Q., Xuan, W., Ling, T., Zhang, B., & Shen, W. (2007). Involvement of carbon monoxide produced by heme oxygenase in ABA-induced stomatal closure in *Vicia faba* and its proposed signal transduction pathway. *Chinese Science Bulletin*, **52**(17), 2365-2373.

Chandok, M. R., Ytterberg, A. J., van Wijk, K. J., & Klessig, D. F. (2003). The pathogen-inducible nitric oxide synthase (iNOS) in plants is a variant of the P protein of the glycine decarboxylase complex. *Cell*, **113**(4), 469-482.



Clapham, D. E. (1995). Calcium signaling. *Cell*, **80**(2), 259-268.

Corpas, F. J., & Barroso, J. B. (2015). Nitric oxide from a “green” perspective. *Nitric Oxide*, **45**, 15-19.

Das, A., Trammell, S. A., & Hecht, M. H. (2006). Electrochemical and ligand binding studies of a *de novo* heme protein. *Biophysical Chemistry*, **123**(2-3), 102-112.

Davis, K. L., Martin, E., Turko, I. V., & Murad, F. (2001). Novel effects of nitric oxide. *Annual Review of Pharmacology and Toxicology*, **41**(1), 203-236.

Dayton, M. A., Ewing, A. G., & Wightman, R. M. (1980). Response of microvoltammetric electrodes to homogeneous catalytic and slow heterogeneous charge-transfer reactions. *Analytical Chemistry*, **52**(14), 2392-2396.

- Denninger, J. W., & Marletta, M. A. (1999). Guanylate cyclase and the NO/cGMP signalling pathway. *Biochimica et Biophysica Acta (BBA)-Bioenergetics*, **1411**(2-3), 334-350.
- Dhlamini, Z., Spillane, C., Moss, J. P., Ruane, J., Urquia, N., & Sonnino, A. (2005). *Status of research and application of crop biotechnologies in developing countries: preliminary assessment*. FAO.
- Dodd, A. N., Kudla, J., & Sanders, D. (2010). The language of calcium signalling. *Annual Review of Plant Biology*, **61**, 593-620.
- Domingos, P., Prado, A. M., Wong, A., Gehring, C., & Feijo, J. A. (2015). Nitric oxide: a multitasked signalling gas in plants. *Molecular Plant*, **8**(4), 506-520.
- Donaldson, L., Ludidi, N., Knight, M. R., Gehring, C., & Denby, K. (2004). Salt and osmotic stress cause rapid increases in *Arabidopsis thaliana* cGMP levels. *FEBS letters*, **569**(1-3), 317-320.
- Drøbak, B. K., & Watkins, P. A. (2000). Inositol (1, 4, 5) trisphosphate production in plant cells: an early response to salinity and hyperosmotic stress. *FEBS letters*, **481**(3), 240-244.
- Dubovskaya, L. V., Bakakina, Y. S., Kolesneva, E. V., Sodel, D. L., McAinsh, M. R., Hetherington, A. M., & Volotovski, I. D. (2011). cGMP-dependent ABA-induced stomatal closure in the ABA-insensitive *Arabidopsis* mutant *abi1-1*. *New Phytologist*, **191**(1), 57-69.
- Dulak, J., & Józkwicz, A. (2003). Carbon monoxide-a "new" gaseous modulator of gene expression. *Acta Biochimica Polonica-English edition*, **50**(1), 31-48.
- Durner, J., Wendehenne, D., & Klessig, D. F. (1998). Defense gene induction in tobacco by nitric oxide, cyclic GMP, and cyclic ADP-ribose. *Proceedings of the National Academy of Sciences*, **95**(17), 10328-10333.

Durzan, D. J., & Pedroso, M. C. (2002). Nitric oxide and reactive nitrogen oxide species in plants. *Biotechnology and Genetic Engineering Reviews*, **19**(1), 293-338.

Feng, J. J., Zhao, G., Xu, J. J., & Chen, H. Y. (2005). Direct electrochemistry and electrocatalysis of heme proteins immobilized on gold nanoparticles stabilized by chitosan. *Analytical Biochemistry*, **342**(2), 280-286.

Fleming, B. D., Bell, S. G., Wong, L. L., & Bond, A. M. (2007). The electrochemistry of a heme-containing enzyme, CYP199A2, adsorbed directly onto a pyrolytic graphite electrode. *Journal of Electroanalytical Chemistry*, **611**(1-2), 149-154.

Förstermann, U., & Sessa, W. C. (2011). Nitric oxide synthases: regulation and function. *European Heart Journal*, **33**(7), 829-837.

Fröhlich, A., & Durner, J. (2011). The hunt for plant nitric oxide synthase (NOS): is one really needed?. *Plant Science*, **181**(4), 401-404.

Fufezan, C., Zhang, J., & Gunner, M. R. (2008). Ligand preference and orientation in b- and c-type heme-binding proteins. *Proteins: Structure, Function, and Bioinformatics*, **73**(3), 690-704.

Fujita, M., Fujita, Y., Noutoshi, Y., Takahashi, F., Narusaka, Y., Yamaguchi-Shinozaki, K., & Shinozaki, K. (2006). Crosstalk between abiotic and biotic stress responses: a current view from the points of convergence in the stress signaling networks. *Current Opinion in Plant Biology*, **9**(4), 436-442.

Garcia-Mata, C., & Lamattina, L. (2003). Abscisic acid, nitric oxide and stomatal closure—is nitrate reductase one of the missing links?. *Trends in plant Science*, **8**(1), 20-26.

- Gaupels, F., Kuruthukulangarakoola, G. T., & Durner, J. (2011). Upstream and downstream signals of nitric oxide in pathogen defence. *Current Opinion in Plant Biology*, **14**(6), 707-714.
- Gehring, C. (2010). Adenyl cyclases and cAMP in plant signalling-past and present. *Cell Communication and Signalling*, **8**(1), 15.
- Gorton, L., Lindgren, A., Larsson, T., Munteanu, F. D., Ruzgas, T., & Gazaryan, I. (1999). Direct electron transfer between heme-containing enzymes and electrodes as basis for third generation biosensors. *Analytica Chimica Acta*, **400**(1-3), 91-108.
- Grondin, A., Rodrigues, O., Verdoucq, L., Merlot, S., Leonhardt, N., & Maurel, C. (2015). Aquaporins contribute to ABA-triggered stomatal closure through OST1-mediated phosphorylation. *The Plant Cell*, **27**(7), 1945-1954.
- Gross, I., & Durner, J. (2016). In search of enzymes with a role in 3', 5'-cyclic guanosine monophosphate metabolism in plants. *Frontiers in Plant Science*, **7**, 576.
- Gupta, K. J., Fernie, A. R., Kaiser, W. M., & van Dongen, J. T. (2011). On the origins of nitric oxide. *Trends in Plant Science*, **16**(3), 160-168.
- Haeseleer, F., Imanishi, Y., Sokal, I., Filipek, S., & Palczewski, K. (2002). Calcium-binding proteins: intracellular sensors from the calmodulin superfamily. *Biochemical and Biophysical Research Communications*, **290**(2), 615-623.
- Haines, R. J., Corbin, K. D., Pendleton, L. C., & Eichler, D. C. (2012). Protein kinase Ca phosphorylates a novel argininosuccinate synthase site at serine 328 during calcium-dependent stimulation of endothelial nitric-oxide synthase in vascular endothelial cells. *Journal of Biological Chemistry*, **287**(31), 26168-26176.

Hao, F., Zhao, S., Dong, H., Zhang, H., Sun, L., & Miao, C. (2010). Nia1 and Nia2 are involved in exogenous salicylic acid-induced Nitric Oxide generation and stomatal closure in *Arabidopsis*. *Journal of Integrative Plant Biology*, **52**(3), 298-307.

Heinemann, S. H., Hoshi, T., Westerhausen, M., & Schiller, A. (2014). Carbon monoxide—physiology, detection and controlled release. *Chemical Communications*, **50**(28), 3644-3660.

Henares, B. M., Higgins, K. E., & Boon, E. M. (2012). Discovery of a nitric oxide responsive quorum sensing circuit in *Vibrio harveyi*. *ACS Chemical Biology*, **7**(8), 1331-1336.

Hepler, P. K. (2005). Calcium: a central regulator of plant growth and development. *The Plant Cell*, **17**(8), 2142-2155.

Hetherington, A. M., & Brownlee, C. (2004). The generation of Ca<sup>2+</sup> signals in plants. *Annual Review of Plant Biology*, **55**, 401-427.

Hirschi, K. D., Zhen, R. G., Cunningham, K. W., Rea, P. A., & Fink, G. R. (1996). CAX1, an H<sup>+</sup>/Ca<sup>2+</sup> antiporter from *Arabidopsis*. *Proceedings of the National Academy of Sciences*, **93**(16), 8782-8786.

Hong, J., Zhao, Y. X., Xiao, B. L., Moosavi-Movahedi, A. A., Ghourchian, H., & Sheibani, N. (2013). Direct electrochemistry of hemoglobin immobilized on a functionalized multi-walled carbon nanotubes and gold nanoparticles nanocomplex-modified glassy carbon electrode. *Sensors*, **13**(7), 8595-8611.

Hu, X., Neill, S. J., Tang, Z., & Cai, W. (2005). Nitric oxide mediates gravitropic bending in soybean roots. *Plant Physiology*, **137**(2), 663-670.

Ignaszak, A., Hendricks, N., Waryo, T., Songa, E., Jahed, N., Ngece, R., & Iwuoha, E. I. (2009). Novel therapeutic biosensor for indinavir—A protease inhibitor antiretroviral drug. *Journal of Pharmaceutical and Biomedical Analysis*, **49**(2), 498-501.

Isner, J. C., & Maathuis, F. J. (2011). Measurement of cellular cGMP in plant cells and tissues using the endogenous fluorescent reporter FlincG. *The Plant Journal*, **65**(2), 329-334.

Ito, M., Takahashi, H., Sawasaki, T., Ohnishi, K., Hikichi, Y., & Kiba, A. (2014). Novel type of adenylyl cyclase participates in tabtoxinine- $\beta$ -lactam-induced cell death and occurrence of wildfire disease in *Nicotiana benthamiana*. *Plant Signaling and Behavior*, **9**(1), 27420.

Iwuoha, E. I., Joseph, S., Zhang, Z., Smyth, M. R., Fuhr, U., & de Montellano, P. R. O. (1998). Drug metabolism biosensors: electrochemical reactivities of cytochrome P450<sub>cam</sub> immobilised in synthetic vesicular systems. *Journal of Pharmaceutical and Biomedical Analysis*, **17**(6-7), 1101-1110.

Joudoi, T., Shichiri, Y., Kamizono, N., Akaike, T., Sawa, T., Yoshitake, J., & Iwai, S. (2013). Nitrated cyclic GMP modulates guard cell signalling in Arabidopsis. *The Plant Cell*, **25**(2), 558-571.

Kim, K., Rhee, S. G., & Stadtman, E. R. (1985). Nonenzymatic cleavage of proteins by reactive oxygen species generated by dithiothreitol and iron. *Journal of Biological Chemistry*, **260**(29), 15394-15397.

Koch, K. W., & Stryer, L. (1988). Highly cooperative feedback control of retinal rod guanylate cyclase by calcium ions. *Nature*, **334**(6177), 64.

Kokhan, O., Shinkarev, V. P., & Wraight, C. A. (2010). Binding of Imidazole to the Heme of Cytochrome c1 and Inhibition of the bc1 Complex from *Rhodobacter sphaeroides* I. EQUILIBRIUM AND MODELING STUDIES. *Journal of Biological Chemistry*, **285**(29), 22513-22521.

Kreno, L. E., Leong, K., Farha, O. K., Allendorf, M., Van Duyne, R. P., & Hupp, J. T. (2011). Metal–organic framework materials as chemical sensors. *Chemical Reviews*, **112**(2), 1105-1125.

Kwezi, L., Meier, S., Mungur, L., Ruzvidzo, O., Irving, H., & Gehring, C. (2007). The *Arabidopsis thaliana* brassinosteroid receptor (*AtBRI1*) contains a domain that functions as a guanylyl cyclase *in vitro*. *PLoS one*, **2**(5), e449.

Leitner, M., Vandelle, E., Gaupels, F., Bellin, D., & Delledonne, M. (2009). NO signals in the haze: nitric oxide signalling in plant defence. *Current Opinion in Plant Biology*, **12**(4), 451-458.

Lemtiri-Chlieh, F., Thomas, L., Marondedze, C., Irving, H., & Gehring, C. A. (2011). *Cyclic nucleotides and nucleotide cyclases in plant stress responses*. InTech.

Lewis, D. F., & Pratt, J. M. (1998). The P450 catalytic cycle and oxygenation mechanism. *Drug Metabolism Reviews*, **30**(4), 739-786.

Liu, J., & Zhu, J. K. (1998). A calcium sensor homolog required for plant salt tolerance. *Science*, **280**(5371), 1943-1945.

Liu, K., Xu, S., Xuan, W., Ling, T., Cao, Z., Huang, B., & Shen, W. (2007). Carbon monoxide counteracts the inhibition of seed germination and alleviates oxidative damage caused by salt stress in *Oryza sativa*. *Plant Science*, **172**(3), 544-555.



Liu, Y., Xu, S., Ling, T., Xu, L., & Shen, W. (2010). Heme oxygenase/carbon monoxide system participates in regulating wheat seed germination under osmotic stress involving the nitric oxide pathway. *Journal of Plant Physiology*, **167**(16), 1371-1379.

Ludidi, N., & Gehring, C. (2003). Identification of a novel protein with guanylyl cyclase activity in *Arabidopsis thaliana*. *Journal of Biological Chemistry*, **278**(8), 6490-6494.

Mabbott, G. A. (1983). An introduction to cyclic voltammetry. *Journal of Chemical Education*, **60**(9), 697.

Magyar, Z., Mészáros, T., Miskolczi, P., Deák, M., Fehér, A., Brown, S., & Bakó, L. (1997). Cell cycle phase specificity of putative cyclin-dependent kinase variants in synchronized alfalfa cells. *The Plant Cell*, **9**(2), 223-235.

Mahajan, S., & Tuteja, N. (2005). Cold, salinity and drought stresses: an overview. *Archives of Biochemistry and Biophysics*, **444**(2), 139-158.

Malakhov, M. P., Mattern, M. R., Malakhova, O. A., Drinker, M., Weeks, S. D., & Butt, T. R. (2004). SUMO fusions and SUMO-specific protease for efficient expression and purification of proteins. *Journal of Structural and Functional Genomics*, **5**(1-2), 75-86.

Mansy, S. S., Olson, J. S., Gonzalez, G., & Gilles-Gonzalez, M. A. (1998). Imidazole is a sensitive probe of steric hindrance in the distal pockets of oxygen-binding heme proteins. *Biochemistry*, **37**(36), 12452-12457.

Marcus, R. A. (1964). Chemical and electrochemical electron-transfer theory. *Annual Review of Physical Chemistry*, **15**(1), 155-196.

Martinez-Atienza, J., Van Ingelgem, C., Roef, L., & Maathuis, F. J. (2007). Plant cyclic nucleotide signalling: facts and fiction. *Plant Signalling and Behavior*, **2**(6), 540-543.

Meier, S., Ruzvidzo, O., Morse, M., Donaldson, L., Kwezi, L., & Gehring, C. (2010). The Arabidopsis wall associated kinase-like 10 gene encodes a functional guanylyl cyclase and is co-expressed with pathogen defense related genes. *PLoS one*, **5**(1), 8904.

Migita, C. T., Matera, K. M., Ikeda-Saito, M., Olson, J. S., Fujii, H., Yoshimura, T., & Yoshida, T. (1998). The oxygen and carbon monoxide reactions of heme oxygenase. *Journal of Biological Chemistry*, **273**(2), 945-949.

Migneault, I., Dartiguenave, C., Bertrand, M. J., & Waldron, K. C. (2004). Glutaraldehyde: behavior in aqueous solution, reaction with proteins, and application to enzyme crosslinking. *Biotechniques*, **37**(5), 790-806.

Monteiro, D., Liu, Q., Lisboa, S., Scherer, G. E. F., Quader, H., & Malho, R. (2005). Phosphoinositides and phosphatidic acid regulate pollen tube growth and reorientation through modulation of  $[Ca^{2+}]_c$  and membrane secretion. *Journal of Experimental Botany*, **56**(416), 1665-1674.

Moreau, M., Lindermayr, C., Durner, J., & Klessig, D. F. (2010). NO synthesis and signalling in plants—where do we stand?. *Physiologia Plantarum*, **138**(4), 372-383.

Mori, V., & Bertotti, M. (2000). Nitric oxide solutions: standardisation by chronoamperometry using a platinum disc microelectrode. *Analyst*, **125**(9), 1629-1632.

Motterlini, R. (2007). Carbon monoxide-releasing molecules (CO-RMs): vasodilatory, anti-ischaemic and anti-inflammatory activities. *Biochemistry Society*, **35**, 1142-1146.

Moutinho, A., Hussey, P. J., Trewavas, A. J., & Malho, R. (2001). cAMP acts as a second messenger in pollen tube growth and reorientation. *Proceedings of the National Academy of Sciences*, **98**(18), 10481-10486.

Mulaudzi, T. (2011). *Structural and functional characterisation of a novel signalling molecule in Arabidopsis thaliana* (Doctoral dissertation).

Mulaudzi, T., Ludidi, N., Ruzvidzo, O., Morse, M., Hendricks, N., Iwuoha, E., & Gehring, C. (2011). Identification of a novel *Arabidopsis thaliana* nitric oxide-binding molecule with guanylate cyclase activity *in vitro*. *FEBS letters*, **585**(17), 2693-2697.

Müller, H., Bracken, A. P., Vernell, R., Moroni, M. C., Christians, F., Grassilli, E., & Helin, K. (2001). E2Fs regulate the expression of genes involved in differentiation, development, proliferation, and apoptosis. *Genes and Development*, **15**(3), 267-285.

Müller, U. L. I. (1997). The nitric oxide system in insects. *Progress in Neurobiology*, **51**(3), 363-381.

Murad, F. (1999). Cellular signalling with nitric oxide and cyclic GMP. *Brazilian Journal of Medical and Biological Research*, **32**(11), 1317-1327.

Pachauri, R. K. (2007). Andy Reisinger, eds. 2008. *Climate Change 2007: Synthesis Report*.

Pagnussat, G. C., Lanteri, M. L., & Lamattina, L. (2003). Nitric oxide and cyclic GMP are messengers in the indole acetic acid-induced adventitious rooting process. *Plant Physiology*, **132**(3), 1241-1248.

- Parani, M., Rudrabhatla, S., Myers, R., Weirich, H., Smith, B., Leaman, D. W., & Goldman, S. L. (2004). Microarray analysis of nitric oxide responsive transcripts in Arabidopsis. *Plant Biotechnology Journal*, **2**(4), 359-366.
- Perez-Zoghbi, J. F., Bai, Y., & Sanderson, M. J. (2010). Nitric oxide induces airway smooth muscle cell relaxation by decreasing the frequency of agonist-induced  $Ca^{2+}$  oscillations. *The Journal of General Physiology*, **135**(3), 247-259.
- Pfeiffer, S., Janistyn, B., Jessner, G., Pichorner, H., & Ebermann, R. (1994). Gaseous nitric oxide stimulates guanosine-3', 5'-cyclic monophosphate (cGMP) formation in spruce needles. *Phytochemistry*, **36**(2), 259-262.
- Pietrobon, M., Zamparo, I., Maritan, M., Franchi, S. A., Pozzan, T., & Lodovichi, C. (2011). Interplay among cGMP, cAMP, and  $Ca^{2+}$  in living olfactory sensory neurons *in vitro* and *in vivo*. *Journal of Neuroscience*, **31**(23), 8395-8405.
- Planchet, E., Jagadis Gupta, K., Sonoda, M., & Kaiser, W. M. (2005). Nitric oxide emission from tobacco leaves and cell suspensions: rate limiting factors and evidence for the involvement of mitochondrial electron transport. *The Plant Journal*, **41**(5), 732-743.
- Planchet, E., & Kaiser, W. M. (2006). Nitric oxide production in plants: facts and fictions. *Plant Signalling and Behavior*, **1**(2), 46-51.
- Potocký, M., Eliáš, M., Profotová, B., Novotná, Z., Valentová, O., & Žárský, V. (2003). Phosphatidic acid produced by phospholipase D is required for tobacco pollen tube growth. *Planta*, **217**(1), 122-130.

Qi, Z., Verma, R., Gehring, C., Yamaguchi, Y., Zhao, Y., Ryan, C. A., & Berkowitz, G. A. (2010).  $\text{Ca}^{2+}$  signalling by plant *Arabidopsis thaliana* Pep peptides depends on *AtPepR1*, a receptor with guanylyl cyclase activity, and cGMP-activated  $\text{Ca}^{2+}$  channels. *Proceedings of the National Academy of Sciences*, **107**(49), 21193-21198.

Ranty, B., Aldon, D., & Galaud, J. P. (2006). Plant calmodulins and calmodulin-related proteins: multifaceted relays to decode calcium signals. *Plant Signaling and Behavior*, **1**(3), 96-104.

Reddy, A. S., Ali, G. S., Celesnik, H., & Day, I. S. (2011). Coping with stresses: roles of calcium- and calcium/calmodulin-regulated gene expression. *The Plant Cell*, **23**(6), 2010-2032.

Rockel, P., Strube, F., Rockel, A., Wildt, J., & Kaiser, W. M. (2002). Regulation of nitric oxide (NO) production by plant nitrate reductase in vivo and in vitro. *Journal of Experimental Botany*, **53**(366), 103-110.

Ruzvidzo, O., Dikobe, B. T., Kawadza, D. T., Mabadahanye, G. H., Chatukuta, P., & Kwezi, L. (2013). Recombinant expression and functional testing of candidate adenylate cyclase domains. *In Cyclic Nucleotide Signaling in Plants*, **1016**, 13-25.

Saitoh, H., Pu, R. T., & Dasso, M. (1997). SUMO-1: wrestling with a new ubiquitin-related modifier. *Trends in Biochemical Sciences*, **22**(10), 374-376.

Schmidt, H. H. (1992).  $\text{NO}\bullet$ ,  $\text{CO}$  and  $\bullet\text{OH}$  endogenous soluble guanylyl cyclase-activating factors. *FEBS letters*, **307**(1), 102-107.

Sedmak, J. J., & Grossberg, S. E. (1977). A rapid, sensitive, and versatile assay for protein using Coomassie brilliant blue G250. *Analytical Biochemistry*, **79**(1-2), 544-552.

Schade, G. W., Hofmann, R. M., & Crutzen, P. J. (1999). CO emissions from degrading plant matter. *Tellus B*, **51**(5), 889-908.

She, X. P., & Song, X. G. (2008). Carbon Monoxide-induced Stomatal Closure Involves Generation of Hydrogen Peroxide in *Vicia faba* Guard Cells. *Journal of Integrative Plant Biology*, **50**(12), 1539-1548.

Shi, H., Ishitani, M., Kim, C., & Zhu, J. K. (2000). The *Arabidopsis thaliana* salt tolerance gene *SOS1* encodes a putative Na<sup>+</sup>/H<sup>+</sup> antiporter. *Proceedings of the national academy of sciences*, **97**(12), 6896-6901.

Šljukić, B., Banks, C. E., & Compton, R. G. (2006). Iron oxide particles are the active sites for hydrogen peroxide sensing at multiwalled carbon nanotube modified electrodes. *Nano Letters*, **6**(7), 1556-1558.

Song, X. G., She, X. P., & Zhang, B. (2008). Carbon monoxide-induced stomatal closure in *Vicia faba* is dependent on nitric oxide synthesis. *Physiologia Plantarum*, **132**(4), 514-525.

Stone, J. R., & Marletta, M. A. (1994). Soluble guanylate cyclase from bovine lung: activation with nitric oxide and carbon monoxide and spectral characterization of the ferrous and ferric states. *Biochemistry*, **33**(18), 5636-5640.

Świeżawska, B., Jaworski, K., Pawełek, A., Grzegorzewska, W., Szewczuk, P., & Szmidt-Jaworska, A. (2014). Molecular cloning and characterization of a novel adenylyl cyclase gene, HpAC1, involved in stress signaling in *Hippeastrum x hybridum*. *Plant Physiology and Biochemistry*, **80**, 41-52.

- Trewavas, A. (1999). Le calcium, c'est la vie: calcium makes waves. *Plant Physiology*, **120**(1), 1-6.
- Trewavas, A. J. (1997). Plant cyclic AMP comes in from the cold. *Nature*, **390**(6661), 657.
- Turek, I., & Gehring, C. (2016). The plant natriuretic peptide receptor is a guanylyl cyclase and enables cGMP-dependent signalling. *Plant Molecular Biology*, **91**(3), 275-286.
- Tuteja, N., & Mahajan, S. (2007). Calcium signalling network in plants: an overview. *Plant Signalling and Behavior*, **2**(2), 79-85.
- Thoonen, R., Sips, P. Y., Bloch, K. D., & Buys, E. S. (2013). Pathophysiology of hypertension in the absence of nitric oxide/cyclic GMP signalling. *Current Hypertension Reports*, **15**(1), 47-58.
- Vielma, A. H., Retamal, M. A., & Schmachtenberg, O. (2012). Nitric oxide signalling in the retina: what have we learned in two decades?. *Brain Research*, **1430**, 112-125.
- Wang, M., & Liao, W. (2016). Carbon monoxide as a signalling molecule in plants. *Frontiers in Plant Science*, **7**, 572.
- Wang, Y., Chen, T., Zhang, C., Hao, H., Liu, P., Zheng, M., & Lin, J. (2009). Nitric oxide modulates the influx of extracellular  $\text{Ca}^{2+}$  and actin filament organization during cell wall construction in *Pinus bungeana* pollen tubes. *New Phytologist*, **182**(4), 851-862.
- Wheeler, J. I., Freihat, L., & Irving, H. R. (2013). A cyclic nucleotide sensitive promoter reporter system suitable for bacteria and plant cells. *BMC Biotechnology*, **13**(1), 97.
- Xu, H., Li, X., Zhang, J., Zhang, Z., & Liu, K. (2009). Electrochemical studies of calcium dobesilate and interaction with DNA. *Microchimica Acta*, **165**(3-4), 415-420.

Xuan, W., Huang, L., Li, M., Huang, B., Xu, S., Liu, H., & Shen, W. (2007). Induction of growth elongation in wheat root segments by heme molecules: a regulatory role of carbon monoxide in plants?. *Plant Growth Regulation*, **52**(1), 41-51.

Xuan, W., Zhu, F. Y., Xu, S., Huang, B. K., Ling, T. F., Qi, J. Y., & Shen, W. B. (2008). The heme oxygenase/carbon monoxide system is involved in the auxin-induced cucumber adventitious rooting process. *Plant Physiology*, **148**(2), 881-893.

Xuan, W., Xu, S., Li, M., Han, B., Zhang, B., Zhang, J., & Cui, J. (2012). Nitric oxide is involved in hemin-induced cucumber adventitious rooting process. *Journal of plant physiology*, **169**(11), 1032-1039.

Yamasaki, H., & Sakihama, Y. (2000). Simultaneous production of nitric oxide and peroxynitrite by plant nitrate reductase: in vitro evidence for the NR-dependent formation of active nitrogen species. *FEBS letters*, **468**(1), 89-92.

Yu, M., Lamattina, L., Spoel, S. H., & Loake, G. J. (2014). Nitric oxide function in plant biology: a redox cue in deconvolution. *New Phytologist*, **202**(4), 1142-1156.

Zhu, C., Yang, G., Li, H., Du, D., & Lin, Y. (2014). Electrochemical sensors and biosensors based on nanomaterials and nanostructures. *Analytical Chemistry*, **87**(1), 230-249.

Zhu, J. K., Liu, J., & Xiong, L. (1998). Genetic analysis of salt tolerance in *Arabidopsis*: evidence for a critical role of potassium nutrition. *The Plant Cell*, **10**(7), 1181-1191.

Zilli, C. G., Santa-Cruz, D. M., & Balestrasse, K. B. (2014). Heme oxygenase-independent endogenous production of carbon monoxide by soybean plants subjected to salt stress. *Environmental and Experimental botany*, **102**, 11-16.



## Appendices

### Appendix I: Determination of *AtNOGC1* protein concentration

**Table 3.1: The absorbance (595 nm) of the standard and unknown samples concentration ( $\mu\text{g/mL}$ ).** Bradford assay was conducted by using FLUOstar OPTIMA (BMG LABTECH, Germany, 2010) multi-detection microplate reader.

<b>Standard concentration (<math>\mu\text{g/mL}</math>)</b>	<b>Absorbance (595 nm)</b>
0	0.248
2.5	0.25
5	0.2535
10	0.258
15	0.2615
25	0.2645
<b><i>AtNOGC1</i> protein Diluent factor</b>	<b>Absorbance (595 nm)</b>
1:50	0.254
1:1000	0.2535

*Equation for the calculation of *AtNOGC1* protein concentration*

Equation 1

1:50

$$y = 0.0007x + 0.2494$$

$$0.254 - 0.2494 = 0.0007x$$

$$x = 6.57 \text{ (50 diluent factor)}$$

$$x = 328.5$$

1:1000

$$y = 0.0007 + 0.2494$$

$$0.2535 - 0.2494 = 0.0007x$$

$$x = 5.86 \text{ (1000 diluent factor)}$$

$$x = 5860$$

Average concentration

$$\frac{328.5 + 5860}{2} = 3094.25 \text{ } \mu\text{g/mL}$$

$$\frac{3094.25}{1000} = 3.1 \text{ mg/mL}$$

Final concentration = 3.1 mg/mL

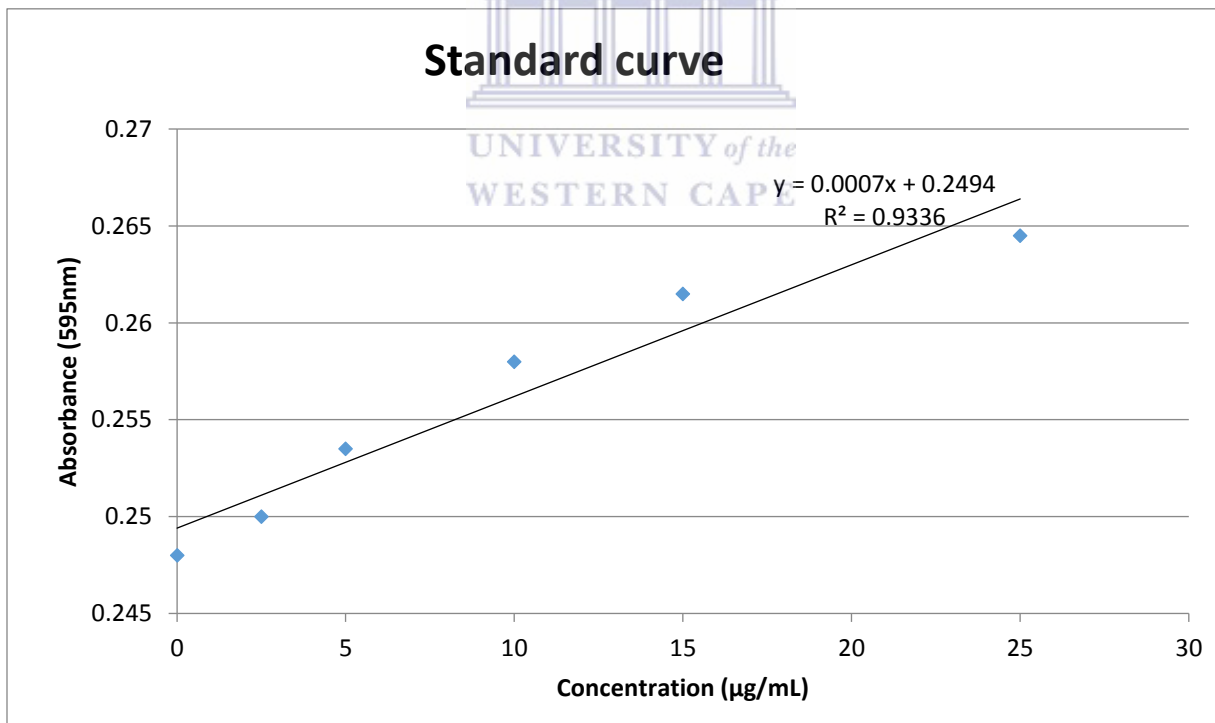


**Figure 3.3: Standard curve of BSA to determine the *At*NOGC1 protein concentration by Bradford assay.** The standard curve plot shows the linear relationship of the absorbance (595 nm) against the BSA concentration (µg/mL). From the linear regression equation the *At*NOGC1 protein concentration was calculated to a final concentration of 3.1 mg/mL.